EMPLOYING INTEGRATED ELECTROMAGNETIC INDUCTION SENSORS FOR SOIL CHARACTERIZATION UNDER DIFFERENT LAND USE CONDITIONS

By

© Clinton Mensah

A thesis submitted to the School of Graduate Studies in partial fulfillment of the requirements for the degree of

Master of Science

Boreal Ecosystems and Agricultural Sciences

School of Science and the Environment

Grenfell Campus

Memorial University of Newfoundland

May 2023

Corner Brook, Newfoundland and Labrador, Canada

Employing integrated electromagnetic induction sensors for soil characterization under different land use conditions

By

Clinton Mensah

A thesis submitted to the School of Graduate Studies

In partial fulfillment of the requirements for the degree of

Master of Science

Boreal Ecosystems and Agricultural Sciences

Approved:

_____

School of Graduate Studies

_____

Supervisor (Dr. Lakshman Galagedara)

_____

Date

Co-Supervisor
Dr. Mano Krishnapillai

Committee member
Dr. Dmitry Sveshnikov

Abstract

This study was conducted to explore the possibility of predicting soil moisture content (SMC) in podzolic soils in western Newfoundland using multi-coil (MC) and multi-frequency (MF) electromagnetic induction (EMI) sensors. Two studies were conducted to assess the effectiveness of apparent electrical conductivity (EC_a) from both MC and MF EMI sensors in characterizing SMC. The first study focused on employing MF-EMI in characterizing SMC under three different land uses in western Newfoundland's podzolic soils. The second study assessed effectiveness of EC_a obtained from the MC and MF-EMI sensors to maximize the representation of SMC taking into consideration organic matter, bulk density and texture using a statistical and geostatistical analysis. Geostatistical analysis from the first study revealed that cokriging of SMC with densely collected EC_a provided an improved characterization accuracy of soil moisture variability across the different land use conditions. The second study found that multiple linear regression (MLR) models were effective in representing SMC variations. Additionally, MC-EMI sensors provided better predictions of SMC than MF-EMI sensors. The findings from this study demonstrate that EMI has the potential to provide an accurate and robust technique for predicting soil moisture in boreal podzolic soils. Furthermore, it is worth noting that the surveys were performed during the wet period, given that MF–EMI is more reliable for ECa variability in wet soils than in dry soils.

General summary

This study examined the spatial variability of geo-referenced electrical conductivity of the soil (ECa) measurements, as a potential tool for characterizing soil properties under different land use conditions. MC and MF EMI sensors were used to analyze podzolic soils, and two kriging interpolation techniques were employed to estimate the accuracy of ECa as an auxiliary variable in predicting SMC under different land use conditions. The results showed that the ECa and SMC were significantly distinct between the natural forest and managed agricultural lands. MC-EMI sensors were more precise than MF-EMI sensors for SMC prediction, and cokriging with ECa as the covariate outperformed ordinary kriging in representing the spatial variation of SMC. This study demonstrates the applicability of georeferenced EMI in accurately representing SMC in boreal podzolic soils in an eco-friendly manner. It also reinforces the ongoing effort of converting natural forests into managed agricultural lands for increasing agricultural production.

Acknowledgements

My gratitude to the Almighty God for his countless blessings, to be able to complete my MSc program. First, I would like to thank my advisor, Dr. Lakshman Galagedara for inviting me to work on this topic with his research team and my co-advisor, Dr. Mano Krishnapillai, for his purposeful advice and encouragement throughout my programme and Dr. Yeukai Katanda, and Dr. Dmitry Sveshnikov as the advisory committee member for their supports and comments.

I equally thank my colleagues of the Hydrology & Agrophysics Group for their help and constructive comments during my thesis research. Special thanks to the Natural Science and Engineering Research Council Discovery Grant (NSERC-DG: RGPIN-2019-04614), Industry, Energy and Technology of the Government of NL (IET Grant: 5404-1962-102) for the financial support and to Memorial University of Newfoundland, School of Science and the Environment, Grenfell Campus of Memorial University, Canada for their support to executing all experiments.

I am also grateful to my friends in Corner Brook particularly Dragan Bruce Malesevic and Albert Sey.

I specially thank all my family members, my parents Mr. Victor and Mrs. Ethel Mensah, my siblings Victor Mensah (Jnr), Darlington Mensah and Sylvester Mensah for their support and encouragement. I also want to thank my special friend Princess Ntim Boateng for her support and understanding.

Clinton Mensah.

Table of Contents

List of tables

List of figures

List of abbreviations

ANOVA - Analysis of variance

BD - Bulk density

CV - Coefficient of variation

DOI - Depth of investigation

dSm^{-1} - DeciSiemens per meter

ECa - Soil apparent electrical conductivity

ECa-38kHz – GEM-2 horizontal coplanar (HCP) configuration

EC25 - Temperature corrected ECa

EMI - Electromagnetic induction

GIS - Geographic information system

GPR - Ground penetrating radar

HCP - Horizontal coplanar

Hp - Primary magnetic field at the receiver coil

Hs - Secondary magnetic field at the receiver coil

KHz - Kilohertz

LCCC - Lin's Concordance Correlation Coefficient

Max Temp - Maximum temperature

Min Temp - Minimum temperature

MC - Multi-coil

MC-EMI HCP 1 - CMD Mini-explorer horizontal coplanar (VCP) configuration for coil 1

MC-EMI HCP 2 - CMD Mini-explorer horizontal coplanar (VCP) configuration for coil 2

MC-EMI HCP 3 - CMD Mini-explorer horizontal coplanar (VCP) configuration for coil 3

MC-EMI VCP 1 - CMD Mini-explorer vertical coplanar (VCP) configuration for coil 1

MC-EMI VCP 2 - CMD Mini-explorer vertical coplanar (VCP) configuration for coil 2

MC-EMI VCP 3 - CMD Mini-explorer vertical coplanar (VCP) configuration for coil 3

MF - Multi-frequency

MLR - Multiple linear regression

MS_a - apparent magnetic susceptibility

n - number of samples

NL - Newfoundland

PD(s) - Pseudo-depth(s)

PET - Potential evapotranspiration

R^2 - Coefficient of determination

RMSE - Root mean square error

Rx – Receiver coil

SMC – Soil moisture content

SOM - Soil organic matter

SE - Standard Error

Std Dev - Standard deviation

t - Measured soil temperature (°C)

TDR - Time domain reflectometry

Tx – Transmitter coil

VIF – Variance inflation factor

VCP - Vertical coplanar

CHAPTER ONE: Introduction

1.1 Background and rationale

Agriculture in the Boreal region is perceived as low intensity, marginal, and insufficient to satisfy the local community's needs. However, this region possesses an unexploited ability to contribute to the global food system by increasing the local food supply (Unc et al. 2021). Considering this, the provincial government of Newfoundland and Labrador (NL) has outlined plans to convert substantial areas of boreal forests into agricultural land as part of the "The Way Forward on Agriculture Initiative" to increase food production (Government of NL 2017).

Converting natural forests to agricultural lands in NL requires intensive long-term soil management practices due to the poor inherent fertility of the predominant coarse to medium textured podzols that limits the food production in the province. Podzols cover approximately 55% of the landmass in NL (Sanborn et al. 2011). They are acidic and have low nutrient status (Enakiev et al. 2018), however, their quality can be improved through practices including, but not limited to, the addition of organic matter and the use of fertilizers.

Soil properties, such as apparent electrical conductivity (EC_a) (Badewa et al. 2018), soil organic matter (SOM) content (Atwell and Wuddivira 2019), and water holding capacity (Adejuwon 1988) naturally vary with land use (Wilson et al. 2011), prevailing temperature and precipitation, (Dale 1987;) and soil type (Wilson et al. 2008). The conversion of natural forest land to agricultural fields also introduces spatial and temporal variability in these soil properties (Atwell and Wuddivira

2019; Niu et al. 2015), which if not monitored, could affect crop planning, and reduce crop yields and return. Furthermore, such conversion induces environmentally damaging effects such as erosion, degradation in air and water quality and a reduction in carbon sequestration.

Quantifying soil properties involves monitoring and understanding the spatial distribution of soil properties, which is crucial in controlling a land's hydrological and ecological function. In the past, landscape mapping of soil properties to monitor and understand the spatial distribution of soil properties was executed employing techniques from the conventional National Cooperative Soil Survey yet these maps lacked adequate detail and precision (Batte 2000; Brevik et al. 2000). Conversely, grid mapping was regarded as an accurate method to map the spatial distribution of surface soil properties across a landscape; however, this technique also proved to be time-consuming and expensive (Burrough et al. 1971). Conventional methods used for mapping surface soil properties have demonstrated their limitations in current research, primarily because they are insufficient when it comes to cover larger areas and exploring deeper soils depths. As a result, these methods are time-consuming and failed to provide a complete overvies of soil composition across large areas. In order to attain a more precise comprehension of soil composition, it is imperative to adopt more comprehensive sampling procedures. Geophysical techniques have emerged as the favoured method of soil mapping due to their ability penetrate deeper into the soil and collect samples over larger area in a less destructive way.

These techniques include ground penetrating radar (GPR), capacitance probes (CPs), active microwaves (AM), passive microwaves (PM), neutron thermalization, nuclear magnetic resonance

(NMR), gamma-ray attenuation, near-surface seismic reflection, aerial photography, self-potential, time domain reflectometry (TDR), and electromagnetic induction (EMI) (Corwin 2008). These techniques employ different operating principles, perform at various scales, and can differentiate individual soil series with high accuracy (Brevik et al. 2006; Binley et al. 2015; Romero-Ruiz et al. 2018).

Geophysical techniques that utilize electromagnetic waves at different frequencies (GPR and EMI) have the added advantage of collecting real-time, high-resolution soil data, non-invasively (Corwin and Lesch 2003). Thus, these techniques can be used to monitor the impacts of conversion of natural forests into managed agricultural lands in regions where the soil is less fertile, such as Newfoundland and the world at large. EMI is favored over GPR due to its speed of data collection (no contact with the ground), relatively low destructive nature, and its ability to collect data in rough terrains, such as wooded areas (Allred et al. 2008; Doolittle and Brevik 2014; Triantafilis and Santos 2013). Apparent electrical conductivity (EC_a) and apparent magnetic susceptibility (MS_a) maps generated from the EMI technique is another option for displaying a high-resolution soil information which is quantitative and can improve understanding of soil distributions (Corwin and Lesch 2003; Geonics 2005). This technique is sensitive in detecting changes in soil properties that are influenced by electrical conductivity (McNeill 1980; Von Hebel et al. 2019; Wang et al. 2021). Lastly, most EMI sensors are lightweight compared to the GPR devices. This has given rise to the production of several commercial EMI sensors. These sensors include but are not limited to the DUALEM-1 and DUALEM-2 meters (Dualem Inc., Milton, Ontario), the profiler EMP-400

(Geophysical Survey Systems Inc., Salem, New Hampshire) and the EM31, EM38, EM38-DD, and EM38-MK2 meters (Geonics Limited, Mississauga, Ontario). The introduction of the multi-coil and multi-frequency EMI sensors as elaborated in Section 1.4 has also proved well suited for soil studies (Doolittle and Brevik 2014; Badewa 2018; Sadatcharam 2019; Altdorf 2020).

The EMI technique has some limitations, such as its inability to work efficiently in all soil environments (Doolittle and Collins 1998) due to the heterogenic nature of soils. The heterogenic nature of soils results in weak relationships between EC_a derived from EMI and the targeted soil properties (Doolittle et al. 2000). The sensitivity of EMI to interferences from close-by features like temperature (Allred et al. 2008), power lines and pumps also affects its use in soil characterization (Schumann and Zaman 2003). Although, the theoretical values of the depth of explorations based on the inter-coil spacing in the EMI technique has been established by McNeill (1980), there are always deviations in the penetration associated with specific land use (Mansourian 2020).

In soil studies, EMI sensors measure the EC_a (Altdorff and Dietrich 2014). EC_a is the depth weighted average of the bulk soil electrical conductivity within a soil volume (Greenhouse and Slaine, 1983; McNeill, 1980) and is influenced by other soil information directly related to crop production, plant growth and the general health of the soil (Kaffka et al. 2005). EC_a is considered a proxy of soil properties (McNeill 1980; Greenhouse and Slaine, 1983), including soil moisture, soil salinity, soil texture, bulk density (BD), SOM and porosity (Niu et al. 2015; Badewa 2018;

Atwell and Wuddivira 2019; Sadatcharam 2019; Altdorf 2020). Recent technological advancements have created accurate field-scale geo-referenced EC_a maps obtained from the combination EMI sensors and global positioning systems (Corwin and Lesch 2019). Geostatistics can be used to analyze soil data and create a raster map to improve soil mapping (Tarr et al. 2005; Medhioub et al. 2019; Dakak et al. 2023). Geostatistical models characterize and interpret the spatial relations of the measured soil property from the sampled data to predict the values of variables at unsampled locations (Goovaerts 1999).

Geostatistics is a branch of statistics that is concerned with the spatial analysis of data. It is employed to analyze and model spatial data, for instance soil properties, in order to gain a better comprehension of the spatial patterns of the data. Tobler's Laws of Geography, which describe the spatial relationships between geographical features, can be utilized in soil studies to comprehend the spatial patterns of soil properties, such as soil texture, organic matter content, and nutrient availability. By understanding the spatial patterns of soil properties, soil scientists can more effectively comprehend how soil properties vary across a landscape and how they may be influenced by environmental factors. This knowledge can then be utilized to inform soil management decisions and to enhance soil fertility and productivity.

Soil properties, such as EC_a and soil moisture, which display continuous spatial variability, are a suitable fit for geostatistical analysis methods since observations that are close to each other are more similar than those that are further apart (Goovaerts 1997). Tarr et al. (2005), Buta et al. (2019),

Kostić et al. (2021) among others have incorporated collecting georeferenced EMI data and interpolating these data using geostatistical techniques such as kriging, cokriging and inverse distance to power method to exhibit good overall fit to the soil surveys. The SURFER® software (Golden, CO, the USA.) is a tool that can be used to implement geostatical techniques (Brevik 2001; Afrizal et al. 2013; Ganjegunte et al. 2014).

Since variations in EC_a measurements are a proxy for several soil properties that are influenced by changes in land use conditions, this study investigates the spatial variability of geo-referenced EC_a data as an effective means to characterize soil properties under different land use conditions. Furthermore, the study investigates two interpolation techniques (ordinary kriging and cokriging) to assess the effectiveness of EC_a as an auxiliary variable in predicting soil moisture variations under different land use conditions. This goal supports the ongoing effort to convert the natural forests into managed agricultural lands for increasing agricultural production.

1.2 Thesis objectives and hypotheses

The utilization of EMI sensors in soil studies remains a relatively unexplored area of research, particularly as it relates to boreal podzolic soils. To date, much of the research has been limited to examining the relationship between soil parameters and EC_a measurements from the MC or MF EMI sensors under a single land use condition. Furthermore, the overall accuracy and efficacy of utilizing integrated EC_a measurements to detect changes in soil moisture, SOM, BD and texture over time has yet to be fully determined. As such, further research is needed to identify the optimal

combination of EMI sensors for accurately measuring soil properties and to bridge the existing knowledge gaps.

In order to address this issue, a unique approach involving the use of EC_a measurements from MC and MF EMI sensors as well as kriging approaches is proposed. This research is expected to provide valuable insights on the accuracy of the MC and MF EMI methods in estimating SMC response to land use changes thus serving as an effective tool in conservation and environmental protection. Ultimately, continued research into EMI for soil studies is essential to fully understand the scope of its applications.

The key objectives of the study were to:

i. utilize multi-frequency EMI in characterizing soil moisture under different land uses in western Newfoundland's podzolic soils.
ii. use multi-frequency and multi-coil electromagnetic induction sensors to improve soil moisture prediction accuracy in different land use.

The hypothesis proposed in this study was that EC_a could vary with changes in soil properties such as soil moisture, SOM, BD, and texture that are affected by a change in land use conditions and can be used as a proxy for these properties based on the relation between EC_a and these targeted soil properties. If these variations can be measured and mapped rapidly and non-destructively employing integrated EMI methods, it will allow for the development of site-specific management practices.

1.3 Thesis organization

The thesis is structured in a manuscript style and divided into four chapters. The thesis has a general introduction chapter, two stand-alone chapters (manuscript format) and the last chapter (chapter four) as a general discussion and conclusion.

Chapter one: This is the general introduction chapter of the thesis. It provides the overview with background information, rationale, objectives and hypothesis of the thesis.

Chapter two: This is the literature review. It encompasses review of relevant literature on basic electromagnetic induction theory, time-domain reflectometry and the soil properties being investigated in the thesis using EMI.

Chapter three (study one): "Multi-frequency electromagnetic induction soil moisture characterization under different land uses in western Newfoundland". EC_a employed in this study were obtained from the multi-frequency EMI device. The chapter evaluates the field scale accuracy of the TDR meter by comparing it with the oven drying method and generates site-specific EC_a - soil moisture regression models. This chapter has been accepted for publication in the Canadian Journal of Soil Science.

Chapter four (study two): "**Using multi-frequency and multi-coil electromagnetic induction sensors to improve soil moisture prediction accuracy in different land use**". This study investigates the effectiveness of EC_a obtained from the multi-coil (CMD Mini-explorer) and multi-frequency (GEM-2) EMI sensors to maximize the representation of soil moisture taking into consideration SOM, BD and soil texture using a statistical and geostatistical methods. The study also confirms the efficiency of EC_a as a surrogate for the soil properties.

Chapter five: The chapter presents an overall discussion about study findings, conclusion and provides recommendations for further studies.

1.4 References

Adejuwon, J.O. and Ekanade, O., 1988. A comparison of soil properties under different land use types in a part of the Nigerian cocoa belt. Catena, 15(3-4), pp.319-331.

Afrizal, R. and Masunaga, T., 2013. Assessment erosion 3D hazard with USLE and surfer tool: a case study of Sumani Watershed in West Sumatra Indonesia. Journal of Tropical Soils, 18(1), pp.81-92.

Allred, B.J., Ehsani, M.R. and Daniels, J.J., 2008. General considerations for geophysical methods applied to agriculture. Handbook of Agricultural Geophysics, pp.3-16.

Altdorff, D. and Dietrich, P., 2014. Delineation of areas with different temporal behavior of soil properties at a landslide affected Alpine hillside using time-lapse electromagnetic data. Environmental Earth Sciences, 72, pp.1357-1366.

Altdorff, D., Sadatcharam, K., Unc, A., Krishnapillai, M. and Galagedara, L., 2020. Comparison of multi-frequency and multi-coil electromagnetic induction (EMI) for mapping properties in shallow podzolic soils. Sensors, 20(8), pp.2330.

Atwell, M.A. and Wuddivira, M.N., 2019. Electromagnetic-induction and spatial analysis for assessing variability in soil properties as a function of land use in tropical savanna ecosystems. SN Applied Sciences, 1(8), pp.856.

Badewa, E., Unc, A., Cheema, M., Kavanagh, V. and Galagedara, L., 2018. Soil moisture mapping using multi-frequency and multi-coil electromagnetic induction sensors on managed podzols. Agronomy, 8(10), pp.224.

Batte, M.T., 2000. Factors influencing the profitability of precision farming systems. Journal of Soil and Water Conservation, 55(1), pp.12-18.

Binley, A., Hubbard, S.S., Huisman, J.A., Revil, A., Robinson, D.A., Singha, K. and Slater, L.D., 2015. The emergence of hydrogeophysics for improved understanding of surface soil processes over multiple scales. Water Resources Research, 51(6), pp.3837-3866.

Brevik, E.C., Fenton, T.E. and Lazari, A., 2006. Soil electrical conductivity as a function of soil water content and implications for soil mapping. Precision Agriculture, 7, pp.393-404.

Brevik, E.C., 2000. A comparison of soil properties in compacted versus non-compacted Bryant soil series twenty-five years after compaction ceased. Soil Survey Horizons, 41(2), pp.52-58.

Burrough, P.A., Beckett, P.H.T. and Jarvis, M.G., 1971. The relation between cost and utility in soil survey (i–iii) 1. Journal of Soil Science, 22(3), pp.359-394.

Buta, M., Paulette, L., Man, T., Bartha, I., Negruşier, C. and Bordea, C., 2019. Spatial assessment of soil salinity by electromagnetic induction survey. Environmental Engineering and Management Journal (EEMJ), 18, pp.2073-2081

Corwin, D.L. and Scudiero, E., 2019. Mapping soil spatial variability with apparent soil electrical conductivity (ECa) directed soil sampling. Soil Science Society of America Journal, 83, pp.3-4.

Corwin, D.L. and Lesch, S.M., 2003. Application of soil electrical conductivity to precision agriculture: theory, principles, and guidelines. Agronomy Journal, 95(3), pp.455-471.

Corwin, D.L., 2008. Past, present, and future trends in soil electrical conductivity measurements using geophysical methods. Handbook of Agricultural Geophysics, pp.17-44.

Dakak, H., Dekkaki, H.C., Zouahri, A., Moussadek, R., Iaaich, H., Yachou, H., Ghanimi, A. and Douaik, A., 2023. Soil salinity prediction and mapping using electromagnetic induction and spatial interpolation. Environmental Sciences Proceedings, 16(1), pp.76.

Dale, V.H., 1997. The relationship between land-use change and climate change. Ecological Applications, 7(3), pp.753-769.

Doolittle, J., Noble, C. and Leinard, B., 2000. An electromagnetic induction survey of a riparian area in southwest Montana. Soil Survey Horizons, 41(2), pp.27-36.

Doolittle, J.A. and Brevik, E.C., 2014. The use of electromagnetic induction techniques in soils studies. Geoderma, 223, pp.33-45.

Doolittle, J.A. and Collins, M.E., 1998. A comparison of EM induction and GPR methods in areas of karst. Geoderma, 85(1), pp.83-102.

Enakiev, Y.I., Bahitova, A.R. and Lapushkin, V.M., 2018. Microelements (Cu, Mo, Zn, Mn, Fe) in corn grain according to their availability in the fallow SOD-Podzolic soil profile. Bulgarian Journal of Agricultural Science, 24(2), pp.285-289.

Ganjegunte, G.K., Sheng, Z. and Clark, J.A., 2014. Soil salinity and sodicity appraisal by electromagnetic induction in soils irrigated to grow cotton. Land Degradation and Development, 25(3), pp.228-235.

Geonics, 2005. EM38. Available from: http://www.geonics.com/html/em38.html (Accessed 17 February 2005).

Goovaerts, P., 1999. Using elevation to aid the geostatistical mapping of rainfall erosivity. Catena, 34(3-4), pp.227-242.

Government of Newfoundland and Labrador, 2017. The Way Forward on Agriculture. Sector Work Plan. Retrieved 20 Nov. 2021. From https://www.gov.NF.ca/ffa/files/agriculture-Sector-Workplan_Final.pdf

Greenhouse, J.P. and Slaine, D.D., 1983. The use of reconnaissance electromagnetic methods to map contaminant migration: These nine case studies can help determine which geophysical techniques are applicable to a given problem. Groundwater Monitoring and Remediation, 3(2), pp.47-59.

Kaffka, S.R., Lesch, S.M., Bali, K.M. and Corwin, D.L., 2005. Site-specific management in salt-affected sugar beet fields using electromagnetic induction. Computers and Electronics in Agriculture, 46(1-3), pp.329-350.

Kostić, M., Rajković, M., Ljubičić, N., Ivošević, B., Radulović, M., Blagojević, D. and Dedović, N., 2021. Georeferenced tractor wheel slip data for prediction of spatial variability in soil physical properties. Precision Agriculture, 22(5), pp.1659-1684.

Mansourian, D., Cornelis, W. and Hermans, T., 2020. Exploring Geophysical Methods for Mapping Soil Strength in Relation to Soil Compaction. Master's thesis. Ghent University.

McNeill, J.D., 1980. Applications of transient electromagnetic techniques Missasauga, ON, Canada: Geonics Limited. pp.17.

Medhioub, E., Bouaziz, M. and Bouaziz, S., 2019. Spatial estimation of soil organic matter content using remote sensing data in southern Tunisia. In Advances in Remote Sensing and Geo Informatics Applications: Proceedings of the 1st Springer Conference of the Arabian Journal of Geosciences (CAJG-1), Tunisia 2018 Springer International Publishing, pp. 215-217.

Niu, C.Y., Musa, A. and Liu, Y., 2015. Analysis of soil moisture condition under different land uses in the arid region of Horqin sandy land, northern China. Solid Earth, 6(4), pp.1157-1167.

Romero-Ruiz, A., Linde, N., Keller, T. and Or, D., 2018. A review of geophysical methods for soil structure characterization. Reviews of Geophysics, 56(4), pp.672-697.

Sadatcharam, K., 2019. Assessing potential applications of multi-coil and multi-frequency electromagnetic induction sensors for agricultural soils in western Newfoundland. Master's thesis. Memorial University of Newfoundland.

Sanborn, P., Lamontagne, L. and Hendershot, W., 2011. Podzolic soils of Canada: Genesis, distribution, and classification. Canadian Journal of Soil Science, 91(5), pp.843-880.

Schumann, A.W. and Zaman, Q.U., 2003. Mapping water table depth by electromagnetic induction. Applied Engineering in Agriculture, 19(6), pp.675.

Tarr, A.B., Moore, K.J., Bullock, D.G., Dixon, P.M. and Burras, C.L., 2005. Improving map accuracy of soil variables using soil electrical conductivity as a covariate. Precision Agriculture, 6(3), pp.255-270.

Triantafilis, J. and Santos, F.M., 2013. Electromagnetic conductivity imaging (EMCI) of soil using a DUALEM-421 and inversion modelling software (EM4Soil). Geoderma, 211, pp.28-38.

Unc, A., Altdorff, D., Abakumov, E., Adl, S., Baldursson, S., Bechtold, M., Cattani, D.J., Firbank, L.G., Grand, S., Guðjónsdóttir, M. and Kallenbach, C., 2021. Expansion of agriculture in northern cold-climate regions: a cross-sectoral perspective on opportunities and challenges. Frontiers in Sustainable Food Systems, 5, pp.663448.

Von Hebel, C., Van Der Kruk, J., Huisman, J.A., Mester, A., Altdorff, D., Endres, A.L., Zimmermann, E., Garré, S. and Vereecken, H., 2019. Calibration, conversion, and quantitative multi-layer inversion of multi-coil rigid-boom electromagnetic induction data. Sensors, 19(21), pp.4753.

Wang, F., Yang, S., Wei, Y., Shi, Q. and Ding, J., 2021. Characterizing soil salinity at multiple depth using electromagnetic induction and remote sensing data with random forests: A case study in Tarim River Basin of southern Xinjiang, China. Science of the Total Environment, 754, pp.142030.

Wilson, B.R., Growns, I. and Lemon, J., 2008. Land-use effects on soil properties on the north-western slopes of New South Wales: implications for soil condition assessment. Soil Research, 46(4), pp.359-367.

CHAPTER TWO: Literature review

2.1 Electromagnetic induction

EMI has been used successfully to estimate soil water variability at field and landscape scales (Corwin 2008; Toushmalani 2010; Calamita et al. 2015; Shanahan et al. 2015; Martini et al. 2017). Michael Faraday first introduced the principle of EMI in the early 19th century. This principle is embedded into a wide range of sensors for soil mapping. The EMI sensor sends an alternating current at set frequency(ies), generating a primary magnetic field via its transmitter coil. This primary magnetic field propagates through the soil and induces an eddy current loop in the soil with the magnitude of these loops directly proportional to the electrical conductivity (EC) in the locality of the loop. The induced eddy current on the conductors now radiates a secondary electromagnetic field proportional to the current flowing within the loop. The eddy current radiates the secondary electromagnetic field by combining the inter-coil space covered by the magnetic field, the frequency of the applied current and the ability of the soil around the sensor to conduct electricity (Gebbers et al. 2007; Hendrickx and Kachanoski 2002). The mode of operation of the EMI (Figure 2.1). The ratio of the primary and secondary magnetic fields measured at the receiver coil (McNeill 1980) is the EC_a (Corwin 2008) (Equation 2.1).

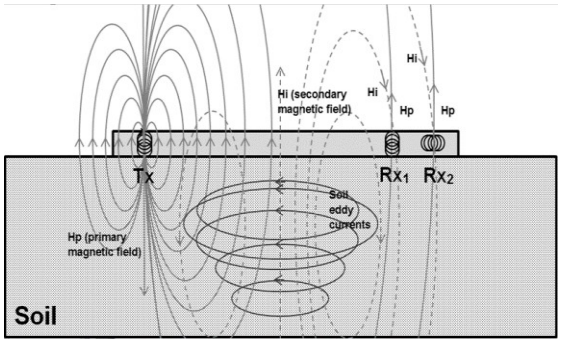

Figure 2.1: Schematic view of EMI operating principles. Tx is the transmitter coil and Rx is the receiver coil (Visconti et al. 2016).

$$EC_a = \frac{4}{\omega \mu o\, S^2}\left(\frac{Hs\ (quadrature)}{Hp}\right) \qquad \text{Equation 2.1}$$

Where (Hs/Hp) is the ratio of the out-of-phase secondary to primary magnetic fields.

Hs = Secondary magnetic field at the receiver coil

Hp = Primary magnetic field at the receiver coil

EC_a = Apparent electrical conductivity

$\omega = 2\pi f$ – angular frequency

f = Frequency (30 kHz for CMD-miniexplorer; 2.8, 18.8, 38.3, 80 kHz for GEM-2)

μ_o = Permeability of free space

S= Inter-coil spacing (m)

Understanding the integrated response of the measurement of EMI involves if the current loops generated below the ground are not affected (McNeill 1980). This assumption results in Equations 2.2 and 2.3 for horizontal and vertical dipole configurations respectively:

$$\varphi\ H(z) = 2 - \frac{4z}{(4z^2+1)^{0.5}} \qquad \text{Equation 2.2}$$

$$\varphi\ \mathrm{V}\ (z) = \frac{4z}{(4z^2+1)^{1.5}} \qquad \text{Equation 2.3}$$

where $\varphi\ H(z)$ and $\varphi\ \mathrm{V}\ (z)$ are the sensitivity function of the EMI sensor (vertical coplanar (VCP) and horizontal coplanar (HCP) modes, respectively) with depth and z is the depth (cm) from the soil surface.

2.1.1 Electromagnetic induction sensors

The CMD Mini-explorer and GEM-2 are commercially available EMI sensors that can measure EC_a reading at depth intervals (Badewa et al. 2018; Sadatcharam et al. 2019; Altdorff et al. 2020).

2.1.1.1 CMD Mini-explorer

The CMD Mini-explorer is a multi-coil EM sensor that operates at 30 kHz frequency and consists of a probe and a handheld control unit. The control unit communicates with the probe through Bluetooth. This EMI sensor has a single transmitter coil and three receiver coils. The inter-coil spacing between the transmitter and receiver coils are 32 cm, 71 cm, and 118 cm. The coils can be oriented in low or high depth range under the VCP or HCP coil configuration (Figure 2.2). In the VCP mode, the sensor can simultaneously sense up to 25, 50 and 90 cm integral depths. In the HCP

mode, the sensor can simultaneously sense up to 50, 100, and 180 cm integral depths (Altdorff et al. 2016). The sensor has a temperature stability of ±1 mS/m per 10°C change in temperature and is suited to outside temperatures between -10°C and +50°C (GF-Instruments 2011).

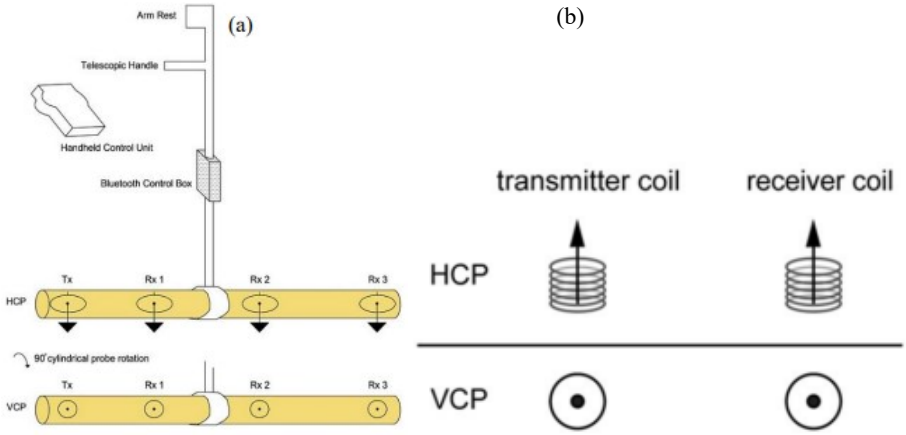

Figure 2.2: The schematic diagram of CMD Mini-explorer at low (VCP) and high (HCP) coil orientations showing the positions of the transmitter coil (Tx), receiver coils (Rx), coil geometry, spacing and orientation (modified from Bonsall et al. 2013).

2.1.1.2 GEM-2

The GEM-2 is a lightweight, digital multi-frequency EM sensor with a single transmitter and receiver coil (Tang et al. 2018; Won et al. 1996). The sensor consists of a ski that encloses all sensing elements, an electronics enclosure that plugs onto the ski, a detachable windows-based display assistant known as IPaq and an external GPS connector. The sensor operates within a frequency range of 0.3 kHz to 90 kHz (Sadatcharam 2019). The sensor has a factory set frequency

file that can be modified to a set of desired frequencies (Geophex Ltd. 2004). The inter-coil spacing between the transmitter and receiver coil is 166 cm. The MF sensor has a bucking coil located at approximately 1 m from the transmitter coil. The bucking coil cuts off the primary field from the receiver sensor (Minsley et al. 2012; Simon et al. 2015). Although the MF sensor allows the user to select multiple frequencies, selecting too many frequencies lowers the resolution (Sadatcharam et al. 2019; Altdorff et al. 2020). The magnitude of the selected operating frequency is inversely proportional to the depth of investigation (DOI); thus; the higher the selected operating frequency, the shallower the DOI. A higher frequency, however, gives a high resolution of the mapped area. The GEM-2 sensor can operate in both HCP and VCP coil configurations (Figure 2.3). Comparatively, the MF sensor can operate at low frequencies hence possesses a higher DOI, whiles, the MC sensor has also been seen to be better suited for detecting small metallic objects in the shallow surface soil (Sadatcharam 2019).

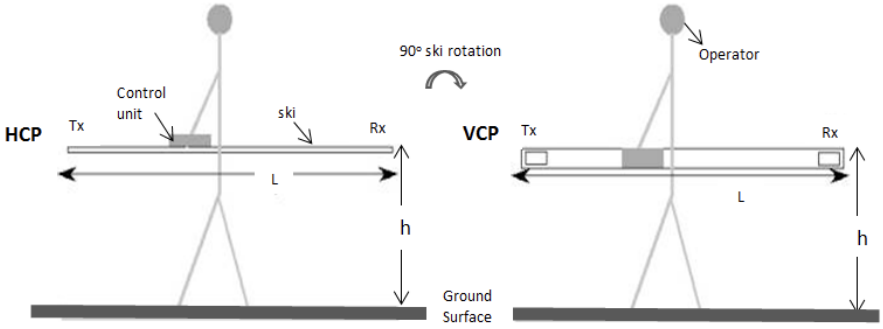

Figure 2.3: The schematic diagram of GEM-2 at low (VCP) and high (HCP) coil orientations (Bonsall et al. 2013).

2.2 Time-domain reflectometry (FieldScout TDR 350)

The underlying principle of TDR involves measuring the travel time of an electromagnetic wave along a waveguide (Figure 2.4). The speed of transmitted wave depends on the soil matrix's bulk dielectric permittivity (Roberto and Guida 2006). TDR measures a soil matrix's volumetric soil moisture content (θv). This θv measured by TDR is an average over the length of the waveguide. Electronics in the FieldScout TDR 350 generate and sense the two-way travel of a high-energy signal through soil, along the instrument's waveguides. The high energy signal information is then converted to θv.

Figure 2.4: The schematic diagram of FieldScout TDR 350 (IMKO 2016).

2.3 Relation between apparent electrical conductivity and desired soil properties

2.3.1 Apparent electrical conductivity

The theoretical foundation relating EC_a and soil properties was developed by Rhoades et al. (1989). The main soil properties that determine EC_a measurements are soil moisture, soil salinity, the

amount of clay in a soil (texture), cation exchange capacity (CEC) and temperature (McNeil 1980; Friedman 2005). Other soil properties associated with EC_a are BD, SOM, soil nutrients and the concentration of ions in a solution (Friedman 2005).

Although, studies have shown soil moisture, soil texture, SOM and soil BD to correlate with EC_a measurements within and across field(s) (Corwin and Lesch 2005), the correlation between EC_a and soil properties is site-specific dependent and is affected by different agronomic practices such as irrigation, tillage, manure application and compaction (Altdorff et al. 2017). EC_a is also affected by porosity, saturation, pore water electrical conductivity. Based on this, Archie (1942) developed an equation used to express the impact of partial saturation on bulk electrical conductivity (σ) (Equation 2.4).

$$\sigma = \varphi^m S^n{}_w \sigma_w \qquad \text{Equation 2.4}$$

where φ is the porosity, S is the saturation and σ is the pore water electrical conductivity. The exponents m and n account for the contribution related to the soil structural form. However, this equation ignores surface conductivity (Revil et al. 2017). Hence, site-specific calibration of EC_a is needed when using EC_a to accurately characterize soil properties (Reedy and Scanlon 2003). An overview of the desired soil properties is given in the next section.

2.3.2 Soil moisture content

Electric current flow within a soil mainly depends on water content, making soil moisture the most crucial soil property influencing EC_a (Brevik and Fenton 2002; Huth and Poulton 2007). Doolittle et al. (1994) indicate that the flow of water down the soil produces pathways for the flow of electric current due to charge displacement from the water molecules. In wet soils, increased chemical reactions and current flow results in a high EC_a values and more contributions from other soil properties (Brevik et al. 2006). On the other hand, chemical reactions and current flow tend to seize in arid soils and influence EC_a (Johnson et al. 2001). Soil moisture varies spatially and temporally in a field and when it is mapped repeatedly on the field, there would be locations that consistently record higher or lower soil moisture values relative to the average soil moisture of the study area (Starr 2005; Guber et al. 2008). This is known as temporal stability in the spatial patterns of the soil moisture (Tallon and Si 2004) and has been correlated to with other soil properties such as soil particle distribution (Starr 2005). The temporal stability in the spatial patterns of soil moisture is crucial in delineating management zones when converting from natural land to managed agricultural land (Starr 2005). A compilation of additional relevant literature measuring soil moisture with EC_a are shown in Table 2.1.

Table 2.1 Compilation of additional relevant literature measuring soil moisture with apparent electrical conductivity

List of additional relevant literature measuring soil moisture with apparent electrical conductivity
De Benedetto et al. (2013); Guo et al. (2016); Pognant et al. (2013); Wunderlich et al. (2013); Chrétien et al. (2014); Gooley et al. (2014); Liao et al. (2014); Misra and Padhi (2014); Fortes et al. (2015); Shanahan et al. (2015); Stadler et al. (2015); Walter et al. (2015); Cho et al. (2016); Neely et al. (2016); Pedrera-Parrilla et al. (2016); Altdorff et al. (2018); Lu et al. (2017); Moghadas et al. (2017); Al Rashid et al. (2018); Rallo et al. (2018); Nocco et al. (2019)

2.3.3 Soil texture

Soil texture represents the relative proportion of clay, sand, and silt in soil (Wang et al. 2010). Clay particles possess a higher ability to retain soil moisture and dissolved solids due to a larger surface area. Hence, they generally have a high EC relative to sand and silt particles (Grisso et al. 2005). In a study by Brevik et al. (2006), the authors indicated wet conditions as the optimal environment for EC_a to distinguish soil types. However, Sudduth et al. (2003) cited that a different result could be expected due to the complex nature of clay-rich soils, highlighting the importance of testing EC_a in wet and dry soils. Soil texture can be determined in the laboratory or in the field. In the laboratory, the hydrometer and pipette methods are the ways to meaure soil texture, the pipette method is more complicated yet precise relative to the hydrometer methods (Wang et al. 2010). On the field, soil texture is determined by hand texturing techniques (Wang et al. 2010). However, both methods are time-consuming and require skilled labor (Wang et al. 2010). EC_a has been used

as a rapid way to determine soil texture variations (Brevik 2006). Soil texture mainly contributes to EC in non-saline soil (Lund 1999; Corwin and Lesch 2005). Soil texture has also been seen to change over time (Kelley 2017). Agricultural practices such as tillage and fertilization due to a change in land use conditions can hasten these changes to be significant over short timeframes (Kelley 2017). A compilation of additional relevant literature measuring soil texture with EC_a are shown in Table 2.2.

Table 2.2 Compilation of additional relevant literature measuring soil texture with apparent electrical conductivity

List of relevant literature measuring soil texture with apparent electrical conductivity
Heil and Schmidhalter (2012); Islam et al. (2012); Mahmood et al. (2012); Nearing et al. (2013); Piikki et al. (2013); Pan et al. (2014); Ciampalini et al. (2015); Pozdnyakov et al. (2015); Rodríguez et al. (2015); Rodrigues Jr. et al. (2015); Stadler et al. (2015); Stepień et al. (2015); Moghadas et al. (2016); Filho et al. (2017); Ganjegunte et al. (2017); García-Tomillo et al. (2017); de Lima et al. (2017); Grubbs et al. (2019); Brogi et al. (2019)

2.3.4 Soil organic matter

SOM is an indicator of the overall health of the soil. Generally, SOM comprises of primary plant remains and decomposed organic compounds that have been combined into more complex molecules (humus) (Morris 2004). Some of the benefits of SOM include providing nutrients and habitat to soil organisms, and binding soil particles into aggregates which improves the water holding capacity of a soil (Polyakov and Lal 2004). Due to the complex structure and composition

of SOM with compounds containing various carbon functional groups (Shi et al. 2006), soil organic carbon is closely related to SOM and is used as an indicator of SOM. In the laboratory, SOM can be determined via the loss-on-ignition method, the Walkley-Black method, automated dry combustion, and humic matter methods. The loss-on-ignition method involves the thermal decomposition of SOM in a muffled furnace (Roper et al. 2019). The Walkley-Black method, Automated dry combustion and Humic matter methods are other techniques used to determine SOM (Roper et al. 2019).

Soils with high SOM tend to have high cation exchange capacity due to having a larger amount of exchange sites. Negatively charged surface attact cations removing them from the soil solution hence ECa is lower since the cations are bound soil colloid surfaces instead of being free in the soil solution. Additionally, SOM can increase the porosity of soil, which can also reduce EC_a. Finally, SOM can also act as a buffer, which can reduce the fluctuations in EC_a due to changes in soil moisture (Tipping 2002). Since SOM has been found to significantly influence EC_a (Martinez et al. 2009), EC_a can be used as a surrogate for SOM variations. Farming activities such as no-till systems, cover cropping and N fertilization due to land use conversion have also been seen to change the SOM significantly (Morris 2004; Sapkota et al. 2012). Past studies have revealed gaps in understanding the mechanisms of how SOM affects EC_a, the effects of different soil types on EC_a, and the effects of different management practices on EC_a. Additionally, there is a lack of data on the effects of SOM on EC_a in different climates and soil types. A compilation of additional relevant literature measuring SOM with EC_a are shown in Table 2.3.

Table 2.3 Compilation of additional relevant literature measuring soil organic matter with apparent electrical conductivity

List of relevant literature measuring soil organic matter with apparent electrical conductivity
Ekwue and Bartholomew (2011); Kweon et al. (2013); Koszinski et al. (2015); Peralta et al. (2015); Pozdnyakov et al. (2015); Altdorff et al. (2016); Huang et al. (2017); Grubbs et al. (2019); Uribeetxebarria et al. (2018); Nocco et al. (2019)

2.3.5 Bulk density

BD is a measure of the mass of soil per unit volume. It is an important factor in determining the EC_a of a soil because it affects the amount of water and air that can be held in the soil. Soils with higher BDs have lower porosities which reduces the ability of ions to move through the soil and decreases the EC_a. Conversely, soils with lower BDs have higher porosities, which increases the ability of ions to move through the soil and increases the EC_a. Changes in soil BD has been found to affect EC_a significantly (Brevik and Fenton 2002). When the BD of soil increases, more finer particles are packed into a unit volume of soil, increasing the contact between soil particles (Rhoades and Corwin 1990; Malicki et al. 1989). The hydraulic properties of a soil have been seen to vary due to changes in BD. Due to smaller pore spaces in compacted soil, little water is required to saturate a compacted soil compared to an uncompacted soil (Brevik and Fenton 2002). Differences in land-use management following land use conversion can alter the BD within a field or between fields that contain otherwise similar soils (Battikhi and Suleiman 1999). A compilation of additional relevant literature measuring BD with EC_a are shown in Table 2.4.

Table 2.4 Compilation of additional relevant literature measuring bulk density with apparent electrical conductivity

List of relevant literature measuring bulk density with apparent electrical conductivity
Ekwue and Bartholomew (2011); Kweon et al. (2013); Koszinski et al. (2015); Peralta et al. (2015); André et al. (2012); Naderi-Boldaji et al. (2014); Rossi et al. (2013); Al-Asadi and Mouazen (2014); Islam et al. (2014); Cho et al. (2016); Filho et al. (2017); Rashid et al. (2018)

Based on the above reviews, I hypothesize that EC_a can be used as a surrogate for the targeted soil properties under different land use conditions and have concluded to investigate the ability to employ an integrated EMI technique (combined MC and MF EMI sensors) to characterize the spatial variability of soil moisture, BD, SOM, and soil texture across three different land use conditions.

2.4 References

Adejuwon, J.O. and Ekanade, O., 1988. A comparison of soil properties under different land use types in a part of the Nigerian cocoa belt. Catena, 15(3-4), pp.319-331.

Afrizal, R. and Masunaga, T., 2013. Assessment erosion 3D hazard with USLE and surfer tool: a case study of Sumani Watershed in West Sumatra Indonesia. Journal of Tropical Soils, 18(1), pp.81-92.

Al-Asadi, R.A. and Mouazen, A.M., 2014. Combining frequency domain reflectometry and visible and near infrared spectroscopy for assessment of soil bulk density. Soil and Tillage Research, 135, pp.60-70.

Allred, B.J., Ehsani, M.R. and Daniels, J.J., 2008. General considerations for geophysical methods applied to agriculture. Handbook of Agricultural Geophysics, pp.3-16.

Altdorff, D. and Dietrich, P., 2014. Delineation of areas with different temporal behavior of soil properties at a landslide affected Alpine hillside using time-lapse electromagnetic data. Environmental Earth Sciences, 72, pp.1357-1366.

Altdorff, D., Bechtold, M., Van der Kruk, J., Vereecken, H. and Huisman, J.A., 2016. Mapping peat layer properties with multi-coil offset electromagnetic induction and laser scanning elevation data. Geoderma, 261, pp.178-189.

Altdorff, D., Sadatcharam, K., Unc, A., Krishnapillai, M. and Galagedara, L., 2020. Comparison of multi-frequency and multi-coil electromagnetic induction (EMI) for mapping properties in shallow podsolic soils. Sensors, 20(8), pp.2330.

Altdorff, D., von Hebel, C., Borchard, N., van der Kruk, J., Bogena, H.R., Vereecken, H. and Huisman, J.A., 2017. Potential of catchment-wide soil water content prediction using electromagnetic induction in a forest ecosystem. Environmental Earth Sciences, 76, pp.1-11.

André, F., Van Leeuwen, C., Saussez, S., Van Durmen, R., Bogaert, P., Moghadas, D., De Resseguier, L., Delvaux, B., Vereecken, H. and Lambot, S., 2012. High-resolution imaging of a vineyard in south of France using ground-penetrating radar, electromagnetic induction and electrical resistivity tomography. Journal of Applied Geophysics, 78, pp.113-122.

Archie, G.E., 1942. The electrical resistivity log as an aid in determining some reservoir characteristics. Transactions of the AIME, 146(01), pp.54-62.

Atwell, M.A. and Wuddivira, M.N., 2019. Electromagnetic-induction and spatial analysis for assessing variability in soil properties as a function of land use in tropical savanna ecosystems. SN Applied Sciences, 1(8), pp.856.

Badewa, E., Unc, A., Cheema, M., Kavanagh, V. and Galagedara, L., 2018. Soil moisture mapping using multi-frequency and multi-coil electromagnetic induction sensors on managed podzols. Agronomy, 8(10), pp.224.

Batte, M.T., 2000. Factors influencing the profitability of precision farming systems. Journal of Soil and Water Conservation, 55(1), pp.12-18.

Battikhi, A.M. and Suleiman, A.A., 1999. Effect of tillage system on soil strength and bulk density of vertisols. Journal of Agronomy and Crop Science, 183(2), pp.81-89.

Binley, A., Hubbard, S.S., Huisman, J.A., Revil, A., Robinson, D.A., Singha, K. and Slater, L.D., 2015. The emergence of hydrogeophysics for improved understanding of subsurface soil processes over multiple scales. Water Resources Research, 51(6), pp.3837-3866.

Brevik, E.C., Fenton, T.E. and Lazari, A., 2003. Differences in EM-38 readings taken above crop residues versus readings taken with instrument-ground contact. Precision Agriculture, 4, pp.351-358.

Brevik, E.C., Fenton, T.E. and Lazari, A., 2006. Soil electrical conductivity as a function of soil water content and implications for soil mapping. Precision Agriculture, 7, pp.393-404.

Brevik, E.C. and Fenton, T.E., 2002. Influence of soil water content, clay, temperature, and carbonate minerals on electrical conductivity readings taken with an EM-38. Soil Survey Horizons, 43(1), pp.9-13.

Brevik, E.C., 2000. A comparison of soil properties in compacted versus non-compacted Bryant soil series twenty-five years after compaction ceased. Soil Survey Horizons, 41(2), pp.52-58.

Brevik, E.C., 2001. Evaluation of selected factors that may influence the application of electromagnetic induction technology to soil science investigations in Iowa. Iowa State University.

Brogi, C., Huisman, J.A., Pätzold, S., Von Hebel, C., Weihermüller, L., Kaufmann, M.S., Van Der Kruk, J. and Vereecken, H., 2019. Large-scale soil mapping using multi-configuration EMI and supervised image classification. Geoderma, 335, pp.133-148.

Buol, S.W. and Stokes, M.L., 1997. Soil profile alteration under long-term, high-input agriculture. Replenishing Soil Fertility in Africa, 51, pp.97-109.

Buta, M., Paulette, L., Man, T., Bartha, I., Negruşier, C. and Bordea, C., 2019. Spatial assessment of soil salinity by electromagnetic induction survey. Environmental Engineering & Management Journal (EEMJ), 18(9), pp.2073-2081

Cho, Y., Sudduth, K.A. and Chung, S.O., 2016. Soil physical property estimation from soil strength and apparent electrical conductivity sensor data. Biosystems Engineering, 152, pp.68-78.

Chrétien, M., Lataste, J.F., Fabre, R. and Denis, A., 2014. Electrical resistivity tomography to understand clay behavior during seasonal water content variations. Engineering Geology, 169, pp.112-123.

Ciampalini, A., André, F., Garfagnoli, F., Grandjean, G., Lambot, S., Chiarantini, L. and Moretti, S., 2015. Improved estimation of soil clay content by the fusion of remote hyperspectral and proximal geophysical sensing. Journal of Applied Geophysics, 116, pp.135-145.

Corwin, D.L., 2008. Past, present, and future trends in soil electrical conductivity measurements using geophysical methods. Handbook of Agricultural Geophysics, pp.17-44.

Corwin, D.L. and Lesch, S.M., 2005. Apparent soil electrical conductivity measurements in agriculture. Computers and Electronics in Agriculture, 46(1-3), pp.11-43.

Corwin, D.L. and Lesch, S.M., 2003. Application of soil electrical conductivity to precision agriculture: theory, principles, and guidelines. Agronomy Journal, 95(3), pp.455-471.

Dakak, H., Dekkaki, H.C., Zouahri, A., Moussadek, R., Iaaich, H., Yachou, H., Ghanimi, A. and Douaik, A., 2023. Soil salinity prediction and mapping using electromagnetic induction and spatial interpolation. Environmental Sciences Proceedings, 16(1), pp.76.

Dale, V.H., 1997. The relationship between land-use change and climate change. Ecological Applications, 7(3), pp.753-769.

De Benedetto, D., Castrignanò, A., Rinaldi, M., Ruggieri, S., Santoro, F., Figorito, B., Gualano, S., Diacono, M. and Tamborrino, R., 2013. An approach for delineating homogeneous zones by using multi-sensor data. Geoderma, 199, pp.117-127.

De Souza Lima, E., Lovera, L.H., Montanari, R., De Souza, Z.M. and Torres, J.L.R., 2017. Spatial variability of apparent electrical conductivity and physicochemical attributes of the soil. Revista Cultura Agronômica, 26(3), pp.469-482.

Doolittle, J.A. and Collins, M.E., 1998. A comparison of EM induction and GPR methods in areas of karst. Geoderma, 85(1), pp.83-102.

Doolittle, J., Noble, C. and Leinard, B., 2000. An electromagnetic induction survey of a riparian area in southwest Montana. Soil Survey Horizons, 41(2), pp.27-36.

Doolittle, J.A. and Brevik, E.C., 2014. The use of electromagnetic induction techniques in soils studies. Geoderma, 223, pp.33-45.

Doolittle, J.A., Sudduth, K.A., Kitchen, N.R. and Indorante, S.J., 1994. Estimating depths to claypans using electromagnetic induction methods. Journal of Soil and Water Conservation, 49(6), pp.572-575.

DualEM, Inc., 2005. DUALEM-1S and Dualem- S User's Manual. Milton, Ontario, Canada.

Enakiev, Y.I., Bahitova, A.R. and Lapushkin, V.M., 2018. Microelements (Cu, Mo, Zn, Mn, Fe) in corn grain according to their availability in the fallow SOD-Podzolic soil profile. Bulgarian Journal of Agricultural Science, 24(2), pp.285-289.

Fortes, R., Millán, S., Prieto, M.H. and Campillo, C., 2015. A methodology based on apparent electrical conductivity and guided soil samples to improve irrigation zoning. Precision Agriculture, 16(4), pp.441-454.

Friedman, S.P., 2005. Soil properties influencing apparent electrical conductivity: a review. Computers and Electronics in Agriculture, 46(1-3), pp.45-70.

Ganjegunte, G.K., Clark, J.A., Sallenave, R., Sevostianova, E., Serena, M., Alvarez, G. and Leinauer, B., 2017. Soil salinity of an urban park after long-term irrigation with saline ground water. Agronomy Journal, 109(6), pp.3011-3018.

Ganjegunte, G.K., Sheng, Z. and Clark, J.A., 2014. Soil salinity and sodicity appraisal by electromagnetic induction in soils irrigated to grow cotton. Land Degradation and Development, 25(3), pp.228-235.

García-Tomillo, A., Mirás-Avalos, J.M., Dafonte-Dafonte, J. and Paz-González, A., 2017. Mapping soil texture using geostatistical interpolation combined with electromagnetic induction measurements. Soil Science, 182(8), pp.278-284.

Gebbers, R., Lück, E. and Heil, K., 2007. Depth sounding with the EM38-detection of soil layering by inversion of apparent electrical conductivity measurements. Precision Agriculture, 7, pp.95-102.

Geonics, 2005. EM38. Available from: http://www.geonics.com/html/em38.html (Accessed 17 February 2005).

GF Instruments, 2011. CMD Electromagnetic conductivity meter user manual V. 1.5. Geophysical Equipment and Services, Czech Republic. Available at: http://www.gfinstruments.cz/index.php?menu=gi&smenu=iem&cont=cmd_&ear=ov.

Gooley, L., Huang, J., Page, D. and Triantafilis, J., 2014. Digital soil mapping of available water content using proximal and remotely sensed data. Soil Use and Management, 30(1), pp.139-151.

Goovaerts, P., 1997. Geostatistics for natural resources evaluation. Oxford University Press on Demand.

Goovaerts, P., 1999. Using elevation to aid the geostatistical mapping of rainfall erosivity. Catena, 34(3-4), pp.227-242.

Government of Newfoundland and Labrador, 2017. The Way Forward on Agriculture. Sector Work Plan. Retrieved 20 Nov. 2021. From https://www.gov.NF.ca/ffa/files/agriculture-Sector-Workplan_Final.pdf

Greco, R. and Guida, A., 2009. TDR water content inverse profiling in layered soils during infiltration and evaporation. In EGU General Assembly Conference Abstracts pp.7038.

Greenhouse, J.P. and Slaine, D.D., 1983. The use of reconnaissance electromagnetic methods to map contaminant migration: These nine case studies can help determine which geophysical techniques are applicable to a given problem. Groundwater Monitoring and Remediation, 3(2), pp.47-59.

Grisso, R.D., Alley, M.M., Holshouser, D.L. and Thomason, W.E., 2005. Precision farming tools. Soil Electrical Conductivity. Virginia State University Cooperative Extension, pp.442–508.

Grubbs, R.A., Straw, C.M., Bowling, W.J., Radcliffe, D.E., Taylor, Z. and Henry, G.M., 2019. Predicting spatial structure of soil physical and chemical properties of golf course fairways using an apparent electrical conductivity sensor. Precision Agriculture, 20(3), pp.496-519.

Guber, A.K., Gish, T.J., Pachepsky, Y.A., van Genuchten, M.T., Daughtry, C.S.T., Nicholson, T.J. and Cady, R.E., 2008. Temporal stability in soil water content patterns across agricultural fields. Catena, 73(1), pp.125-133.

Guo, Y., Shi, Z., Huang, J., Zhou, L., Zhou, Y. and Wang, L., 2016. Characterization of field scale soil variability using remotely and proximally sensed data and response surface method. Stochastic Environmental Research and Risk Assessment, 30, pp.859-869.

Heil, K. and Schmidhalter, U., 2012. Characterisation of soil texture variability using the apparent soil electrical conductivity at a highly variable site. Computers and Geosciences, 39, pp.98-110.

Hendrickx, J.M.H., Kachanoski, R.G., Dane, J.H. and Topp, G.C., 2002. Nonintrusive electromagnetic induction. Methods of Soil Analysis. Part, 4, pp.1297-1306.

Hendrickx, J.M.H., Baerends, B., Raza, Z.I., Sadig, M. and Chaudhry, M.A., 1992. Soil salinity assessment by electromagnetic induction of irrigated land. Soil Science Society of America Journal, 56(6), pp.1933-1941.

Huang, J., Pedrera-Parrilla, A., Vanderlinden, K., Taguas, E.V., Gómez, J.A. and Triantafilis, J., 2017. Potential to map depth-specific soil organic matter content across an olive grove using quasi-2d and quasi-3d inversion of DUALEM-21 data. Catena, 152, pp.207-217.

Huth, N.I. and Poulton, P.L., 2007. An electromagnetic induction method for monitoring variation in soil moisture in agroforestry systems. Soil Research, 45(1), pp.63-72.

Islam, M.M., Meerschman, E., Saey, T., De Smedt, P., Van De Vijver, E. and Van Meirvenne, M., 2012. Comparing apparent electrical conductivity measurements on a paddy field under flooded and drained conditions. Precision Agriculture, 13, pp.384-392.

Islam, M.M., Meerschman, E., Saey, T., De Smedt, P., Van De Vijver, E., Delefortrie, S. and Van Meirvenne, M., 2014. Characterizing compaction variability with an electromagnetic induction sensor in a puddled paddy rice field. Soil Science Society of America Journal, 78(2), pp.579-588.

Johnson, C.K., Doran, J.W., Duke, H.R., Wienhold, B.J., Eskridge, K.M. and Shanahan, J.F., 2001. Field-scale electrical conductivity mapping for delineating soil condition. Soil Science Society of America Journal, 65(6), pp.1829-1837.

Kaffka, S.R., Lesch, S.M., Bali, K.M. and Corwin, D.L., 2005. Site-specific management in salt-affected sugar beet fields using electromagnetic induction. Computers and Electronics in Agriculture, 46(1-3), pp.329-350.

Kelley, J., Higgins, C.W., Pahlow, M. and Noller, J., 2017. Mapping soil texture by electromagnetic induction: a case for regional data coordination. Soil Science Society of America Journal, 81(4), pp.923-931.

Kostić, M., Rajković, M., Ljubičić, N., Ivošević, B., Radulović, M., Blagojević, D. and Dedović, N., 2021. Georeferenced tractor wheel slip data for prediction of spatial variability in soil physical properties. Precision Agriculture, 22(5), pp.1659-1684.

Koszinski, S., Miller, B.A., Hierold, W., Haelbich, H. and Sommer, M., 2015. Spatial modeling of organic carbon in degraded peatland soils of northeast Germany. Soil Science Society of America Journal, 79(5), pp.1496-1508.

Kweon, G., Lund, E. and Maxton, C., 2013. Soil organic matter and cation-exchange capacity sensing with on-the-go electrical conductivity and optical sensors. Geoderma, 199, pp.80-89.

Liao, K.H., Zhu, Q. and Doolittle, J., 2014. Temporal stability of apparent soil electrical conductivity measured by electromagnetic induction techniques. Journal of Mountain Science, 11(1), pp.98-109.

Lu, C., Zhou, Z., Zhu, Q., Lai, X. and Liao, K., 2017. Using residual analysis in electromagnetic induction data interpretation to improve the prediction of soil properties. Catena, 149, pp.176-184.

Lund, E.D., Christy, C.D. and Drummond, P.E., 1999. Practical applications of soil electrical conductivity mapping. Precision Agriculture, 99, pp.771-779.

Mahmood, H.S., Hoogmoed, W.B. and van Henten, E.J., 2012. Sensor data fusion to predict multiple soil properties. Precision Agriculture, 13(6), pp.628-645.

Malicki, M.A., Campbell, E.C. and Hanks, R.J., 1989. Investigations on power factor of the soil electrical impedance as related to moisture, salinity and bulk density. Irrigation Science, 10, pp.55-62.

Mansourian, D., Cornelis, W. and Hermans, T., 2020. Exploring Geophysical Methods for Mapping Soil Strength in Relation to Soil Compaction. Master's thesis. Ghent University.

Martinez, G., Vanderlinden, K., Ordóñez, R. and Muriel, J.L., 2009. Can apparent electrical conductivity improve the spatial characterization of soil organic carbon? Vadose Zone Journal, 8(3), pp.586-593.

Martini, E., Werban, U., Zacharias, S., Pohle, M., Dietrich, P. and Wollschläger, U., 2017. Repeated electromagnetic induction measurements for mapping soil moisture at the field scale: Validation with data from a wireless soil moisture monitoring network. Hydrology and Earth System Sciences, 21(1), pp.495-513.

McNeill, J.D., 1980. Applications of transient electromagnetic techniques. Missasauga, ON, Canada: Geonics Limited. pp.17.

Medhioub, E., Bouaziz, M. and Bouaziz, S., 2019. Spatial estimation of soil organic matter content using remote sensing data in southern Tunisia. In Advances in Remote Sensing and Geo

Informatics Applications: Proceedings of the 1st Springer Conference of the Arabian Journal of Geosciences (CAJG-1), Tunisia 2018 Springer International Publishing, pp. 215-217.

Miller, W. and Miller, W.M., 1978. Soil Survey of De Witt County, Texas. Department of Agriculture, Soil Conservation Service.

Minsley, B.J., Smith, B.D., Hammack, R., Sams, J.I. and Veloski, G., 2012. Calibration and filtering strategies for frequency domain electromagnetic data. Journal of Applied Geophysics, 80, pp.56-66.

Misra, R.K. and Padhi, J., 2014. Assessing field-scale soil water distribution with electromagnetic induction method. Journal of Hydrology, 516, pp.200-209.

Moghadas, D., Jadoon, K.Z. and McCabe, M.F., 2017. Spatiotemporal monitoring of soil water content profiles in an irrigated field using probabilistic inversion of time-lapse EMI data. Advances in Water Resources, 110, pp.238-248.

Moghadas, D., Taghizadeh-Mehrjardi, R. and Triantafilis, J., 2016. Probabilistic inversion of EM38 data for 3D soil mapping in central Iran. Geoderma Regional, 7(2), pp.230-238.

Morris, L.A., 2004. Soil biology and tree growth-soil organic matter forms and functions. Elsevier, pp.1201-1207.

Naderi-Boldaji, M., Sharifi, A., Alimardani, R., Hemmat, A., Keyhani, A., Loonstra, E.H., Weisskopf, P., Stettler, M. and Keller, T., 2013. Use of a triple-sensor fusion system for on-the-go measurement of soil compaction. Soil and Tillage Research, 128, pp.44-53.

Nearing, G.S., Tuller, M., Jones, S.B., Heinse, R. and Meding, M.S., 2013. Electromagnetic induction for mapping textural contrasts of mine tailing deposits. Journal of Applied Geophysics, 89, pp.11-20.

Neely, H.L., Morgan, C.L., Hallmark, C.T., McInnes, K.J. and Molling, C.C., 2016. Apparent electrical conductivity response to spatially variable vertisol properties. Geoderma, 263, pp.168-175.

Niu, C.Y., Musa, A. and Liu, Y., 2015. Analysis of soil moisture condition under different land uses in the arid region of Horqin sandy land, northern China. Solid Earth, 6(4), pp.1157-1167.

Nocco, M.A., Ruark, M.D. and Kucharik, C.J., 2019. Apparent electrical conductivity predicts physical properties of coarse soils. Geoderma, 335, pp.1-11.

Pan, L., Adamchuk, V.I., Prasher, S., Gebbers, R., Taylor, R.S. and Dabas, M., 2014. Vertical soil profiling using a galvanic contact resistivity scanning approach. Sensors, 14(7), pp.13243-13255.

Pedrera-Parrilla, A., Van De Vijver, E., Van Meirvenne, M., Espejo-Pérez, A.J., Giráldez, J.V. and Vanderlinden, K., 2016. Apparent electrical conductivity measurements in an olive orchard under wet and dry soil conditions: significance for clay and soil water content mapping. Precision Agriculture, 17(5), pp.531-545.

Peralta, N.R., Cicore, P.L., Marino, M.A., da Silva, J.R.M. and Costa, J.L., 2015. Use of geophysical survey as a predictor of the edaphic properties variability in soils used for livestock production. Spanish Journal of Agricultural Research, 13(4), pp.1103.

Piikki, K., Söderström, M. and Stenberg, B., 2013. Sensor data fusion for topsoil clay mapping. Geoderma, 199, pp.106-116.

Pognant, D., Canone, D., Previati, M. and Ferraris, S., 2013. Using EM equipment to verify the presence of seepage losses in irrigation canals. Procedia Environmental Sciences, 19, pp.836-845.

Polyakov, V. and Lal, R., 2004. Modeling soil organic matter dynamics as affected by soil water erosion. Environment International, 30(4), pp.547-556.

Pozdnyakov, A.I., Eliseev, P.I. and Pozdnyakov, L.A., 2015. Electrophysical approach to assessing some cultivation and fertility elements of light soils in the humid zone. Eurasian Soil Science, 48(7), pp.726-734.

Rallo, G., Provenzano, G., Castellini, M. and Sirera, À.P., 2018. Application of EMI and FDR sensors to assess the fraction of transpirable soil water over an olive grove. Water, 10(2), pp.168.

Rashid, Q.A., Abuel-Naga, H.M., Leong, E.C., Lu, Y. and Al Abadi, H., 2018. Experimental-artificial intelligence approach for characterizing electrical resistivity of partially saturated clay liners. Applied Clay Science, 156, pp.1-10.

Reedy, R.C. and Scanlon, B.R., 2003. Soil water content monitoring using electromagnetic induction. Journal of Geotechnical and Geoenvironmental Engineering, 129(11), pp.1028-1039.

Revil, A., Coperey, A., Shao, Z., Florsch, N., Fabricius, I.L., Deng, Y., Delsman, J.R., Pauw, P.S., Karaoulis, M., De Louw, P.G.B. and van Baaren, E.S., 2017. Complex conductivity of soils. Water Resources Research, 53(8), pp.7121-7147.

Rhoades, J.D., Manteghi, N.A., Shouse, P.J. and Alves, W.J., 1989. Soil electrical conductivity and soil salinity: New formulations and calibrations. Soil Science Society of America Journal, 53(2), pp.433-439. https://doi.org/10.2136/sssaj1989.03615995005300020020x

Rhoades, J.D., and Corwin, D.L., 1990. Soil electrical conductivity: effects of soil properties and application to soil salinity appraisal. Communications in Soil Science and Plant Analysis, 21(11-12), pp.837-860

Robinet, J., von Hebel, C., Govers, G., van der Kruk, J., Minella, J.P., Schlesner, A., Ameijeiras-Mariño, Y. and Vanderborght, J., 2018. Spatial variability of soil water content and soil electrical conductivity across scales derived from Electromagnetic Induction and Time Domain Reflectometry. Geoderma, 314, pp.160-174.

Rodrigues Jr, F.A., Bramley, R.G.V. and Gobbett, D.L., 2015. Proximal soil sensing for precision agriculture: Simultaneous use of electromagnetic induction and gamma radiometrics in contrasting soils. Geoderma, 243, pp.183-195.

Romero-Ruiz, A., Linde, N., Keller, T. and Or, D., 2018. A review of geophysical methods for soil structure characterization. Reviews of Geophysics, 56(4), pp.672-697.

Roper, W.R., Robarge, W.P., Osmond, D.L. and Heitman, J.L., 2019. Comparing four methods of measuring soil organic matter in North Carolina soils. Soil Science Society of America Journal, 83(2), pp.466-474.

Rossi, R., Amato, M., Pollice, A., Bitella, G., Gomes, J.J., Bochicchio, R. and Baronti, S., 2013. Electrical resistivity tomography to detect the effects of tillage in a soil with a variable rock fragment content. European Journal of Soil Science, 64(2), pp.239-248.

Sadatcharam, K., 2019. Assessing potential applications of multi-coil and multi-frequency electromagnetic induction sensors for agricultural soils in western Newfoundland. Master's thesis. Memorial University of Newfoundland.

Sadatcharam, K., Altdorff, D., Unc, A., Krishnapillai, M. and Galagedara, L., 2020. Depth sensitivity of apparent magnetic susceptibility measurements using multi-coil and multi-frequency electromagnetic induction. Journal of Environmental and Engineering Geophysics, 25(3), pp.301-314. Doi: 10.32389/JEEG20-001.

Sanborn, P., Lamontagne, L. and Hendershot, W., 2011. Podzolic soils of Canada: Genesis, distribution, and classification. Canadian Journal of Soil Science, 91(5), pp.843-880.

Sapkota, T.B., Mazzoncini, M., Bàrberi, P., Antichi, D. and Silvestri, N., 2012. Fifteen years of no till increase soil organic matter, microbial biomass and arthropod diversity in cover crop-based arable cropping systems. Agronomy for Sustainable Development, 32(4), pp.853-863.

Schumann, A.W. and Zaman, Q.U., 2003. Mapping water table depth by electromagnetic induction. Applied Engineering in Agriculture, 19(6), pp.675.

Shanahan, P.W., Binley, A., Whalley, W.R. and Watts, C.W., 2015. The use of electromagnetic induction to monitor changes in soil moisture profiles beneath different wheat genotypes. Soil Science Society of America Journal, 79(2), pp.459-466.

Shi, W., Dell, E., Bowman, D. and Iyyemperumal, K., 2006. Soil enzyme activities and organic matter composition in a turfgrass chronosequence. Plant and Soil, 288(1), pp.285-296.

Silva Filho, A.M., Silva, C.L.B., Oliveira, M.A.A., Pires, T.G., Alves, A.J., Calixto, W.P. and Narciso, M.G., 2017. Geoelectric method applied in correlation between physical characteristics and electrical properties of the soil. Transactions on Environment and Electrical Engineering, 2(2), pp.37-44.

Simon, F.X., Tabbagh, A., Donati, J.C. and Sarris, A., 2019. Permittivity mapping in the VLF–LF range using a multi-frequency EMI device: first tests in archaeological prospection. Near Surface Geophysics, 17(1), pp.27-41.

Stadler, A., Rudolph, S., Kupisch, M., Langensiepen, M., van der Kruk, J. and Ewert, F., 2015. Quantifying the effects of soil variability on crop growth using apparent soil electrical conductivity measurements. European Journal of Agronomy, 64, pp.8-20.

Starr, G.C., 2005. Assessing temporal stability and spatial variability of soil water patterns with implications for precision water management. Agricultural Water Management, 72(3), pp.223-243.

Stępień, M., Samborski, S., Gozdowski, D., Dobers, E.S., Chormański, J. and Szatyłowicz, J., 2015. Assessment of soil texture class on agricultural fields using ECa, Amber NDVI, and topographic properties. Journal of Plant Nutrition and Soil Science, 178(3), pp.523-536.

Sudduth, K.A., Kitchen, N.R., Bollero, G.A., Bullock, D.G. and Wiebold, W.J., 2003. Comparison of electromagnetic induction and direct sensing of soil electrical conductivity. Agronomy Journal, 95(3), pp.472-482.

Tallon, L.K. and Si, B.C., 2015. Representative soil water benchmarking for environmental monitoring. Journal of Environmental Informatics, 4(1), pp.31-39.

Tang, P., Chen, F., Jiang, A., Zhou, W., Wang, H., Leucci, G., de Giorgi, L., Sileo, M., Luo, R., Lasaponara, R. and Masini, N., 2018. Multi-frequency electromagnetic induction survey for

archaeological prospection: Approach and results in Han Hangu Pass and Xishan Yang in China. Surveys in Geophysics, 39(6), pp.1285-1302.

Tarr, A.B., Moore, K.J., Bullock, D.G., Dixon, P.M. and Burras, C.L., 2005. Improving map accuracy of soil variables using soil electrical conductivity as a covariate. Precision Agriculture, 6(3), pp.255-270.

Toushmalani, R., 2010. Application of geophysical methods in agriculture. Australian Journal Basic Applied Science, 4(12), pp.6433-6439.

Unc, A., Altdorff, D., Abakumov, E., Adl, S., Baldursson, S., Bechtold, M., Cattani, D.J., Firbank, L.G., Grand, S., Guðjónsdóttir, M. and Kallenbach, C., 2021. Expansion of agriculture in northern cold-climate regions: a cross-sectoral perspective on opportunities and challenges. Frontiers in Sustainable Food Systems, 5, pp.663448.

Uribeetxebarria, A., Arnó, J., Escolà, A. and Martinez-Casasnovas, J.A., 2018. Apparent electrical conductivity and multivariate analysis of soil properties to assess soil constraints in orchards affected by previous parcelling. Geoderma, 319, pp.185-193.

Von Hebel, C., Van Der Kruk, J., Huisman, J.A., Mester, A., Altdorff, D., Endres, A.L., Zimmermann, E., Garré, S. and Vereecken, H., 2019. Calibration, conversion, and quantitative

multi-layer inversion of multi-coil rigid-boom electromagnetic induction data. Sensors, 19(21), pp.4753.

Walter, J., Lück, E., Bauriegel, A., Richter, C. and Zeitz, J., 2015. Multi-scale analysis of electrical conductivity of peatlands for the assessment of peat properties. European Journal of Soil Science, 66(4), pp.639-650.

Wang, F., Yang, S., Wei, Y., Shi, Q. and Ding, J., 2021. Characterizing soil salinity at multiple depth using electromagnetic induction and remote sensing data with random forests: A case study in Tarim River Basin of southern Xinjiang, China. Science of the Total Environment, 754, pp.142030.

Wang, P., Hu, Z., Yang, J., Wang, F. and Gao, M. 2010. The identification test of soil texture with ground penetrating radar. In 2010 International Conference on Advances in Energy Engineering, pp.81-84.

Wilson, B.R., Growns, I. and Lemon, J., 2008. Land-use effects on soil properties on the north-western slopes of New South Wales: implications for soil condition assessment. Soil Research, 46(4), pp.359-367.

Wilson, B.R., Koen, T.B., Barnes, P., Ghosh, S. and King, D., 2011. Soil carbon and related soil properties along a soil type and land-use intensity gradient, New South Wales, Australia. Soil Use and Management, 27(4), pp.437-447.

Won, I.J., Keiswetter, D.A., Fields, G.R. and Sutton, L.C., 1996. GEM-2: A new multifrequency electromagnetic sensor. Journal of Environmental and Engineering Geophysics, 1(2), pp.129-137.Doi:https://doi.org/10.4133/JEEG1.2.129.

Co-authorship statement for study one

A manuscript based on the chapter 3, entitled "*Multi-frequency electromagnetic induction soil moisture characterization under different land uses in western Newfoundland*" has been accepted to the Canadian Journal of Soil Science (Mensah, C., Katanda, Y., Krishnapillai M., Cheema, M., and Galagedara, L., 2023) (CJSS-2022-0102, in-press). Clinton Mensah, the thesis author was the primary author and Dr. Galagedara (supervisor), was the corresponding and the fifth author. Dr. Katanda (committee member) and Dr. Krishnapillai (co-supervisor) were second and third authors, respectively. Dr. Cheema, a collaborator at the Memorial University of Newfoundland was the fourth author. For the work in chapter 3, the design of the research was developed by Dr. Galagedara with input from all members of the group. Mr. Mensah was responsible for the data collection, analysis, and interpretation and writing of the original manuscript. Dr. Katanda provided specific guidance on statistical analysis, data interpretation and manuscript writing. Dr. Krishnapillai and Dr. Cheema provided inputs for the field experiment, data interpretation and manuscript editing.

[1]

[1] **foot note:** "Mensah, C., Krishnapillai, M. and Galagedara, L. (2022). Multi-frequency electromagnetic induction soil moisture characterization under different land uses in western Newfoundland. Joint Annual Meeting of the Canadian Soil Science Society (CSSS) Alberta Soil Science Workshop (ASSW) on "Soil Science for Sustainable Development", May 23 – 27, 2022. Edmonton, AB, Canada. doi.org: 10.13140/RG.2.2.20880.28161 (oral presentation)".

CHAPTER THREE: Study one

Multi-frequency electromagnetic induction soil moisture characterization under different land uses in western Newfoundland

Clinton Mensah [1], Yeukai Katanda[1], Mano Krishnapillai [1], Mumtaz Cheema [1], Lakshman Galagedara [1*]

[1] School of Science and the Environment, Memorial University of Newfoundland, Corner Brook, NL, A2H 5G4, Canada
* Corresponding author: lgalagedara@grenfell.mun.ca

Abstract

Identifying and characterizing the spatial patterns in soil moisture variability under different land use conditions is crucial for agriculture, forestry, civil and environmental engineering. Yet, employing multi-frequency electromagnetic induction (EMI) techniques to carry out this task is under-represented in boreal podzolic soils. This study: (i) compared four frequencies (2.8 ~ 80 kHz) for shallow mapping of soil moisture measured with a time-domain reflectometry at 0 – 20 cm soil depth under three different land-use conditions (agricultural land, field road, and a recently cleared natural forest); (ii) developed a relationship between apparent electrical conductivity (EC_a) measured using multi-frequency EMI (GEM-2) and soil moisture; and (iii) assessed the effectiveness of EC_a as an auxiliary variable in predicting soil moisture variations under different land use conditions. The means of EC_a measurements were calculated for the exact sampling location (ground truth data) in each land use condition at a research site, Pasadena, Newfoundland. Soil moisture–EC_a linear regression models for the three land-use conditions were only statistically significant for 38.3 kHz frequency and were further analyzed. Further statistical analysis revealed that EC_a was primarily controlled by soil moisture for the three land-use conditions, with the natural

forest possessing the highest mean EC_a and soil moisture. Geostatistical analysis revealed that cokriging EC_a with less densely collected soil moisture improved the characterization accuracy of soil moisture variability across the different land use conditions. These results reveal the effectiveness of the georeferenced MF-EMI technique to rapidly assess intra-field soil moisture variability under different land uses.

Keywords: Apparent electrical conductivity, land uses, electromagnetic induction, multi-frequency, volumetric soil moisture content

3.1 Introduction

Agricultural production in Newfoundland and Labrador (NL) is limited by the poor inherent fertility of the predominantly coarse to medium textured podzols. These soils are acidic and have low nutrient status (Enakiev et al. 2018). In 2017, the provincial government outlined plans to convert substantial areas of boreal forests into agricultural land as part of the 'The Way Forward on Agriculture Initiative' to increase food production (Government of Newfoundland and Labrador, 2017). The conversion of natural forest land to agricultural fields can introduce spatial and temporal variability in soil properties (Atwell and Wuddivira 2019; Niu et al. 2015). Soil properties naturally vary with land use (Guo et al. 2023), temperature and precipitation as well as soil type (Wu et al. 2023). Properties, such as electrical conductivity (EC) (Tiwari et al. 2019), soil organic matter (Atwell and Wuddivira 2019), and water holding capacity (Bai et al. 2019) have been reported to respond to land use changes. Monitoring such changes is critical for efficient

management, particularly in regions with low inherent production capacity such as those in Newfoundland.

Soil moisture is a vital parameter for optimizing site-specific management and ecosystem sustainability (Yu et al. 2018). Understanding spatial variability in soil moisture is key for effective management of hydrology and water resources (Guo et al. 2020), agriculture and irrigation (Funes et al. 2019), and rock and soil mechanics (Susha et al. 2014). Additionally, EC is important for monitoring the fertility and the chemical status of soils. Conventional methods of sampling and analyzing soil moisture or EC (such as gravimetric sampling, neutron probes, and gypsum blocks) can be destructive, labour-intensive, time-consuming, and provide point information (Calamita et al. 2015; Badewa et al. 2018). Alternatively, geophysical methods, such as electromagnetic induction (EMI) and time-domain reflectometry (TDR) can be used to characterize soil EC or soil moisture variability more rapidly, non-invasively and less laboriously (Altdroff et al. 2018; Badewa et al. 2018; Sadatcharam 2019). EMI and TDR employ electromagnetic waves to measure apparent electrical conductivity (EC_a) and dielectric permittivity, respectively. EC_a is defined as the depth weighted average of the bulk soil EC within a soil volume and is considered a proxy of soil properties including soil moisture (Badewa 2018; Altdorff 2020). Geophysical techniques present an expeditious way for monitoring the spatiotemporal variability of soil moisture.

EMI sensors operate by inducing an alternating current (EM waves in kHz) within the soil via the primary electromagnetic field generated from the transmitting coil and measuring the resultant

secondary field via the receiving coil (Von Hebel et al. 2019). The amplitude, phase differences, and inter-coil spacing between the primary and resultant fields are then used to determine an "apparent" value for soil EC (Simon et al. 2020). There are two types of EMI sensors that are commercially available, multi-coil (MC) and multi-frequency (MF) EMI sensors. The MC sensor operates at a fixed frequency and has multiple coil separations (Altdorff et al. 2020). The depth of investigation for this type of sensor depends on the coil separation; thus, the higher the inter-coil spacing between the transmitter and receiver coils, the higher the depth of investigation (Deidda et al. 2020; Sadatcharam et al. 2020). The bucking coil cuts off the primary influence at the receiver coil (Calamita et al. 2015). The MF–EMI instruments with slingram geometry (dipole-dipole) can be used for conventional soil characterization (Lück et al. 2022) as well as simultaneous mapping of soil EC_a and magnetic susceptibility (Sadatcharam et al. 2020). Altdorff et al. (2020) compared the performance of MF and MC EMI sensors in shallow podzols and concluded superior performance from the MF sensor. Similarly, Sadatcharam (2019) found the MF–EMI sensor to be more reliable for EC_a variability in wet soils than in dry soils.

Over the years, geostatistical techniques have been used as interpolation tools to effectively estimate and provide unbiased predictions at unsampled locations (Srivastava et al. 2019). Kriging and cokriging are widely used interpolation techniques (Belkhiri et al. 2020); the former is used when a variable displays spatial dependence whiles the latter is employed when other properties have been densely sampled in comparison to the target variable (Rostami et al. 2020). The extensively sampled variable (covariate) is usually measured more cheaply, and quickly than the

target variable. EC_a measured using EMI sensors can be used as a covariate for mapping of soil moisture (Tarr et al. 2005; Naimi et al. 2021). Spatial variability in soil moisture can be predicted by ordinary kriging from the limited soil samples and by cokriging when a strong statistically significant relationship exists between soil moisture and an easily measured auxiliary variable. Previous studies suggest superior prediction accuracy of cokriging compared to ordinary kriging (Belkhiri et al. 2020). Altdorff et al. (2017) used ordinary kriging with EC_a data to investigate the performance of EMI sensors in forest ecosystems and reported strong similarities between spatial EC_a and soil moisture patterns. Similarly, Atwell and Wuddivira (2019) reported variable effectiveness of EC_a data from EMI sensors for characterizing soil moisture in forests, agricultural land, grasslands, quarries, and residential areas. Lastly, Carrière et al (2020) reported a stronger relationship between EC_a and estimated soil depth in forest systems compared to managed systems (cedar plantation).

The use of EMI and the comparison of co-kriging and ordinary kriging under different land uses is a novel dimension to soil studies in NL because it allows for a more comprehensive understanding of the soil properties in the region. By comparing the results of co-kriging and ordinary kriging under different land uses, researchers can gain a better understanding of how soil properties vary both spatially and temporally across different land uses in the study area. This information can then be used to delineate mangament zones based on the variability of the soil porperties and inform land management decisions, such as which land uses are best suited for certain soil types. Overall, the use of EMI and the comparison of co-kriging and ordinary kriging under different land uses

provides a novel dimension to soil studies in Newfoundland, allowing for a more comprehensive understanding of the soil properties and their variability in the study area.

Converted lands for agricultural purposes usually combine varying agronomic practices, which tends to significantly affect the EC_a – soil moisture relation making it necessary to have an accurate site-specific soil moisture prediction. This research aims to apply an MF–EMI sensor to map soil moisture variability under natural forests and managed agricultural land in Western Newfoundland. The GEM-2 MF sensor employed in this study produces sensitive and thermally stable measurements (Briggs et al. 2019). Specifically, this work seeks to: (i) compare the different frequencies in the 2.8 – 80 kHz range for shallow mapping of volumetric soil moisture under the different land use conditions; (ii) evaluate the relationship between EC_a measured using MF–EMI and soil moisture; and (iii) assess the effectiveness of EC_a as an auxiliary variable to predict soil moisture variations under different land use conditions. Although previous studies using EMI techniques to characterize soil moisture have been done in agricultural land in Newfoundland (Altdorff et al. 2018; Badewa et al. 2018; Sadatcharam et al. 2020; Altdorff et al. 2020), no study has investigated the use of EMI sensors under different land use types concurrently. It is worthwhile to test the technique under different conditions to assess its usefulness to support various academic, industrial, and government projects being carried out in the province and other sub-regions. Also, the use of EC_a as a covariate in cokriging is yet to be done in the province. To our knowledge, very few studies have used geostatistical techniques with geophysical data as covariates for predicting soil moisture.

3.2 Materials and methods

3.2.1 Study area

This study was conducted on three different land use conditions: an agricultural field, a recently cleared natural forest and a field road at the Western Agriculture Center and Research Station, Pasadena (49.0130° N, 57.5894° W), Newfoundland (Figure 3.1). The study site is managed by the Department of Fisheries, Forestry and Agriculture, Government of Newfoundland, Canada. The soil in the study site is generally classified as a reddish-brown to brown Podzol developed on a gravelly sandy fluvial deposit with >100 cm depth to bedrock and a 2% – 5% slope (Croquet 2016). The area of the agricultural land was 924 m^2 and included a rotation of corn, canola, faba bean, wheat, and oats/peas. The field road was adjacent to the agricultural land and was 240 m^2 in area, serving as access for equipment, vehicles, and people to the other parts of the field. A 50 m^2 area was selected from a recently cleared natural forest to compare its EC_a and soil moisture data with the other land use conditions of interest (agricultural land and field road) (Figure 3.1). Before the commencement of EC_a and soil moisture measurements, soil texture, soil BD and SOM for the different land uses were determined by collecting soils sample from each land use.

To assess a range of soil properties, several analytical methods were employed. For soil moisture, the gravimetric method was used; for soil texture, the hydrometer method; for BD, the oven-drying method; and for SOM, the loss-on-ignition method (Table 3.1). Each of these methods offer an accurate and reliable way of measuring the respective soil characteristics and provide a comprehensive overview of the soil. Through the use of these analytical techniques, the soil can be

thoroughly investigated and the underlying properties can be accurately and reliably determined. Based on three month data (1 Sep. – 30 Nov. 2021) from the nearby Deer Lake weather station A (http://climate.weather.gc.ca), the area received a total rainfall of 409 mm and had an average mean temperature of 8.18 °C (Figure 3.2)

Table 3.1 Basic soil properties of agricultural land, natural forest and field road obtained from ground truthing and laboratory analysis (n = 9)

Basic soil properties	Agricultural land	Natural forest	Field road
Sand (%)	68.2 ± 2.04	65.2 ± 1.98	70.4 ± 3.41
Silt (%)	18.7 ± 2.31	17.3 ± 2.01	19.2 ± 2.98
Clay (%)	14.1 ± 1.92	18.5 ± 2.46	11.4 ± 3.17
Soil Texture	Sandy loam	Sandy loam	Sandy loam
Bulk density (g cm^{-3})	1.26 ± 0.21	0.90 ± 0.29	1.29 ± 0.14
Soil organic matter (% dry weight)	3.87 ± 1.08	9.37 ± 2.30	2.08 ± 0.44

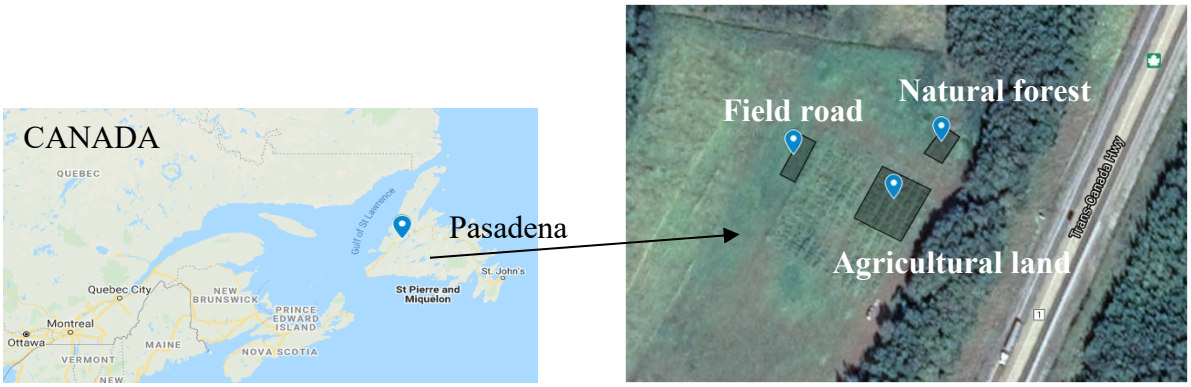

Figure 3.1: The location of the different land use conditions in Western Agriculture Center and Research Station, Pasadena, Newfoundland, Canada (49.0130° N, 57.5894° W).

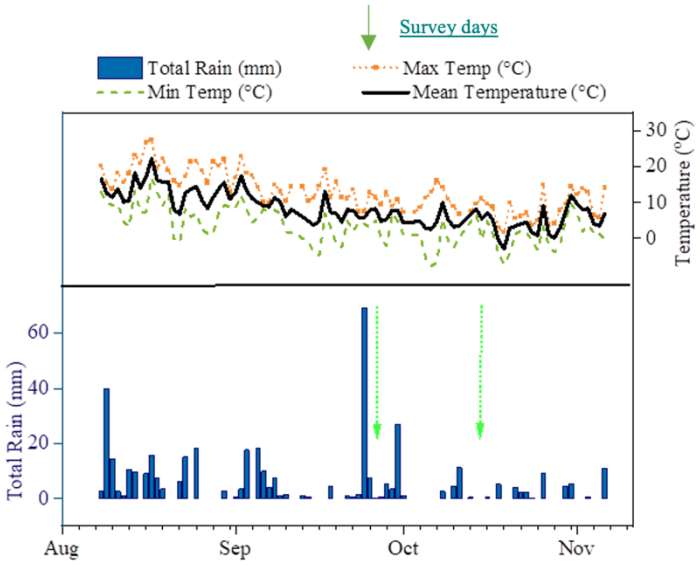

Figure 3.2: Daily total rainfall, minimun, maximum, and mean temperature from Aug. 2021 to Nov. 2021 for the study area from Deer Lake weather station A.

3.2.2 Electromagnetic induction (EMI) survey

EC_a data were recorded from the three land use conditions: Agricultural land, field road, and natural forest using EMI surveys. For each land use condition, a GEM-2 MF–EMI sensor (Geophex, Ltd., Raleigh, NC, USA) was used to simultaneously collect EC_a data at four different frequencies (2.8, 18.3, 38.3, and 80.0 kHz). The selected frequencies were chosen due to their suitability for shallow podzolic soil investigations (Won et al. 1996). During each survey, a 1 m line spacing was maintained. A global positioning system (GPS) was attached to the EMI sensor to enable the production of georeferenced maps. Before each survey, the EMI sensor was warmed up for at least 30 minutes to prevent data drift and ensure high-quality data as proposed by Robinson et al (2004).

During each survey, the MF–EMI sensor was positioned such that the transmitter coil was always ahead of the receiver coil and was carried with the supplied shoulder strap at an average height of about 1 m above the ground. Both the vertical coplanar (VCP) and horizontal coplanar (HCP) coil orientation modes were used when collecting data on agricultural land, field road, and natural forest as done by previous researchers in the same area (Altdorff et al. 2018; Badewa et al. 2018; Sadatcharam et al. 2020). The MF surveys were carried out in a bi-directional order over the three land use conditions.

Soil temperature was measured at 0 – 20 cm depth for all three land use conditions using a soil temperature probe. Among the several models suggested for the correction of the temperature effect on the mobility of dissolved ions, the 'corrected Sheets and Hendrickx model' was adopted in this

study as displayed in Equation 3.1. According to Ma et al (2011), this model was adopted because it performs better in most situations and for a wide range of temperatures.

$$EC_{25} = EC_t \times (0.4470 + 1.4034\, e^{-t/26.815}) \quad \text{Equation 3.1}$$

EC_t is the EC_a data collected at measured soil temperature, t (°C) and EC_{25} is the temperature corrected EC_a. Negative values were considered noise and subsequently eliminated.

The surveys were carried out during a wet period (20 Oct. and 8 Nov. 2021; Figure 3.2) based on the total rainfall data available by the nearby Deer Lake weather station A (http://climate.weather.gc.ca). The surveys were carried out in the wet period because MF–EMI is more reliable for EC_a variability in wet soils than in dry soils (Sadatcharam 2019).

3.2.3 Soil moisture content data recording and time-domain calibration

Soil moisture was measured at nine (9) sampling points at 0 – 20 cm depth in the agricultural land, field road and natural forest volumetrically using a hand-held TDR (FieldScout TDR 350, Spectrum Technologies, Aurora, IL, USA) with a probe length of 20 cm and gravimetrically via oven drying on 20 Oct. and 8 Nov. 2021. The 0 – 20 cm depth was considered because it is an active interface between the soil, vegetation, atmosphere, and human activities mostly affected by precipitation, infiltration, and canopy cover (Choi et al. 2007). Soil moisture data measured gravimetrically were converted to volumetric soil moisture (Carter and Gregorich 2007) and correlated with the TDR data measured using Lin's Concordance Correlation Coefficient (LCCC) and Root mean square error (RMSE) performance criteria to obtain the field scale accuracy of the TDR meter. Lin's Concordance Correlation Coefficient prediction matrix measures the accuracy

of the prediction along a 1:1 line to evaluate the agreement between paired readings (Lawrence and Lin 1989) and is of the form:

$(2s_{xy})/(s_x^2 + s_y^2 + (x^* - y^*)^2)$ Equation 3.2

where $s_x^2 = \frac{1}{N}\sum_{i=1}^{n}(xi - x*)^2$, $s_y^2 = \frac{1}{N}\sum_{i=1}^{n}(yi - y*)^2$, $s_{xy} = \frac{1}{N}\sum_{i=1}^{n}(xi - x*)(yi - y*)$

x^* and y^* are sample means for populations X and Y, and xi and yi are paired ith values from populations X and Y. The value of the index is scaled between −1 and 1, with a value of 1 representing complete agreement between all paired sites.

3.2.4 Descriptive statistics

Descriptive statistics (boxplot and coefficient of variation – CV) were conducted to evaluate the variability of EC_a and soil moisture data on both survey dates. Across all the study sites, the relationship between EC_a and soil moisture was not statistically significant ($p > 0.05$) for 2.85, 18.33 and 80.01 kHz frequencies in both HCP and VCP modes; hence were not further analyzed. However, the relationships were significant ($p < 0.05$) for the soil EC_a measured with a frequency of 38.31 kHz in HCP mode across all study sites on both survey days; thus, only the 38.31 kHz in HCP mode was considered for further analysis. A similar result was seen by Altdorff et al (2018), Badewa et al (2018) and Sadatcharam et al (2020) on a nearby field at the Western Agriculture Center and Research Station. Kolmogorov-Smirnov frequency distribution analysis revealed that all soil properties investigated in this study were normally distributed on both survey days.

3.2.5 Analysis of variance

One-way analysis of variance (ANOVA) was used to examine the differences in soil EC_a and soil moisture across the different land use conditions. The normality of residuals was assessed using Kolmogorov-Smirnov test, and least square means were compared using the Fisher LSD test at 5% significance.

3.2.6 Correlation and regression

The strength of the relationships between EC_a and soil moisture for each land use were assessed using Pearson correlation analysis. A strong relationship between the auxiliary variable and target variable has been seen as an efficacy of cokriging (Tarr et al. 2005). Linear regression was used to characterize the relationship between soil moisture and EC_a and to generate predictive models of soil moisture under each land use using EC_a from the first survey day. The models were validated by fitting them to the EC_a data from the second sampling day to predict soil moisture for the second sampling day. The model performances were evaluated using the level of agreement (accuracy) between the predicted and measured soil moisture for the second day using LCCC prediction matrix and RMSE. All statistical analyses were performed with Minitab 17 (Minitab 17 Statistical Software 2010).

3.2.7 Geostatistical analysis

Ordinary kriging was used to prepare interpolated maps of EC_a. The spatial prediction of the unmeasured points was given by the line sum of observed values (Equation 3.3).

$$Z*(x_o)= \sum^{n}{}_{i=1} =1\lambda_i Z(x_i)$$ Equation 3.3

where $Z*(x_o)$ is the predicted value at the unmeasured position x_o, Z(xi) is the measured value at position x_i, λ_i is the weighting coefficient from the measured position to x_o and n is the number of positions within the neighborhood searching.

A total of 4202, 1303, and 1062 EC_a data were collected (observed values) from the agricultural land, field road and natural forest, respectively. Soil moisture was less sampled (9 data points) compared to EC_a in this study, hence, in addition to ordinary kriging, cokriging was used for soil moisture mapping. Cokriging is the multivariate equivalent of ordinary kriging. The main difference is that cokriging has a secondary variable (covariate) (Equation 3.4).

$\sum^{n}_{vl=1} \sum^{n}_{i=1} \lambda_{il} \lambda_{lv}\gamma(x_i,x_j)- \mu_v = \gamma_{uv}(x_i,x_p)$ where j = 1, ..., n and u = 1, ..., v

$$\sum^{nl}_{i=1} \lambda_{il} = \begin{matrix} 1 & 1 = u \\ 0 & 1 \neq u \end{matrix}$$ Equation 3.4

where u and v are the target and covariate variables, respectively. The two variates u and v are cross-correlated, and the covariate contributes to the estimation of the target variate.

The EC_a data collected on the agricultural land, field road and natural forest, respectively were used as covariates for soil moisture predictions with cokriging. To assess the effectiveness of EC_a as an auxiliary variable for improving soil moisture mapping predictions, ordinary kriging was compared to cokriging.

Several variogram models (linear, exponential, circular, gaussian, spherical and power model) were considered for creating EC_a and soil moisture maps using ordinary kriging or cokriging. The variogram models with the lowest RMSE based on the cross-validation results were selected (Sówka et al. 2020). Cross-validation works by singly removing each point in the sampling scheme and predicting its value based on kriging the remaining data. All variograms were assumed to be isotropic. The ordinary kriging and cokriging under each land use were compared using Surfer 24 (Golden Software Inc. 2022). Interpolated maps were then created using Surfer 24 (Golden Software Inc. 2022).

3.3 Results and discussion

The development of policies in recent times to maintain water resources require evidence-based information on the spatial distribution of soil moisture under different land uses (Gebrehiwot et al. 2021). This approach to measuring soil moisture in different land use conditions has the potential to improve land-unit mapping, agricultural planning, and afforestation activities (Stavi et al. 2019).

3.3.1 Calibration of TDR

There was a significant strong positive correlation (LCCC = 0.9) between measured volumetric moisture content with the TDR and the calculated volumetric moisture content using the gravimetric analysis and bulk density for 0-20 cm depth with a low RMSE (1.09 %) as seen in Figure 3.3. This result is similar to that is reported by Topp et al. (1980) and Badewa et al. (2018).

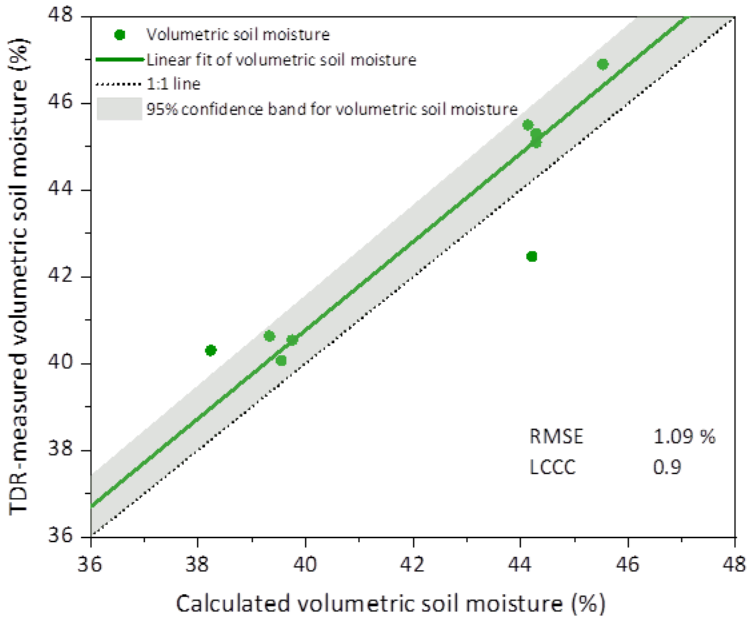

Figure 3.3: Relationship between the measured volumetric moisture content with the TDR and the calculated volumetric moisture content using the gravimetric analysis and bulk density for 0-20 cm depth.

3.3.2 Descriptive statistics

Several factors including but not limited to land use can influence the variation in soil properties (Atwell and Wuddivira 2019). All other factors besides land use were kept constant during soil data collection, therefore the variations in soil EC_a and soil moisture were used as a measure of sensitivity to land use. The coefficient of variation (CV) of the soil EC_a and soil moisture within land uses was used as a reflection of the spatial sensitivity of EC_a and soil moisture. According to the classification of Warrick (1998), the CV of EC_a for agricultural land and field road were moderate ($15\% < CV < 35\%$) while that of the natural forest was low ($CV < 15\%$) for the first

survey day (Figure 3.4). For the second survey day (Figure 3.4), the CVs for EC_a for the three different land use conditions were low based on the classification of Warrick (1998). The agricultural land had the highest CV in EC_a among the three land use conditions indicating this land use was most sensitive to EC_a changes. This was primarily attributed to fertilizer inputs in this land use as discussed in Atwell and Wuddivira (2019). The CV for the soil moisture was low for all three land use conditions for both survey days (CV < 15%) (Figure 3.5). Natural forest showed the lowest CV in soil moisture indicating a more stable spatial pattern in the soil moisture. Agricultural land and field road showed a higher CV in soil moisture, indicating that factors such as human disturbance can increase the spatial heterogeneity of soil moisture as also discussed in Guo et al (2020).

The range of EC_a was most extensive in the natural forest relative to the agricultural land, and field road for both survey days. The higher EC_a range may be ascribed to higher soil organic matter found in the natural forest relative to the other land use conditions. This result is similar to the observation by Atwell and Wuddivira (2019). The range of EC_a values in the agricultural land was greater than that in the field road, and this may be due to fertilizer application which potentially leads to increased soil ionization (Kaufmann et al. 2020).

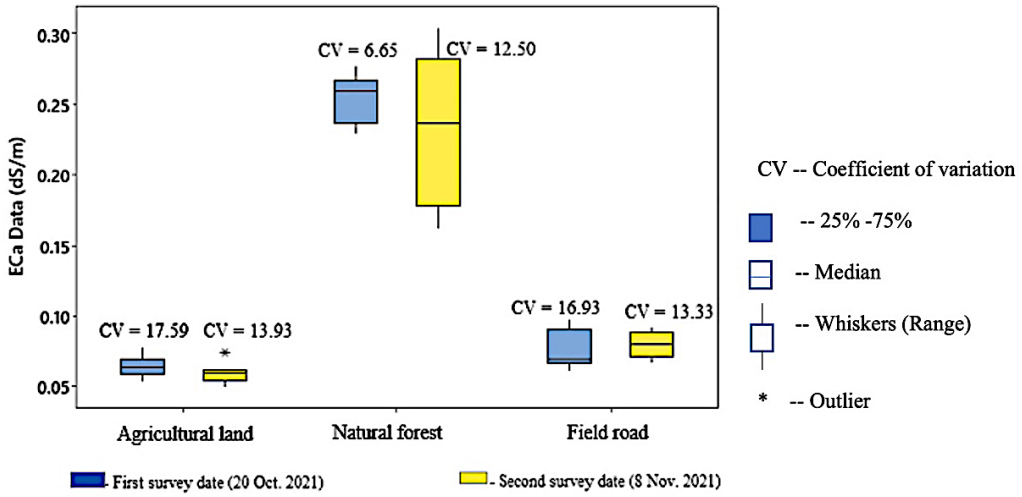

Figure 3.4: Spatial variability of apparent electrical conductivity (ECa) data ranges by box and whisker plots (* - outlier value) with coefficient of variation for the different land use conditions on two survey days.

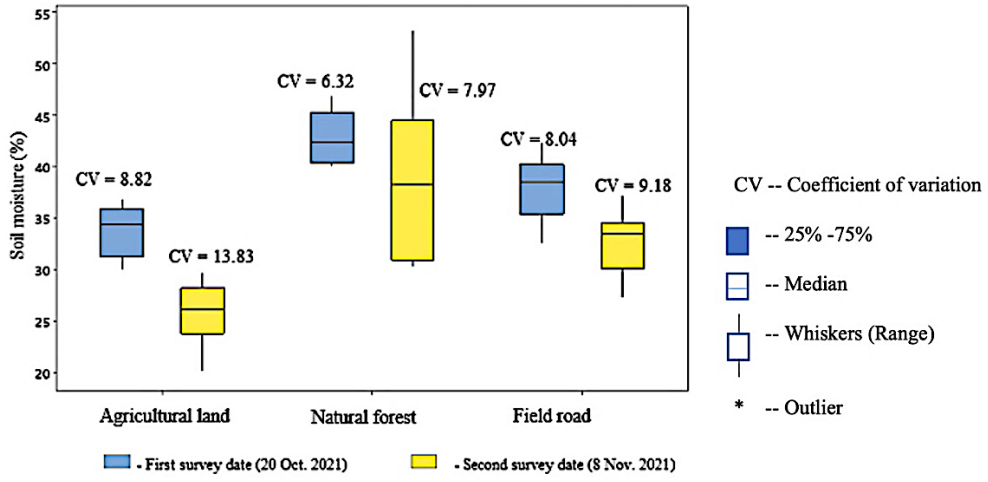

Figure 3.5: Spatial variability of soil moisture data ranges by box and whisker plots (* - outlier value) with coefficient of variation for the different land use conditions on two survey days.

3.3.3 Analysis of variance

The mean EC_a for the natural forest was higher than agricultural land and field road for the first survey day (20 Oct. 2021) and for the second survey day (8 Nov. 2021) (Table 3.2). Generally, soils with high clay contents possess continuous moisture-filled pores that easily conduct electricity relative to sandy soils (Rhoades et al. 1989). Natural forest had a higher clay and soil organic matter content relative to the other land use conditions as shown in Table 3.1 leading to a higher water holding capacity (Atwell and Wuddivira 2019). The lowest EC_a mean was recorded in the agricultural land. This was related to the fact that EC_a surveys on agricultural land were carried out during the harvesting period hence the crops on this land could have utilized most of the applied fertilizer leading to low EC_a readings. The frequent use of the field road as an access route could have increased the soils compaction hence leading to a relatively higher EC_a than in the agricultural land (Machado et al. 2014).

The soil moisture mean values were higher on the first survey day than on the second survey day (Table 3.2) which potentially could be due to a higher total rainfall (mm) on the first survey day (84.2 mm) relative to the second survey day (19.3 mm) as seen in Figure 3.2. The total rainfalls were calculated for ten days before each survey date. The mean soil moisture values were higher in the natural forest relative to the agricultural land and field road (Table 3.2). This was ascribed to the deep litter layer (relatively high soil organic matter) found in this land use. The deep litter can potentially reduce surface evaporation and can improve vertical infiltration effectively by preventing rainfall splashing as well as surface runoff. By improving vertical infiltration, the

presence of the litter facilitates the formation of an aerobic environment that accelerates the decomposition of root systems and improves soil porosity by providing a network of continuous root channels. This finding agrees with that of Morris (2004). The availability of high soil organic matter in coarser textured soils such as podzolic soils also tends to expand the volume of soil pores that retain water against gravitational drainage, increasing the water holding capacity in the natural forest as observed by Morris (2004). The low soil moisture in agricultural land and field road was ascribed to the higher rate of evaporation that existed in the surface horizon of the agricultural land and field road than on the natural forest due to factors such as ploughing, which reduces soil water evaporation by creating a capillary barrier at the surface horizon (Gao et al. 2011). In addition, the agricultural land and field road had relatively higher surface runoff due to surface crusting and compaction, causing them to have a lower infiltration than in the natural forest.

One-way analysis of variances (ANOVA) revealed that EC_a data were not significantly different between the agricultural land and field road, possibly due to the proximity and similar soil characteristics between these land use conditions; however, EC_a in natural land was significantly different from agricultural land and field road as seen in Table 3.2. In contrast, soil moisture was found to be significantly different among the three land use conditions ($p < 0.005$) for both survey days as shown in Table 3.2. These statistics proved that soil EC_a and soil moisture differences existed between the land use conditions as indicated by Xu et al (2021) and Gao et al (2011). Although soil EC_a is dynamic, the results indicate that soil moisture is more sensitive to land use

conditions relative to soil EC_a in this study area. In the Aripo savannas, soil moisture has also been seen to be more sensitive to land use conditions relative to soil EC_a (Atwell and Wuddivira 2019).

Table 3.2 Analysis of variance of apparent electrical conductivity (EC_a) and soil moisture content measurement between agricultural land, natural forest, and the field road at 95% confidence

Effects	N	EC_a (dS m^{-1})		Soil moisture (%)	
Land use		Survey Day 1	Survey Day 2	Survey Day 1	Survey Day 2
Natural forest	9	0.25 [a] ***	0.23 [a] ***	42.98 [a] ***	38.23 [a] ***
Field road	9	0.08 [b] **	0.07 [b] **	38.01 [b] **	32.67 [b] **
Agricultural land	9	0.06 [b] **	0.05 [b] **	33.71 [c] **	25.98 [c] **
Standard Error		0.0063	0.0147	1.30	2.47

Means that do not share a common letter are significantly different according to Fisher's Least Significant Difference Test. Significance is reported at 0.05 (**)

3.3.4 Pearson correlation analysis

There were significant positive correlations between EC_a and soil moisture for all three land use conditions (Figure 3.6). There was a strong relationship between EC_a and soil moisture in the field road and the natural forest whiles the agricultural land showed a relatively weaker relationship between EC_a and soil moisture on both survey days as shown in Figure 3.6. The correlation results show that EC_a values in the study area increase with water content and potentially ions retained in

soil solution. The positive correlation between EC_a and soil moisture corroborates with previous studies (Tang et al. 2020; Wang et al. 2020) in agricultural lands in other sub-regions.

3.3.5 Regression analysis

Regression analysis showed EC_a explained more than 70% of the variation in soil moisture in the field road and the natural forest. On the other hand, EC_a explained relatively lower (59%) variation in soil moisture in the agricultural land (Figure 3.6). A possible explanation of the lower R^2 in the agricultural land could be because the agricultural land is a managed ecosystem with the presence of fertilizer resulting in an increase in the concentration of dissolved ions and, consequently, in the pore water electrical conductivity (EC_w) contributing to a higher variability in EC_a. Also, due to heavy compaction and shallow water depth in some areas of the agricultural land it resulted in poor drainage in certain zones of the field. These factors could have affected EC_a – soil moisture relation (Archie 1942; Corwin and Lesch 2005; Altdorff et al. 2018). The regression results for each land use conditions on both survey days indicate that EC_a is primarily controlled by soil moisture for these study sites.

Validation of the generated regression models using LCCC and RMSE obtained by comparing the predicted volumetric soil moisture using EC_a data with linear regression models to the measured volumetric soil moisture with TDR revealed that predictions of soil moisture from site specific linear regression models exhibited much certainty on the land use conditions with higher soil moisture (natural forest) compared to the land uses with lower soil moisture (agricultural land and

field road) as seen in Figure 3.7. No significant differences existed between the regressions for agricultural land and field road. The fitted linear regression developed between EC_a and soil moisture in the natural forest (LCCC = 0.7, RMSE = 3.87 %) provided the highest prediction accuracy relative to the other land use conditions. These findings indicate that moist soils are more favourable for EC_a surveys, as also suggested by Brevik et al (2006) and Sadatcharam et al (2020). Although several regression models were developed to predict soil moisture during data processing, the site-specific models produced the most accurate soil moisture predictions as seen by Drummond et al (2003) and Altdorff et al (2018).

Systematic deviations in soil moisture (Figure 3.7) have been reported by Bogena et al. (2007) to be magnified in soils with lower EC_a ($\sim$0.06 dS m^{-1}). These EC_a values reported by Bogena et al. (2007) are similar to those recorded in the agricultural land and field road in our study (Table 3.2). A further explanation for the under-estimation and over-estimation is the disparity of sampling depths between TDR and EMI sensor (Altdorff et al. 2017; Calamita et al. 2015). TDR probes were installed vertically at 0-20 cm depth and the EMI sensors have an effective integral depth of 0-250 cm. Another factor could be the effect of soil temperature on the sensor's electronics as also mentioned by Bogena et al. (2007). However, the effect of temperature on the instrument and therefore measured EC_a of the soil in our study area has not yet been studied, and its influence on the results of the experiment is beyond the scope of this paper.

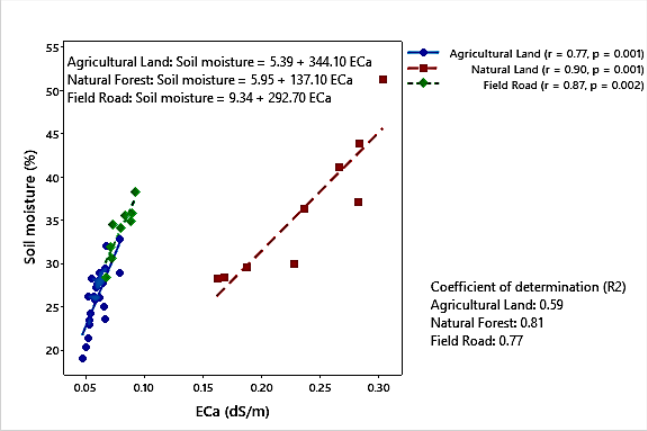

Figure 3.6: The site-specific relationship between ECa and volumetric soil moisture with Pearson correlation coefficient (r) and coefficients of determination (R^2) under each land use.

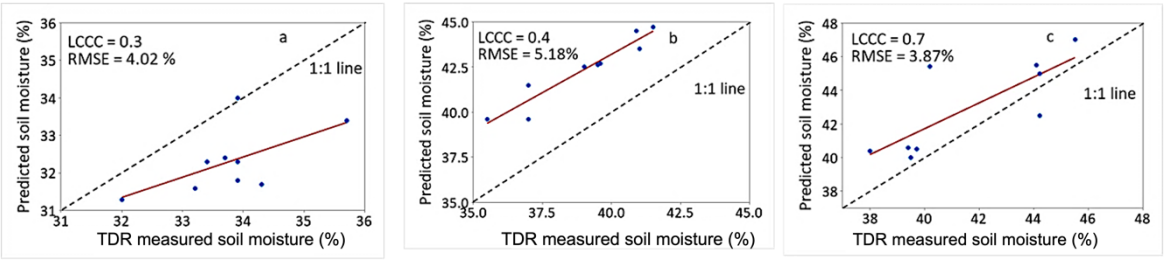

Figure 3.7: Relationship between predicted soil moisture from linear regression models and TDR measured soil moisture under agricultural land (a), field road (b) and natural forest (c) with Lin's concordance correlation coefficient and root mean square error.

3.3.6 Interpolated maps

Visual differences generally existed between the maps of soil moisture obtained from kriging and those from cokriging. The maps obtained from cokriging were less smooth and showed more local detail in their representation of the soil moisture variability. However, the trends in variability of soil moisture in both methods were similar. These findings agree with that of Tarr et al. (2005).

The parameters used in fitting the variograms for each interpolated map are displayed in Table 3.3. The various variograms are displayed in Appendix A1-A6.

3.3.6.1 Agricultural land

The interpolated spatial maps for EC_a (38.3 kHz) for the agricultural land for the two survey dates are displayed in Figures 3.8a and 3.9a. EC_a values for this land use ranged from 0.05 – 0.2 dS m^{-1}. In this land use, spherical (Figure. A1 (a)) and Gaussian models (Figure. A2 (a)) displayed the best fitting models for the spatio-temporal representation of EC_a in ordinary kriging for the first and second day respectively. The variograms provided a clear insight of EC_a spatial structure of both sampling days. Positive nugget values were found for the EC_a variograms on both survey days (Table 3.3). This could be due to the variation in EC_a associated with short-range variability of soil properties such as soil moisture content, ionic composition, and topography (Narjary et al. 2019). The lower range (3 m) on the second day compared to the first day (19.2 m) (Table 3.3) suggests that the spatial autocorrelation of EC_a increased on the second day (Liu et al. 2017). The increase in RMSE between the first day (RMSE = 0.05 dS m^{-1}) and second day (RMSE = 0.09 dS m^{-1}) obtained from cross-validation (Table 3.3) indicates a reduction in prediction accuracy possibly due to an increase in spatial heterogeneity of EC_a as displayed in the interpolated map (Figure 3.9a). The nugget:sill ratio was used to classify the spatial dependence of EC_a. Ratio values lower than 25% and higher than 75% corresponded to strong and weak spatial dependence, respectively, while the ratio values between 25% and 75% corresponded to moderate spatial dependence (Chang et al. 1998). EC_a in the agricultural land use exhibited a strong spatial dependence on the first day and a moderate spatial dependence on the second day (Table 3.3).

This land use generally had low EC_a scattered across the map with the highest EC_a region in the agricultural land observed on the lower left region of the map for the first survey day. The interpolated EC_a maps for the second survey date generally revealed lower EC_a values relative to the first survey date which is consistent with the trend of the measured EC_a data.

The spherical variogram model was the best fit for the spatio-temporal representation of soil moisture in both cokriging Figure A3 (a) and A4 (a)) and ordinary kriging (Figure A6 (a) and A6 (a)) for both survey days. The presence of nugget effect in the ordinary kriged soil moisture maps could be attributed to measurement errors (Kathuria et al. 2019). The maps obtained from cokriging (Figure 3.10a and 3.12a) revealed less smoothness in their depiction of soil moisture variation compared to the ordinary kriged maps (Figure 3.11a and 3.13a). The range values varied slightly between both interpolation techniques on both survey days indicating a slight variation in the spatial autocorrelation of soil moisture (Table 3.3).

The land use was generally dry with the highest soil moisture observed as a small pocket on the northern section of the map. The land use exhibited a strong spatial dependence on the first day and a moderate spatial dependence on the second day. The accuracies of the soil moisture map obtained from cross-validation were higher with cokriging (RMSE = 0.45 % and 0.47 % for day 1 and day 2 respectively) relative to ordinary kriging prediction (RMSE = 0.62 % and 1.72 % for day 1 and day 2 respectively) revealing the effectiveness of using EC_a as a covariate in creating more accurate soil moisture maps relative to ordinary kriging in this land use.

3.3.6.2 Field Road

The interpolated spatial maps of EC_a for the field road ranged between 0.05 – 0.2 dS m^{-1} for the two survey dates (Figures 3.8b and 3.9b). In this land use, spherical models produced the best fit for the spatio-temporal representation of EC_a in ordinary kriging for both days (Figure A1 (b) and A2 (b)). The model had a nugget effect of 0.2 and a range of 12 m on both survey days (Table 3.3). The lower nugget value on this land use compared to the agricultural land could be attributed to the local scale decrease in EC_a variation in the field road (Narjary et al. 2019). The RMSE obtained from cross-validation did not change between the first and second day (RMSE = 0.04 dS m^{-1}) (Table 3.3). The land use exhibited a strong spatial dependence on both survey days (nugget:sill = 8%) (Table 3.3). The field road generally had low EC_a scattered across the map with the highest EC_a found in the upper region of the map on both days (Figures 3.8b and 3.9b). This interpolated EC_a maps for the second survey date generally revealed lower EC_a values relative to the first survey date. A similar pattern was observed in the agricultural land as described above.

For soil moisture, the spherical variogram model presented the best fit in both cokriging (Figure A3 (b) and A4 (b)) and ordinary kriging (Figure A5 (b) and A6 (b)) for the first and second survey days. There were no nugget effects in both approaches (Table 3.3). Maps obtained from cokriging (Figures 3.10b and 3.12b) displayed less smoothness in their depiction of soil moisture variation compared to maps from ordinary kriging (Figures 3.11b and 3.13b). The ranges in soil moisture values obtained from both interpolation techniques did not differ between the two survey days (2 m) (Table 3.3). This suggests that the spatial autocorrelation of soil moisture was not significantly

affected by either interpolation technique or time. The accuracies of the soil moisture map obtained from cross-validation was higher in the cokriging prediction relative to ordinary kriging prediction for the first and second survey days (RMSE = 0.03 % and 0.45 % vs. RMSE = 0.49 % and 0.82 %, respectively) (Table 3.3). This revealed the effectiveness of using EC_a as a covariate in creating more accurate soil moisture maps relative to ordinary kriging in this land use. This result corroborates findings from Tarr et al. (2005) who reported superior effectiveness of cokriging relative to ordinary kriging for soil properties such as soil moisture and organic matter.

3.3.6.3 Natural Forest

The power variogram model (Figure A1 (c) and A2 (c)) displayed the best fit for the spatial representation of EC_a in ordinary kriging for the two survey days (Figures 3.8c and 3.9c). The variogram parameters did not change between survey days in this land use (Table 3.3). The model had a nugget effect of 0.2 and a range of 1 m in this land use (Table 3.3), suggesting the presence of spatial autocorrelation possibly due measurement errors when collecting EC_a measurements (Haining 2009; Liu et al. 2017). The land use exhibited moderate spatial dependence on both survey days (nugget:sill = 40%) (Table 3.3). The RMSE obtained from cross validation was lower on the first day (RMSE = 0.14 dS m^{-1}) compared to the second day (RMSE = 0.24 dS m^{-1}) (Table 3.3) indicating a reduction in prediction accuracy. This was possibly due to the higher soil moisture content on the first survey day relative to the second survey day (Table 3.2). Prediction accuracy of EC_a is expected to increase with soil moisture (Sadatcharam et al. 2020). The natural forest generally had the highest EC_a readings compared to the other land use conditions. This is consistent

with the higher soil organic matter in the natural forest compared to the other land use types. Soil organic matter improves nutrient retention (Lal 2020), cation exchange capacity (Wulanningtyas et al. 2021), moisture retention (Chalise et al. 2019) and electrical conductivity (Pouladi et al. 2019). Similar to the agricultural land and field road, the interpolated EC_a maps for the second survey date showed lower EC_a values than those for the first survey date.

For the first survey day, the spherical model produced the best fit for the spatial representation of soil moisture in cokriging (Figure A3 (c)) and ordinary kriging (Figure A5 (c)). On the other hand, the Gaussian model was the best fitting model for the ordinary and cokriging (Figure A4 (c)) for the second day. There were no nugget effects in both interpolation methods (Table 3.3). This could mean there were minimal errors associated with data collection (Lui et al. 2017). The maps obtained from cokriging (Figures 3.10c and 3.12c) revealed less smoothness and more local detail in its depiction of soil moisture variation compared to the ordinary kriged maps (Figures 3.11c and 3.13c). This is consistent with what was observed in the other land uses. The range values did not change (2 m) between interpolation methods on the first day (Table 3.3). A similar finding was seen on the second day (2.5 m) indicating that the spatial autocorrelation of soil moisture did not vary with interpolation technique but varied with time. This land use was wetter compared to the other land use conditions. The accuracies of the soil moisture map obtained from cross-validation was higher in the cokriging prediction (RMSE = 0.02 % and 0.18 % for day 1 and day 2 respectively) than in the ordinary kriging prediction (RMSE = 0.13 % and 0.25 % for day 1 and

day 2 respectively) (Table 3.3) revealing the effectiveness of using EC_a as a covariate in creating more accurate soil moisture maps relative to ordinary kriging in this land use.

Table 3.3 Geostatistical parameters for ordinary kriging and cokriging analysis and cross validation results (root mean square error) of apparent conductivity and soil moisture content for 20 Oct and 8 Nov. 2021 survey

Variables	First survey day						Second survey day					
	Interpolation technique	Model	Nugget	Sill	Range	RMSE	Interpolation technique	Model	Nugget	Sill	Range	RMSE
EC_a												
Agricultural land	Ordinary kriging	Spherical	0.3	1.5	19.2	0.05	Ordinary kriging	Gaussian	2.3	4.8	3.0	0.09
Field road		Spherical	0.2	2.5	12.0	0.04		Spherical	0.2	2.5	12.0	0.04
Natural forest		Power	0.2	0.5	1.0	0.14		Power	0.2	0.5	1.0	0.24
Soil moisture												
Agricultural land	Ordinary kriging	Spherical	6.2	10.2	8.0	0.13	Ordinary kriging	Spherical	6.2	10.2	8.0	0.25
Field road		Spherical	0.0	7.7	2.0	0.49		Spherical	0.0	7.0	2.0	1.72
Natural forest		Spherical	0.0	6.0	2.0	0.62		Gaussian	0.0	10.0	2.5	0.82
Agricultural land	Cokriging	Spherical	0.0	1.0	9.0	0.02	Cokriging	Spherical	11.0	13.0	9.0	0.18
Field road		Spherical	0.0	7.0	2.0	0.03		Spherical	0.0	9.4	8.0	0.45
Natural forest		Spherical	0.0	7.4	2.0	0.45		Gaussian	0.0	10.0	2.5	0.47

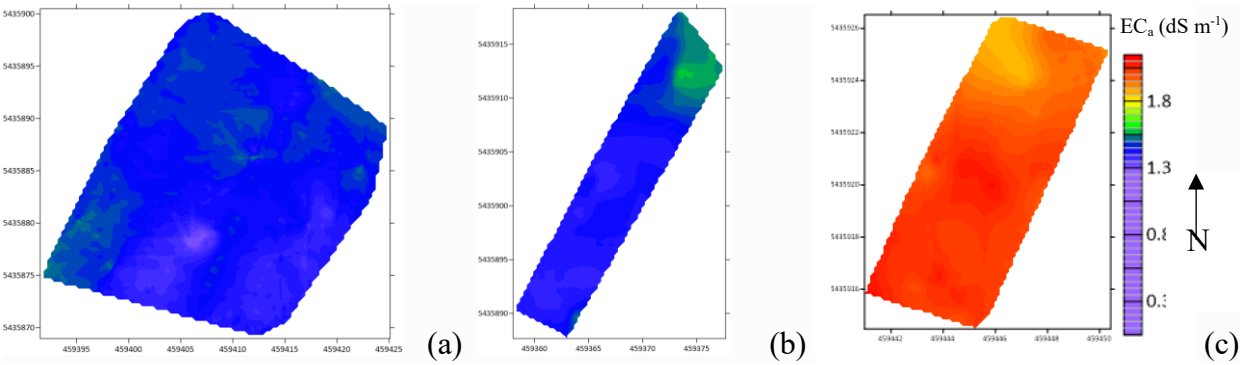

Figure 3.8: Spatial variability maps of apparent electrical conductivity (ECa) (a) Agricultural land; (b) Field road; (c) Natural forest obtained from ordinary kriging for first survey day.

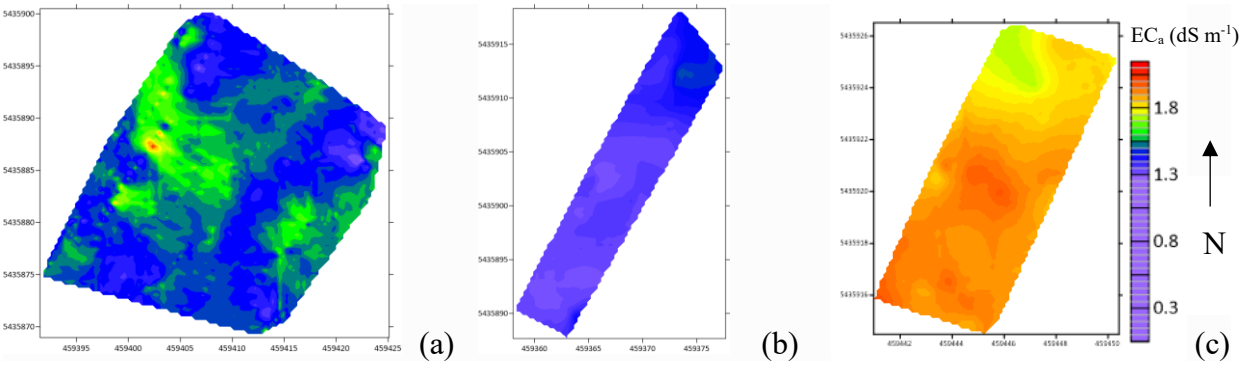

Figure 3.9: Spatial variability maps of apparent electrical conductivity (ECa) (a) Agricultural land; (b) Field road; (c) Natural forest obtained from ordinary kriging for second survey day.

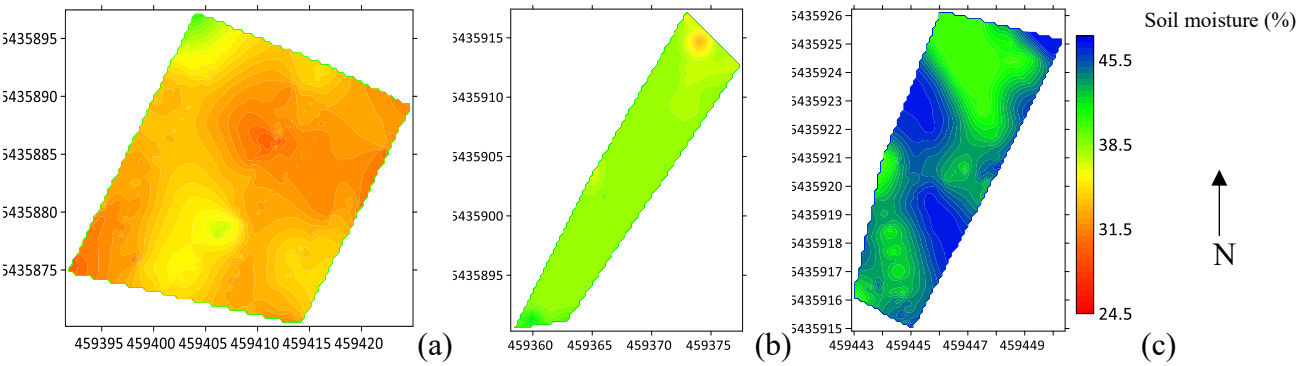

Figure 3.10: Spatial variability maps of soil moisture content (a) Agricultural land; (b) Field road; (c) Natural forest obtained from cokriging for first survey day with apparent electrical conductivity (ECa) as covariate.

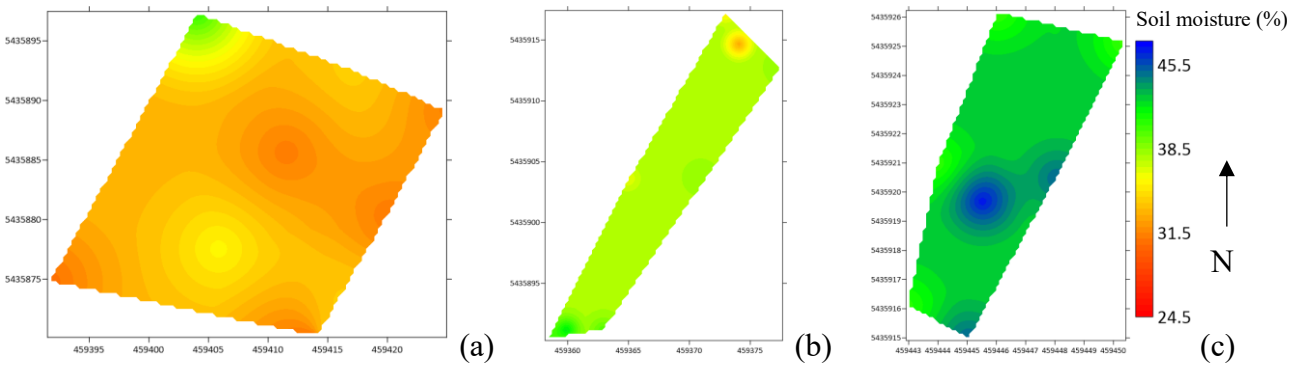

Figure 3.11: Spatial variability maps of soil moisture content (a) Agricultural land; (b) Field road; (c) Natural forest obtained from ordinary kriging for first survey day.

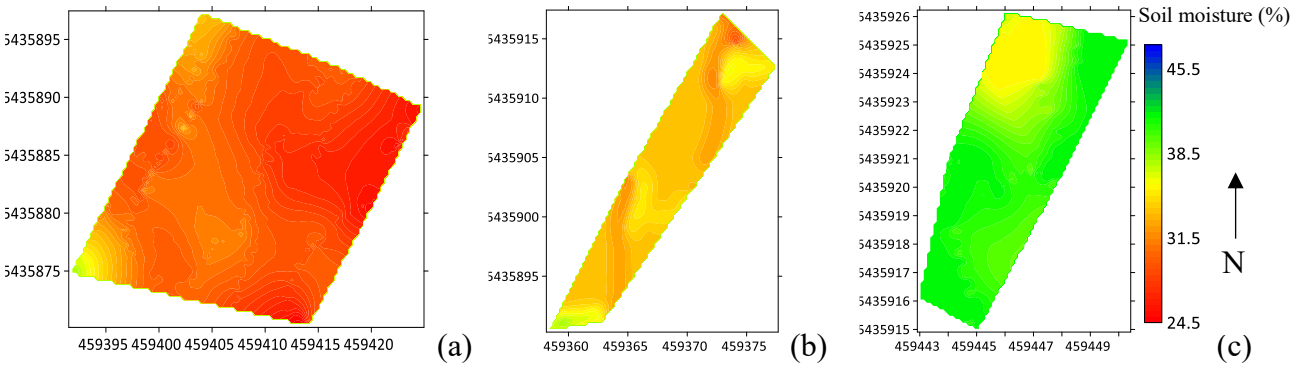

Figure 3.12: Spatial variability maps of soil moisture content (a) Agricultural land; (b) Field road; (c) Natural forest obtained from cokriging for second survey day with apparent electrical conductivity (ECa) as covariate.

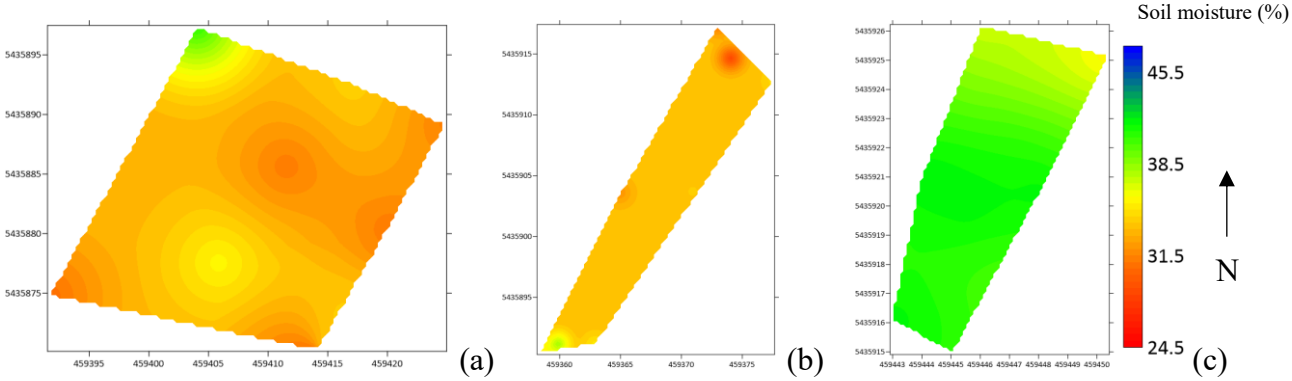

Figure 3.13: Spatial variability maps of soil moisture content (a) Agricultural land; (b) Field road; (c) Natural forest obtained from ordinary kriging for second survey day.

3.4 Conclusion

This study demonstrates that proximal surveys of EC_a using GEM-2 could be a helpful surrogate for assessing intra-field variability of soil moisture. This was achieved by analyzing the relationships between EC_a and soil moisture measurements from three different land use conditions (agricultural land, recently cleared natural forest and field road) on a boreal podzolic soil. The strong influence of soil moisture on EC_a under the different land use conditions from the generated linear regression was indicative that soil moisture was a major driver of EC_a in the study area. Mapping of soil moisture using cokriging with EC_a as a covariate produced more local detail than maps produced using ordinary kriging. There were improvements in the prediction accuracies of soil moisture maps when the cokriging technique was applied compared to the ordinary kriging. This suggests that EC_a obtained using EMI has the potential as a robust auxiliary variable for accurately predicting soil moisture in boreal podzolic soils. The best prediction was found in the natural forest, the land use type that had the strongest correlation between soil moisture and EC_a. These results suggest that cokriging of soil moisture with densely sampled EC_a as covariates improves the characterization accuracy of soil moisture variability in the study area. This study reveals the effectiveness of the georeferenced MF-EMI technique to rapidly assess intra-field variability under different land uses. Such surveys may rapidly map the spatial variability of intra-field soil moisture under different land use conditions. It is recommended that more studies should be carried out on other subregions for further validation.

3.5 Authors contribution statement

Clinton Mensah: Data curation, Formal analysis, Investigation, Methodology, Software, Validation, Visualization, Writing – original draft; **Yeukai Katanda:** Formal Analysis, Validation, Visualization, Writing – review & editing; **Mano Krishnapillai:** Methodology, Supervision, Validation, Writing – review & editing; **Mumtaz Cheema:** Resources, Validation, Writing – review & editing; **Lakshman Galagedara:** Conceptualization, Funding acquisition, Methodology, Project administration, Resources, Supervision, Validation, Writing – review & editing.

3.6 Funding statement

The authors would like to acknowledge the financial support from the Natural Science and Engineering Research Council Discovery Grant (NSERC-DG: RGPIN-2019-04614), Industry, Energy, and Technology of the Government of NL (IET Grant: 5404-1962-102) and the Memorial University of Newfoundland (MUN).

3.7 Acknowledgement

Special thanks to Dr. Dmitry Sveshnikov for the guidance and constructive comments given for the methodology and data analysis. We thank Sashini Pathirana and Salman Afzal for their assistance in collecting the EMI and soil moisture data, respectively. We also thank Sabrina Ellsworth, Dr. Vanessa Kavanagh and Adrian David Reid from the Department of Fisheries, Forestry and Agriculture of the Government of NL, Canada for providing necessary facilities and management of the Clean Tech Crop Rotation Experimental site at the Western Agriculture Center and Research Station in Pasadena, Newfoundland.

3.8 Conflicts of interest

"The authors declare no conflict of interest" in this experiment-based study. A comprehensive study design was prepared and executed without having any influence. The findings presented in this article were obtained from the experiments and compared with the published peer-reviewed journal articles' findings.

3.9 Data availability

Data generated or analyzed during this study are available from the corresponding author upon reasonable request.

Appendix 1

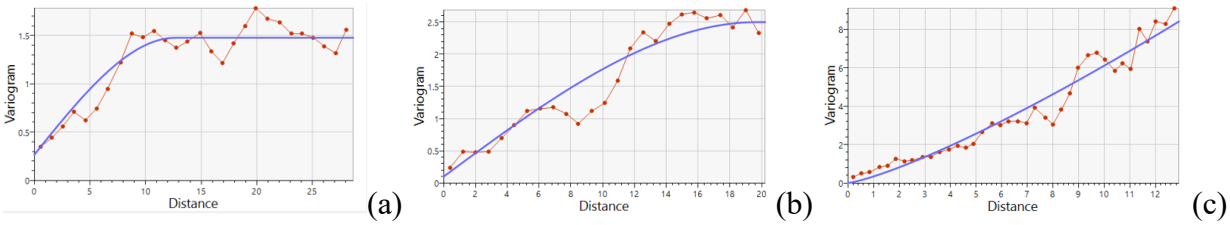

Figure A1: Variogram models of apparent electrical conductivity obtained from ordinary kriging for agricultural land (a), field road (b) and natural forest (c) for first survey day.

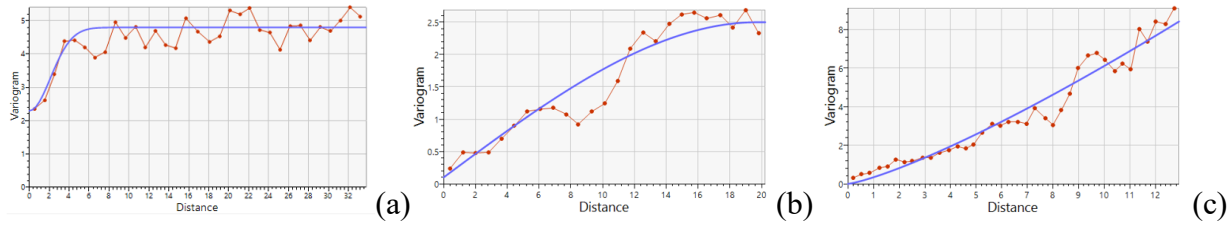

Figure A2: Variogram models of apparent electrical conductivity obtained from ordinary kriging for agricultural land (a), field road (b) and natural forest (c) for second survey day.

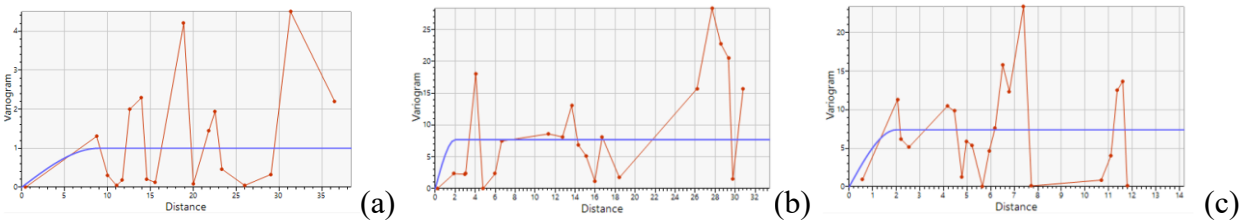

Figure A3: Variogram models of soil moisture obtained from cokriging for agricultural land (a), field road (b) and natural forest (c) for first survey day.

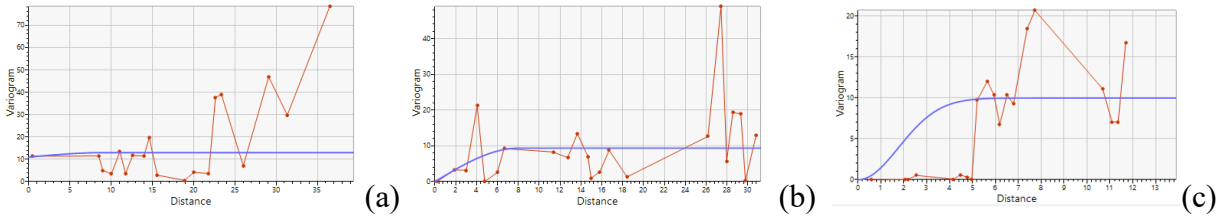

Figure A4: Variogram models of soil moisture obtained from cokriging for agricultural land (a), field road (b) and natural forest (c) for second survey day.

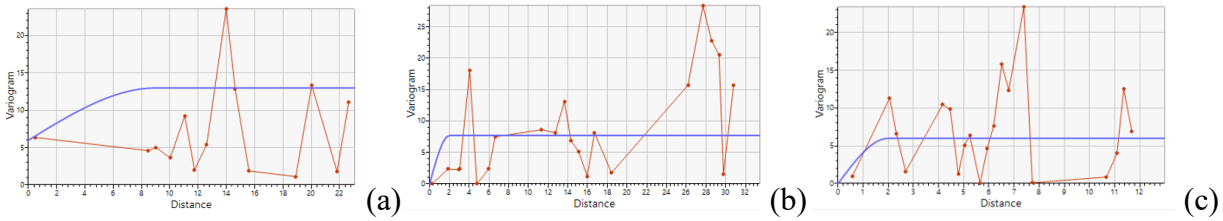

Figure A5: Variogram models of soil moisture obtained from ordinary kriging for agricultural land (a), field road (b) and natural forest (c) for first survey day.

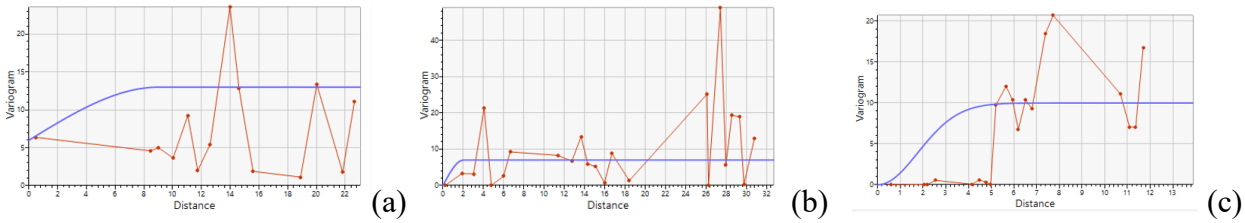

Figure A6: Variogram models of soil moisture obtained from ordinary kriging for agricultural land (a), field road (b) and natural forest (c) for second survey day.

3.10 References

Altdorff, D., Galagedara, L., Nadeem, M., Cheema, M. and Unc, A., 2018. Effect of agronomic treatments on the accuracy of soil moisture mapping by electromagnetic induction. Catena, 164, pp.96-106.

Altdorff, D., Sadatcharam, K., Unc, A., Krishnapillai, M. and Galagedara, L., 2020. Comparison of multi-frequency and multi-coil electromagnetic induction (EMI) for mapping properties in shallow podsolic soils. Sensors, 20(8), pp.2330.

Archie, G.E., 1942. The electrical resistivity log as an aid in determining some reservoir characteristics. Transactions of the AIME, 146(01), pp.54-62.

Atwell, M.A. and Wuddivira, M.N., 2019. Electromagnetic-induction and spatial analysis for assessing variability in soil properties as a function of land use in tropical savanna ecosystems. SN Applied Sciences, 1(8), pp.856.

Badewa, E., Unc, A., Cheema, M., Kavanagh, V. and Galagedara, L., 2018. Soil moisture mapping using multi-frequency and multi-coil electromagnetic induction sensors on managed podzols. Agronomy, 8(10), pp.224. Doi:https://doi.org/10.3390/agronomy8100224.

Bai, Y., Ochuodho, T.O. and Yang, J., 2019. Impact of land use and climate change on water-related ecosystem services in Kentucky, USA. Ecological Indicators, 102, pp.51-64.

Belkhiri, L., Tiri, A. and Mouni, L., 2020. Spatial distribution of the groundwater quality using kriging and co-kriging interpolations. Groundwater for Sustainable Development, 11, pp.100473.

Briggs, M.A., Wang, C., Day-Lewis, F.D., Williams, K.H., Dong, W. and Lane, J.W., 2019. Return flows from beaver ponds enhance floodplain-to-river metals exchange in alluvial mountain catchments. Science of the Total Environment, 685, pp.357-369.

Calamita, G., Perrone, A., Brocca, L., Onorati, B. and Manfreda, S., 2015. Field test of a multi-frequency electromagnetic induction sensor for soil moisture monitoring in southern Italy test sites. Journal of Hydrology, 529, pp.316-329.Doi:https://doi.org/10.1016/j.jhydrol.2015.07.023.

Carrière, S.D., Martin-StPaul, N.K., Doussan, C., Courbet, F., Davi, H. and Simioni, G., 2021. Electromagnetic induction is a fast and non-destructive approach to estimate the influence of surface heterogeneity on forest canopy structure. Water, 13(22), pp.3218.

Chalise, K.S., Singh, S., Wegner, B.R., Kumar, S., Pérez-Gutiérrez, J.D., Osborne, S.L., Nleya, T., Guzman, J. and Rohila, J.S., 2019. Cover crops and returning residue impact on soil organic carbon, bulk density, penetration resistance, water retention, infiltration, and soybean yield. Agronomy Journal, 111(1), pp.99-108.

Choi, M. and Jacobs, J.M., 2007. Soil moisture variability of root zone profiles within SMEX02 remote sensing footprints. Advances in Water Resources, 30(4), pp.883-896. https://doi.org/10.1016/j.advwatres.2006.07.007.

Corwin, D.L. and Lesch, S.M., 2005. Apparent soil electrical conductivity measurements in agriculture. Computers and Electronics in Agriculture, 46(1-3), pp.11-43.

Croquet, E.G., 2016. Late Wisconsinan paleosols and macrofossils in Chehalis Valley: paleoenvironmental reconstruction and regional significance (Doctoral dissertation, Science: Department of Earth Sciences).

Deidda, G.P., De Carlo, L., Caputo, M.C. and Cassiani, G., 2022. Frequency domain electromagnetic induction imaging: An effective method to see inside a capped landfill. Waste Management, 144, pp.29-40.

Drummond, S.T., Sudduth, K.A., Joshi, A., Birrell, S.J. and Kitchen, N.R., 2003. Statistical and neural methods for site–specific yield prediction. Transactions of the ASAE, 46(1), pp.5. Doi:10.13031/2013.12541.

Enakiev, Y.I., Bahitova, A.R. and Lapushkin, V.M., 2018. Microelements (Cu, Mo, Zn, Mn, Fe) in corn grain according to their availability in the fallow SOD-Podzolic soil profile. Bulgarian Journal of Agricultural Science, 24(2), pp.285-289.

Franzen, D.W., 2018. Soil variability and fertility management. Precision Agriculture Basics, pp.79-92.

Funes, I., Savé, R., Rovira, P., Molowny-Horas, R., Alcañiz, J.M., Ascaso, E., Herms, I., Herrero, C., Boixadera, J. and Vayreda, J., 2019. Agricultural soil organic carbon stocks in the north-eastern Iberian Peninsula: Drivers and spatial variability. Science of the Total Environment, 668, pp.283-294.

Gao, X., Wu, P., Zhao, X., Shi, Y., Wang, J. and Zhang, B., 2011. Soil moisture variability along transects over a well-developed gully in the Loess Plateau, China. Catena, 87(3), pp.357-367.

Gebrehiwot, S.G., Bewket, W., Mengistu, T., Nuredin, H., Ferrari, C.A. and Bishop, K., 2021. Monitoring and assessment of environmental resources in the changing landscape of Ethiopia: a focus on forests and water. Environmental Monitoring and Assessment, 193(10), pp.1-13.

Government of Newfoundland and Labrador, 2017. The way forward on agriculture. sector work plan. Retrieved 20 Nov. 2021. From https://www.gov.NF.ca/ffa/files/agriculture-Sector-Workplan_Final.pdf.

Guo, X., Fu, Q., Hang, Y., Lu, H., Gao, F. and Si, J., 2020. Spatial variability of soil moisture in relation to land use types and topographic features on hillslopes in the black soil (mollisols) area of northeast China. Sustainability, 12(9), pp.3552.

Guo, Y., Boughton, E.H., Liao, H.L., Sonnier, G. and Qiu, J., 2023. Direct and indirect pathways of land management effects on wetland plant litter decomposition. Science of the Total Environment, 854, pp.158789.

Haining, R.P., 2009. Spatial autocorrelation and the quantitative revolution. Geographical Analysis, 41(4), pp.364-374.

Kathuria, D., Mohanty, B.P. and Katzfuss, M., 2019. A nonstationary geostatistical framework for soil moisture prediction in the presence of surface heterogeneity. Water Resources Research, 55(1), pp.729-753.

Kaufmann, M.S., von Hebel, C., Weihermüller, L., Baumecker, M., Döring, T., Schweitzer, K., Hobley, E., Bauke, S.L., Amelung, W., Vereecken, H. and van der Kruk, J., 2020. Effect of fertilizers and irrigation on multi-configuration electromagnetic induction measurements. Soil Use and Management, 36(1), pp.104-116.

Lal, R., 2020. Soil organic matter and water retention. Agronomy Journal, 112(5), pp.3265-3277.

Lawrence, I. and Lin, K., 1989. A concordance correlation coefficient to evaluate reproducibility. Biometrics, pp.255-268.

Lück, E., Guillemoteau, J., Tronicke, J., Klose, J. and Trost, B., 2022. Geophysical sensors for mapping soil layers–a comparative case study using different electrical and electromagnetic sensors. in information and communication technologies for agriculture—Theme I: Sensors pp.267-287. Cham: Springer International Publishing.

Liu, L.L., Cheng, Y.M., Jiang, S.H., Zhang, S.H., Wang, X.M. and Wu, Z.H., 2017. Effects of spatial autocorrelation structure of permeability on seepage through an embankment on a soil foundation. Computers and Geotechnics, 87, pp.62-75.

Ma, R., McBratney, A., Whelan, B., Minasny, B. and Short, M., 2011. Comparing temperature correction models for soil electrical conductivity measurement. Precision Agriculture, 12, pp.55-66.

Machado, F.C., Montanari, R., Shiratsuchi, L.S., Lovera, L.H. and Lima, E.D.S., 2015. Spatial dependence of electrical conductivity and chemical properties of the soil by electromagnetic induction. Revista Brasileira de Ciência do Solo, 39, pp.1112-1120.

Moral, F.J., Terrón, J.M. and Da Silva, J.M., 2010. Delineation of management zones using mobile measurements of soil apparent electrical conductivity and multivariate geostatistical techniques. Soil and Tillage Research, 106(2), pp.335-343. Doi:https://doi.org/10.1016/j.still.2009.12.002.

Morris, L.A., 2004. Soil biology and tree growth-soil organic matter forms and functions. Elsevier, pp.1201-1207

Naimi, S., Ayoubi, S., Zeraatpisheh, M. and Dematte, J.A.M., 2021. Ground observations and environmental covariates integration for mapping of soil salinity: a machine learning-based approach. Remote Sensing, 13(23), pp.4825.

Niu, C.Y., Musa, A. and Liu, Y., 2015. Analysis of soil moisture condition under different land uses in the arid region of Horqin sandy land, northern China. Solid Earth, 6(4), pp.1157-1167. Doi:https://doi.org/10.5194/se-6-1157-2015.

Pouladi, N., Møller, A.B., Tabatabai, S. and Greve, M.H., 2019. Mapping soil organic matter contents at field level with Cubist, Random forest, and kriging. Geoderma, 342, pp.85-92.

Robinson, D.A., Lebron, I., Lesch, S.M. and Shouse, P., 2004. Minimizing drift in electrical conductivity measurements in high temperature environments using the EM-38. Soil Science Society of America Journal, 68(2), pp.339-345. Doi: https://doi.org/10.2136/sssaj2004.3390.

Rostami, A.A., Karimi, V., Khatibi, R. and Pradhan, B., 2020. An investigation into seasonal variations of groundwater nitrate by spatial modelling strategies at two levels by kriging and co-kriging models. Journal of Environmental Management, 270, pp.110843.

Sadatcharam, K., 2019. Assessing potential applications of multi-coil and multi-frequency electromagnetic induction sensors for agricultural soils in western Newfoundland. Master's thesis. Memorial University of Newfoundland.

Sadatcharam, K., Altdorff, D., Unc, A., Krishnapillai, M. and Galagedara, L., 2020. Depth Sensitivity of Apparent Magnetic Susceptibility Measurements using Multi-coil and Multi-frequency Electromagnetic Induction. Journal of Environmental and Engineering Geophysics, 25(3), pp.301-314.

Sheets, K.R. and Hendrickx, J.M., 1995. Noninvasive soil water content measurement using electromagnetic induction. Water Resources Research, 31(10), pp.2401-2409.

Simon, F.X., Pareilh-Peyrou, M., Buvat, S., Mayoral, A., Labazuy, P., Kelfoun, K. and Tabbagh, A., 2020. Quantifying multiple electromagnetic properties in EMI surveys: A case study of hydromorphic soils in a volcanic context–The Lac du Puy (France). Geoderma, 361, pp.114084.

Sówka, I., Badura, M., Pawnuk, M., Szymański, P. and Batog, P., 2020. The use of the GIS tools in the analysis of air quality on the selected University campus in Poland. Archives of Environmental Protection, 46(1), pp.100-106.

Srivastava, P.K., Pandey, P.C., Petropoulos, G.P., Kourgialas, N.N., Pandey, V. and Singh, U., 2019. GIS and remote sensing aided information for soil moisture estimation: A comparative study of interpolation techniques. Resources, 8(2), pp.70.

Stavi, I., 2019. Seeking environmental sustainability in dryland forestry. Forests, 10(9), pp.737.

Susha, S.U., Singh, D.N. and Baghini, M.S., 2014. A critical review of soil moisture measurement. Measurement, 54, pp.92-105. https://doi.org/10.1016/j.measurement.2014.04.007.

Tang, S., Farooque, A.A., Bos, M. and Abbas, F., 2020. Modelling DUALEM-2 measured soil conductivity as a function of measuring depth to correlate with soil moisture content and potato tuber yield. Precision Agriculture, 21(3), pp.484-502

Tarr, A.B., Moore, K.J., Bullock, D.G., Dixon, P.M. and Burras, C.L., 2005. Improving map accuracy of soil variables using soil electrical conductivity as a covariate. Precision Agriculture, 6(3), pp.255-270.

Tiwari, S., Singh, C., Boudh, S., Rai, P.K., Gupta, V.K. and Singh, J.S., 2019. Land use change: A key ecological disturbance declines soil microbial biomass in dry tropical uplands. Journal of Environmental Management, 242, pp.1-10.

Topp, G.C., Davis, J.L. and Annan, A.P., 1980. Electromagnetic determination of soil water content: Measurements in coaxial transmission lines. Water Resources Research, 16(3), pp.574-582. Doi:https://doi.org/10.1029/WR016i003p00574.

Von Hebel, C., Van Der Kruk, J., Huisman, J.A., Mester, A., Altdorff, D., Endres, A.L., Zimmermann, E., Garré, S. and Vereecken, H., 2019. Calibration, conversion, and quantitative multi-layer inversion of multi-coil rigid-boom electromagnetic induction data. Sensors, 19(21), pp.4753.

Wang, J., Sun, Q., Shang, J., Zhang, J., Wu, F., Zhou, G. and Dai, Q., 2020. A new approach for estimating soil salinity using a low-cost soil sensor in situ: A case study in saline regions of China's East Coast. Remote Sensing, 12(2), pp.239.

Warrick, A.W., 1988. Additional solutions for steady-state evaporation from a shallow water table. Soil Science, 146, pp.63-66.

Wu, W., Chen, G., Meng, T., Li, C., Feng, H., Si, B. and Siddique, K.H., 2023. Effect of different vegetation restoration on soil properties in the semi-arid Loess Plateau of China. Catena, 220, pp.106630.

Wuddivira, M.N., Robinson, D.A., Lebron, I., Bréchet, L., Atwell, M., De Caires, S., Oatham, M., Jones, S.B., Abdu, H., Verma, A.K. and Tuller, M., 2012. Estimation of soil clay content from hygroscopic water content measurements. Soil Science Society of America Journal, 76(5), pp.1529-1535.

Wulanningtyas, H.S., Gong, Y., Li, P., Sakagami, N., Nishiwaki, J. and Komatsuzaki, M., 2021. A cover crop and no-tillage system for enhancing soil health by increasing soil organic matter in soybean cultivation. Soil and Tillage Research, 205, pp.104749.

Xu, G., Huang, M., Li, P., Li, Z. and Wang, Y., 2021. Effects of land use on spatial and temporal distribution of soil moisture within profiles. Environmental Earth Sciences, 80, pp.1-12.

Yu, B., Liu, G., Liu, Q., Wang, X., Feng, J. and Huang, C., 2018. Soil moisture variations at different topographic domains and land use types in the semi-arid Loess Plateau, China. Catena, 165, pp.125-132. https://doi.org/10.1016/j.catena.2018.01.020.

Zhou, Q., Wu, Y., Guo, Z., Hu, J. and Jin, P., 2020. A generalized hierarchical co-Kriging model for multi-fidelity data fusion. Structural and Multidisciplinary Optimization, 62(4), pp.1885-1904.

Co-authorship statement for study-two

A manuscript based on chapter 4 (Study-two), entitled "*Using multi-frequency and multi-coil electromagnetic induction sensors to improve soil moisture prediction accuracy in different land use*" submitted to Environmental Research Communication (ERC-101303) of IOPscience and under review. Clinton Mensah, the primary author of the thesis, was supported by Dr. Galagedara (supervisor) as the corresponding and fifth author. Dr. Katanda (committee member) and Dr. Krishnapillai (co-supervisor) were the second and third authors, respectively. Dr. Cheema, a collaborator at the Memorial University of Newfoundland was the fourth author. The research design for the work in Chapter 4 was developed by Dr. Galagedara with input from all members of the group. Mr. Mensah was responsible for the data collection, analysis, interpretation, and writing of the manuscript. Dr. Katanda provided guidance on statistical analysis, data interpretation, and manuscript writing. Dr. Krishnapillai and Dr. Cheema provided inputs for the field experiment, data interpretation, and manuscript editing.

[2]

[2] **foot note:** "Mensah, C., Galagedara, L., Katanda, Y., Krishnapillai, M. and Cheema, M. 2023. Using multi-frequency and multi-coil electromagnetic induction sensors to improve soil moisture prediction accuracy in different land use. CSBE/SCGAB AGM and Technical Conference, 23-26 July 2023, Lethbridge, Alberta, Canada (Oral - Accepted)".

CHAPTER FOUR: Study two

Using multi-frequency and multi-coil electromagnetic induction sensors to improve soil moisture prediction accuracy in different land use.

Clinton Mensah [1], Yeukai Katanda[1], Mano Krishnapillai [1], Mumtaz Cheema [1], Lakshman Galagedara [1*]

[1] School of Science and the Environment, Memorial University of Newfoundland and Labrador, Corner Brook, NL A2H 5G4, Canada
* Corresponding author: lgalagedara@grenfell.mun.ca

Abstract

Investigating the shallow depth of podzolic soils is challenging due to its complex nature. Near-surface geophysical techniques, such as electromagnetic induction (EMI), can significantly help investigate podzolic soils. Multi-coil (MC-EMI) and multi-frequency (MF-EMI) sensors were selected to maximize soil moisture (SMC) prediction in this study. The objectives of this study were (i) comparing apparent electrical conductivity (EC_a) measurements from the MC and MF-EMI sensors under different land use conditions. (ii) investigating the spatial variation of apparent electrical conductivity (EC_a), soil moisture content (SMC), texture, soil organic matter (SOM), and bulk density (BD) under different land use conditions (iii) using statistical and geostatistical analysis to evaluate the effectiveness of EC_a measurements in characterizing SMC under different land use conditions, taking into consideration the texture, SOM, and BD contents in each land use. The results of the study showed that MC-EMI sensors had more coil orientations showing statistically significant relations (p-value $\leq$ 0.05) with SMC relative to the MF-EMI sensor. Multiple linear regression (MLR) models were also shown to be more effective in representing SMC variations (higher coefficient of determination and lower root mean square error) than simple

linear regression models. MC-EMI sensors provided better predictions of SMC than the MF-EMI sensor, likely because the differences in sampling depths between the TDR measured SMC and MF-EMI sensor were much greater than those between TDR measured SMC and MC-EMI sensor. Lastly, cokriging of measured SMC offered more accurate maps than cokriging of predicted SMC obtained from MLR across different land use conditions. This study shows that EMI has the potential as a robust technique for accurately predicting soil moisture in boreal podzolic soils.

Keywords: apparent electrical conductivity, electromagnetic induction, multi-frequency, multi-coil.

4.1 Introduction

Soil properties vary at diverse spatial scales mainly due to factors such as soil management (Kilic et al. 2012), and land use (Saglam and Dengiz, 2012). Understanding how soil properties respond to different agricultural management practices is crucial in optimizing agricultural operations and inputs. Understanding spatial variations can be achieved by applying a suite of advanced information, data analysis, and communication technologies such as remote sensing (geophysical techniques), geographic information systems (GIS), global positioning systems (GPS), and artificial intelligence (Sishodia et al. 2020). Conventional methods of sampling and analyzing soil properties such as moisture content (SMC), texture, organic matter (SOM), and bulk density (BD) to understand spatial variability tend to be destructive, time consuming and expensive. Consequently, these methods can hinder timely decision-making due to the sparse representation of the desired soil property's spatial variation (Allred et al. 2008). New geophysical techniques,

such as electromagnetic induction (EMI) provides a rapid, reliable, and non-destructive assessment of surface soil properties pertinent to crop growth at small and large scales (Farzamian et al. 2019; Narjary et al. 2019). This led to use of a wide range of portable EMI sensors including the EM-31, EM-34, EM-61, CMD-mini-explorer, and the GEM-2 (Buta et al. 2019).

EMI technique operates by inducing an alternating current (EM waves in kHz) via the primary electromagnetic field generated from the transmitting coil of the EMI sensor and measuring the resultant secondary field from the receiving coil on the sensor (Von Hebel et al. 2019). The amplitude, phase differences, and inter-coil spacing between the primary and resultant fields are then used to determine an "apparent" value for soil electrical conductivity (EC_a) (McNeill 1980). EC_a is a robust and easily measurable soil parameter that is correlated with other key soil parameters such as SMC (Nocco et al. 2019), texture (Grubbs et al. 2019), SOM (Grubbs et al. 2019), and BD (Al Rashid et al. 2018) and can be used to improve the estimation of these soil properties when a spatial correlation is developed. However, developing relationships between EC_a and soil properties are a complex task due to multicollinearity between several predictor soil properties. Multicollinearity is a phenomenon that can lead to unreliable results when conducting statistical analyses, such as soil studies in which soil properties such as BD, SOM, and soil texture are measured. This can occur when soil properties are measured in different locations or at different times, thus presenting the issue of multicollinearity that can affect the quality of results. To reduce the effects of multicollinearity, methods such as principal component analysis, partial least squares regression, and ridge regression are employed. Furthermore, multiple linear regression (MLR) models with interaction terms can be used to identify multicollinearity between predictor variables. Additionally, multivariate statistical and geostatistical methods such as MLR and cokriging can be

utilized to improve estimates of soil properties by integrating EC_a measured with EMI sensors as a covariate. Hence, due to its potential to produce unreliable results, multicollinearity must be addressed to ensure accurate analyses.

EMI sensors, specifically the MF sensors have one coil separation and multiple operating frequencies, whereas MC sensors have a fixed frequency and multiple coil separations (Altdorff et al. 2020). In the MF sensor the magnitude of the selected operating frequency is inversely proportional to the depth of investigation (DOI) (Badewa et al. 2018; Sadatcharam et al. 2019). Thus, a higher operating frequency results in shallower DOI and higher data resolution of the mapped area. For the MC sensor, the DOI is dependent on the coil separation thus, the higher the inter-coil spacing between the transmitter and receiver coils, the higher the depth of investigation and *vice versa*. Due to lower operating frequencies, MF sensors can operate at higher DOIs compared to MC sensors (Sadatcharam et al. 2019). Both sensors can be configured to operate in two coil orientations, horizontal or vertical dipole mode. The DOI for the vertical dipole mode is approximately twice of that in the horizontal dipole mode (McNeill 1980). The choice of a sensor is dependent on several factors such as the depth resolution of the integral signals and its adaptation to outside temperatures (Sadatcharam 2019), and both EMI sensors employed in this study have shown to satisfy these criteria. EMI sensors could be a useful tool when delineating soil properties in the growing agricultural industry in Newfoundland and Labrador (NL), Canada.

The NL provincial government is bolstering the growth of local food production by committing substantial areas of the boreal forests into agricultural fields (Government of Newfoundland and Labrador 2017). Using rapid and non-destructive tools such as EMI sensors to characterize the

spatial variability of vital soil properties can support the timely decision making and development of recommendations for site-specific management practices. This study investigates the role of EMI sensors for mapping EC_a under different land use conditions and agricultural management practices. Specifically, this work aims to (i) compare EC_a data generated from multi-coil (MC) and multi-frequency (MF) EMI data, (ii) inspect the spatial variation of EC_a, SMC, texture, SOM, and BD under different land use and management practices, and (iii) evaluate the effectiveness of EC_a measurement to characterize SMC under agricultural land, field road and natural forest by considering the texture, SOM, and BD contents in each land use in Western NL, Canada. This work is important for supporting researchers, policy makers, and land managers with valuable information that can facilitate land use planning, site specific management and developing agricultural management recommendations to enhance food production in the province.

4.2 Materials and methods

4.2.1 Study area

This study was conducted on three land use conditions: an agricultural field, a natural forest, and a field road at the Western Agriculture Center and Research Station, Pasadena (49.0130° N, 57.5894° W), NL, Canada (Figure 4.1). The Department of Fisheries, Forestry, and Agriculture, Government of NL manages the study site. The soil at the study site was classified as a reddish-brown to brown Podzol developed on a gravelly sandy fluvial deposit with >100 cm depth to bedrock and a 2% – 5% slope (Croquet 2016). The area of the agricultural land considered was 924 m^2 and included three oats/peas. The field road was adjacent to the agricultural land and 240 m2 in area, serving as access year crop rotation of corn, with canola, faba bean, wheat, and for

equipment, vehicles, and people to the other parts of the field. A 50 m^2 area was selected from a recently cleared natural forest to compare its investigated soil properties data with the other land use conditions of interest (agricultural land and field road) (Figure 4.1). The area received a total rainfall of 409 mm and had an average mean temperature of 8.18 °C (Figure 4.2) based on three-month data (1 Sep. – 30 Nov. 2021) from the nearby Deer Lake weather station A. (http://climate.weather.gc.ca.). The daily total precipitation and temperature (minimum, maximum and mean) data obtained from Deer Lake weather station A were used to calculate the daily PET. Potential evapotranspiration (PET) was calculated using the modified Hargreaves-Samani equation (Equation 4.1) for the Deer Lake weather station A (Perera, 2021).

$$PET = 0.0018 \frac{Ra}{\lambda} (T_{max} - T_{min})^{0.5411} (T_{mean} + 19.6605) \quad \text{Equation 4.1}$$

where T_{max} is the daily maximum temperature, T_{min} is the daily minimum temperature, T_{mean} is the daily mean temperature, Ra is the extraterrestrial radiation ($MJ/m^2/day$), and λ is the latent heat of vaporization = 2.45 (MJ/kg).

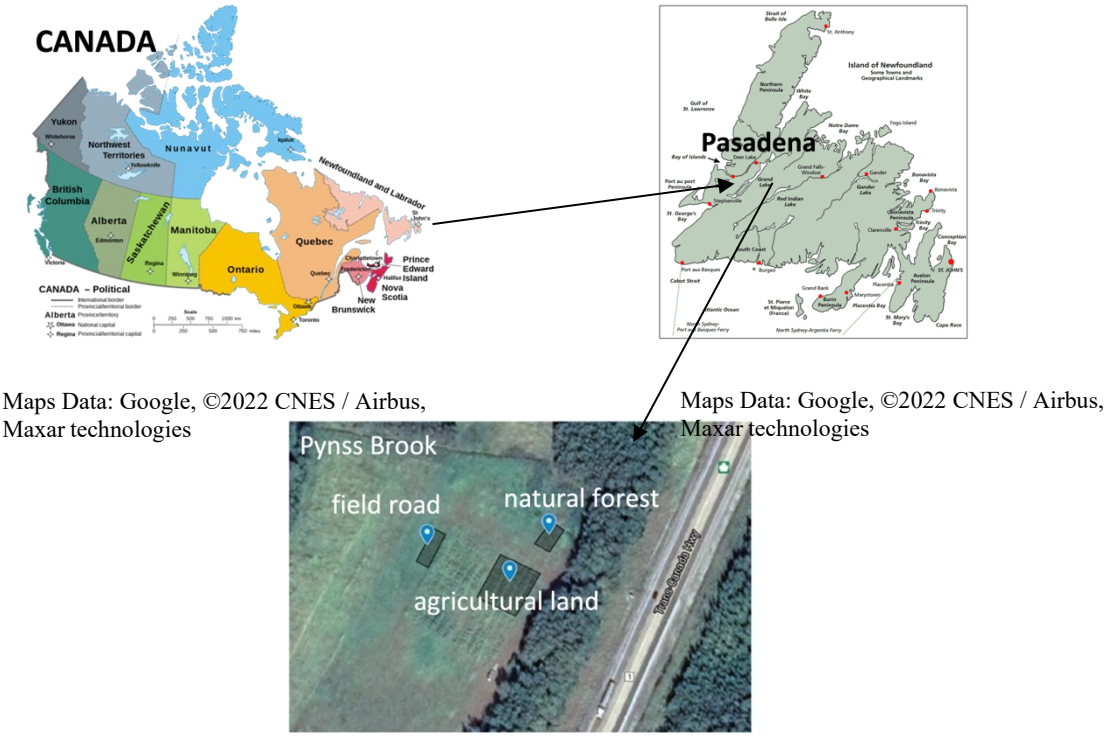

Figure 4.1: The location of the different land use conditions in Western Agriculture Center and Research Station, Pasadena, Newfoundland and Labrador, Canada (49.0130° N, 57.5894° W).

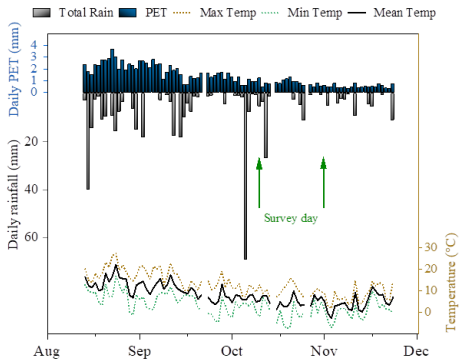

*Max Temp – Maximum Temperature, Min Temp – Minimum Temperature, PET – Potential Evapotranspiration, Mean Temp – Mean Temperature

Figure 4.2: Daily total rainfall, potential evapotranspiration (PET) and mean temperature from Aug. 2021 to Nov. 2021 for the study area from Deer Lake weather station A.

4.2.2 Soil sampling and analysis

Soil samples were collected at a depth of 0 – 20 cm (Figure 4.3) and analysed for a variety of properties, including texture (by hydrometer method), SOM (by loss on ignition), SMC and BD for the different land uses using protocols from Carter and Gregorich (2007). SMC was measured using time domain reflectometry (TDR) by vertically installing a 20 cm probe at each sampling time. For each sampling location, TDR data were collected at 9 different points, and the average value was used.

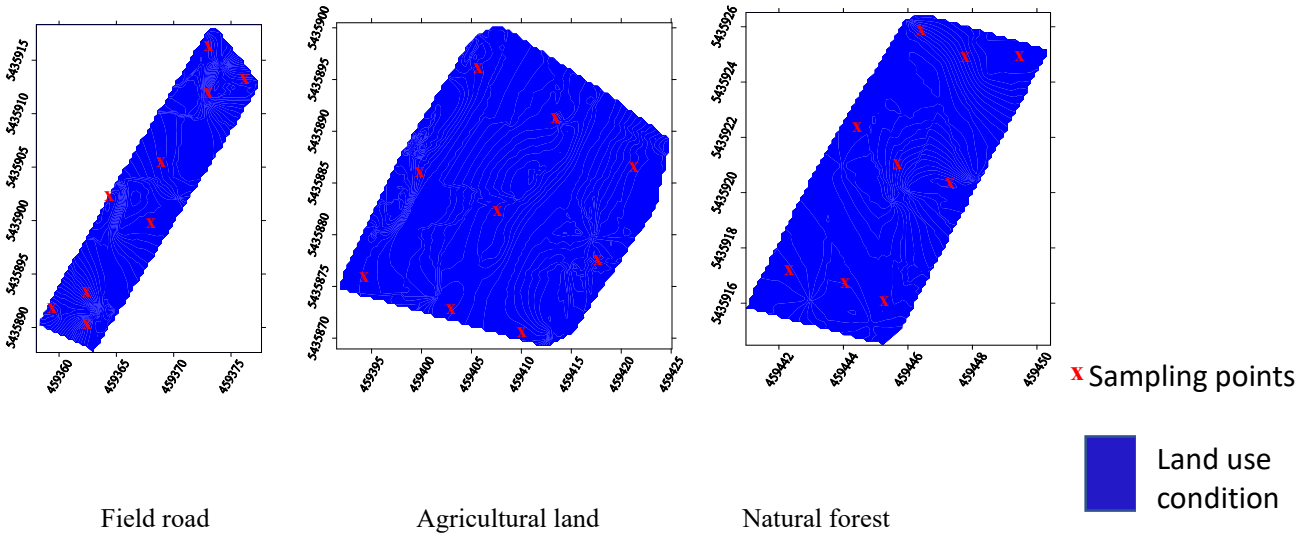

Figure 4.3: The sampling points of the different land use conditions in Western Agriculture Center and Research Station, Passadena, Newfoundland and Labrador, Canada.

4.2.3 Electromagnetic induction survey

We used CMD-mini-explorer (multi-coil (MC)) and the GEM-2 (multi-frequency (MF)) EMI sensors to map soil spatial and temporal variability of $EC_{a.}$ EMI surveys were conducted using both sensors across the different land use conditions on 20 Oct., 11 Nov. 2021. Both sensors were operated in the horizontal and vertical coplanar coil orientations as done by previous researchers in the same area (Altdorff et al. 2018; Badewa et al. 2018; Sadatcharam et al. 2020). All three coils were simultaneously used when employing the CMD mini-explorer while four different frequencies (2.8, 18.3, 38.3, and 80.0 kHz) were manually set to simultaneously measure soil EC_a when using the GEM-2 MF–EMI sensor. The theoretical depth of investigation (DOI) for the CMD mini-explorer at three coils spacing (0.32, 0.71, and 1.18 m) was 25, 50, and 90 cm and 50, 100, and 180 cm for VCP and HCP coil orientations, respectively (GF instruments, Brno, Czech Republic). In the GEM-2 sensor, the DOI for the GEM-2 sensor at coil separation 1.66m are 125 and 250 cm for VCP and HCP coil orientations, respectively (Geophex, Ltd., Raleigh, USA). The selected frequencies have been reported to be suitable for shallow surface soil investigations (Won et al. 1996). The EMI surveys were carried out in a bi-directional order over the three land use conditions while maintaining a 1 m line spacing. A global positioning system (GPS) was attached to the EMI sensors to enable the collection of georeferenced data, thus the production of georeferenced maps. Before each survey, the instrument was warmed up for at least 30 min for temperature adaptation to prevent data drift and ensure high-quality data, as protocols developed by Robinson et al. (2004).

Soil temperature was measured at the 0 – 20 cm depth for all three land use conditions using a soil temperature probe. The "Sheets and Hendrickx temperature correction model" adopted from Sheets and Hendrickx (1995) was used to correct soil temperature (Equation 4.2).

$$EC_{25} = EC_t \times (0.4470 + 1.4034\, e^{-t/26.815}) \quad \text{Equation 4.2}$$

where EC_t is the EC_a data collected at measured soil temperature (°C), EC_{25} is the temperature corrected EC_a at 25°C, and t is the soil temperature. Negative values observations were considered noise and subsequently eliminated.

4.2.4 Statistical analysis

Descriptive statistics and analysis of variance (ANOVA) of measured EC_a, BD, SMC, SOM, and texture were carried out under different land use and management practices using Minitab (Minitab 17 Statistical Software 2010). The residuals for all parameters were tested for normality using the Kolmogorov-Smirnov normality test. Pearson's correlation analysis was performed to determine the strength of the correlation between EC_a and the other soil properties under different land use conditions. The study area in question was characterized by a low clay content and a rocky nature, which impeded the correlation between the electrical conductivity of the soil (EC_a) and its other properties. It is common knowledge that soil properties are often related, but the unique geological conditions of this particular research site complicated the attempts to make such a connection. Furthermore, the implications of this finding are significant as it can potentially provide insight into the soil conditions of the region and their impact on overall soil quality; hence, a 90% confidence interval was used to assess the precision of estimated statistics in this study. A 90% confidence interval has also been used been used by Badewa et al. (2018) to examine the strength

of the EC_a – SMC relationship. To determine the attributes, which were the most influencing predictors of EC_a, MLR was performed using backward elimination of least important variables. The MLR equations obtained from the first survey day data were used to predict SMC for the second survey day under each land use. The measured SMC using TDR on the second day and the predicted SMC by employing MLR models were compared using a 1:1 plot and root mean square error (RMSE). The slope and the intercept of the prediction lines of measured and predicted SMC under each land use were compared statistically with those of the 1:1 line.

Pseudoreplication is a common problem in soil studies, as it occurs when a single sample is used to represent multiple plots or treatments. This can lead to inaccurate results, as the sample may not be representative of the entire area. To avoid pseudoreplication, multiple samples were taken from each plot and analyzed separately. Pseudo-replication was not an issue, and no statistical assumptions were violated. To further explore the potential of EC_a, the MLR equation was rearranged to make EC_a the response variable while the other variables remained temporally unchanged. Despite being a predictor variable, it was used to assess its potential as a response variable. To further explore the effect of properties such as texture, BD and SOM on SMC is outside the scope of this study.

The variance inflation factor (VIF) obtained from each regression model was used to identify if multi-collinearity existed in the models. The VIF measures the amount of variance of the estimated regression coefficient that is magnified if the independent variables are correlated. VIF is calculated as

$$\frac{1}{1-R^2}$$ Equation 4.3

A VIF =1 indicates that multi-collinearity does not exist between predictors, whereas VIFs ranging between 1 and 5 indicate moderately correlated variables. On the other hand, VIF greater than 5 indicate multi-collinearity among the predictors (Shrestha et al. 2020). If multicollinearity exists, further analyses, such as principal component analysis, partial least squares regression, and ridge regression can be employed to reduce the effects of the multicollinearity and gain more accurate results. All statistical analyses were performed with Minitab 17 (Minitab 17 Statistical Software 2010).

4.2.5 Geostatistical analysis

Cokriging with EC_a as a covariate was performed on the measured SMC and EC_a as a covariate on predicted SMC data from the most accurate generated regression models. Cokriging uses multiple datasets to investigate graphs of cross-correlation and autocorrelation (Equation 4.4).

$$\sum^{n}_{vl=1} \sum^{n_i}_{i=1} \lambda_{il}\, \lambda_{lv} \gamma(x_i,x_j) - \mu_v = \gamma_{uv}(x_i,x_p) \text{ where } j = 1, \ldots, n \text{ and } u = 1, ..., v$$

$$\sum^{nl}_{i=1} \lambda_{il} = \begin{matrix} 1 & 1 = u \\ 0 & 1 \neq u \end{matrix} \qquad \text{Equation 4.4}$$

where u and v are the target and covariate variables, respectively. The two variates u and v are cross-correlated, and the covariate contributes to the estimation of the target variate.

Variograms describing the spatial dependence of a spatially random field were used to analyze the spatial structure of SMC. Several variogram models (linear, exponential, circular, gaussian, spherical, and power model) were considered when performing cokriging for creating SMC maps. Each variogram was characterized by three parameters: range, sill, and nugget. The nugget/sill ratios were used to characterize the spatial dependence of observations. Spatial dependence was

characterized as strong (below 25%), moderate (25% and 75%), or weak (above 75%). The variogram model with the lowest RMSE based on the cross-validation (jackknifing) results were selected (Sówka et al. 2020). The leave-one-out cross-validation works by singly removing each point in the sampling scheme and predicting its value based on kriging the remaining data. All variograms were assumed to be isotropic. Interpolated maps were then created using Surfer 24 (Golden Software Inc. 2022).

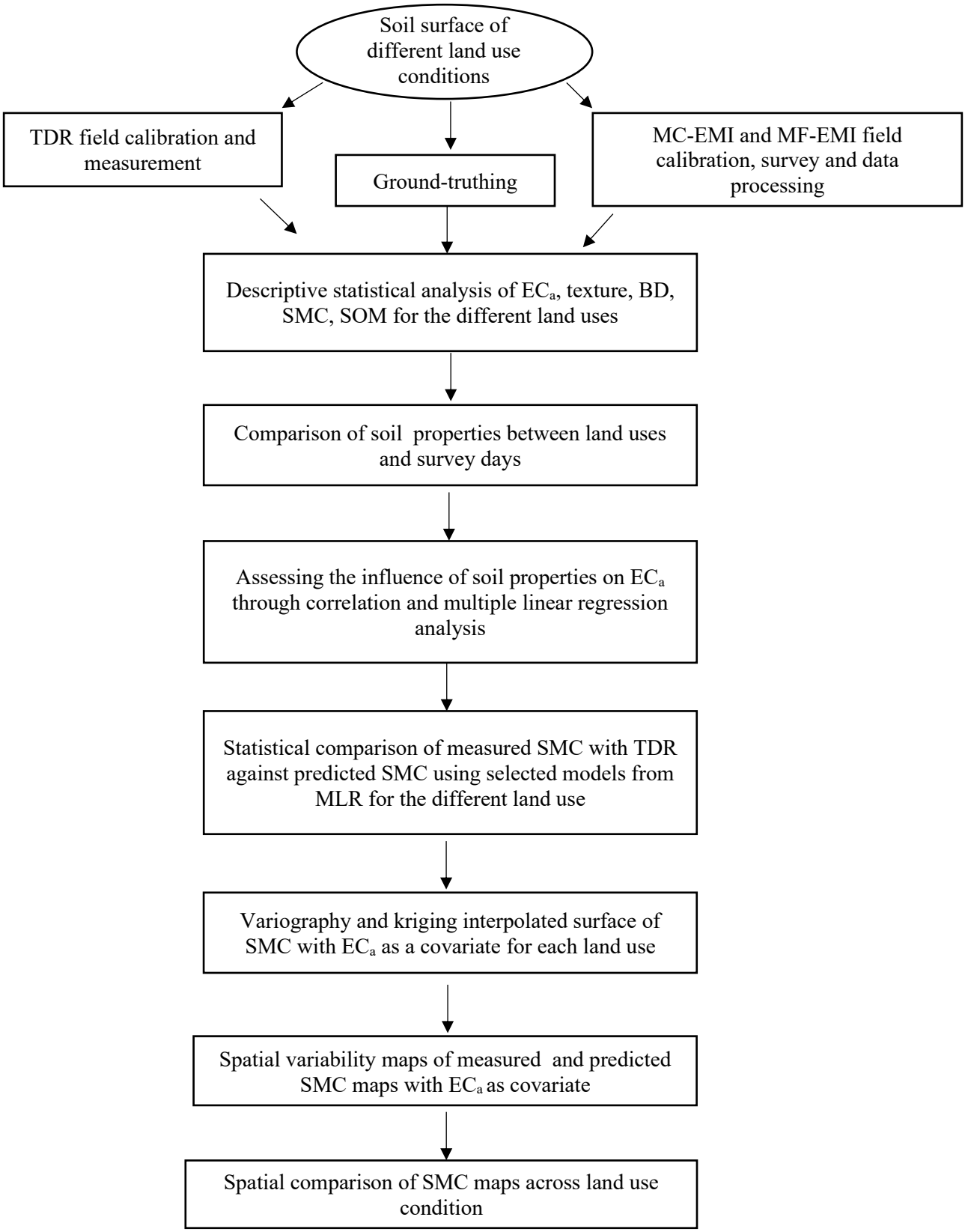

Figure 4.4: The workflow of methodology used in the study.

4.3 Results and discussion

4.3.1 Descriptive statistics and analysis of variance

4.3.1.1 Soil texture

The conversion of forests into managed agricultural land is known to cause a deterioration of soil physical properties, leaving the land more susceptible to erosion. Soil erosion has a profound effect on the soil, as it can reduce soil depth, altering the texture and leading to the loss of essential nutrients and organic matter. This can have profound impacts on both the soil and the local ecosystem (Lobe et al. 2001). Therefore, it is imperative that strong steps are taken to mitigate soil erosion, to protect the environment and preserve the land for future generations.

Soil texture class was a sandy loam for all three land use conditions (Table 4.1). Sand and silt content did not change under the different land use conditions whereas clay content increased significantly from the converted lands to the natural forest. It has been suggested that vegetation-covered land increases the clay content of sandy loam soil relative to bare lands. Root growth, litter decomposition and the formation of humus predominant in the natural forest are thought to influence the fixation of fine soil particles and SOM (Xia et al. 2020). It is evident that the difference in clay content between natural forest and converted lands reflects the impacts of land use on the soil erosion process. This is because erosion is a selective process with respect to particle size distribution (Rhoton et al. 1979).

ANOVA provides evidence that land use impacts resulting from soil erosion are reflected to some degree in the soil texture. Thus, it is important to consider the implications of land use on erosion when assessing the soil texture. The soil texture attributes (sand and clay) of the sandy loam soil in the study area exhibited low sensitivity (CV < 15%). It is well-known that soil texture is an intrinsic soil property that reflects the parent material rather than the environmental conditions, thus it was reasonable to assume that texture would exhibit low sensitivity to land use. However, the results of ANOVA indicated that the texture (clay content) was significantly different between natural forest and the converted land.

4.3.1.2 Bulk density

Soil BD is an important indicator of soil compaction and health. According to Kakaire et al. (2015), a higher soil bulk density implies less water held by the soil at field capacity, while a lower density indicates soils which are less compacted and have greater water retention. This finding is corroborated by the work of Ravina (2012), who determined that soil bulk density was lower in a native forest relative to a converted land.

BD was determined at 0-10 cm and 10-20 cm soil depth intervals. Land use conversions from natural forests to managed lands affects the compaction, porosity, and BD in soil (Kar et al. 2022). Generally, BD was in the order of agricultural land > field road > natural forest (Table 4.1 and Table 4.2). The lower BD in the natural forest compared to the other land use types could be due to a favorable soil structure under forest vegetation and a steady soil environment devoid of anthropogenic activities over long periods. BD is significantly higher in the converted lands, likely

due to direct influences such as compaction caused by agricultural field practices, as well as indirect influences such as the effects of use on SOM (Franzluebbers et al. 2000; Murty et al. 2002). Converting natural forests to agricultural land significantly increases BD (Ayoubi et al. 2014) possibly due to soil compaction and loss of soil organic carbon that occur because of soil plowing and manipulation (Nieto et al. 2010). BD increased with depth under the different land use conditions.

These results could be attributed to the dynamism of organic carbon and the dissipation of organic components, which are present in greater concentrations at shallower depths, are likely to have a diluting effect, thereby reducing the BD (Bronick and Lal 2005; Nwite et al. 2018). The CV of BD within each land use was generally low (CV< 15%). Variations in BD among different land use conditions were found to be minimal at deeper layers (10-20cm) when compared to the surface soil layer (0-10cm) (Table 4.1 and 4.2) thus indicating that various land use practices have a greater impact on soil BD at shallower depth compared to deeper depths.

4.3.1.3 Soil organic matter

It is well established that cultivated soils generally have a lower organic matter content compared to native ecosystems, due to the increased aeration of soil which accelerates the decomposition of soil organic matter (Kizilkaya and Dengiz 2010). Soil organic matter (SOM) is critical for improving the physical properties of soil, increasing cation exchange capacity and water-holding capacity, and for increasing soil structural stability by binding particles into aggregates (Leeper and Uren 1993). Anthropogenic activities such as tillage (hoeing, plowing), biomass burning,

residual removal, overgrazing, and drainage are thought to be responsible for the decreased SOM content observed under different land use at various elevations (Roose and Barthes 2001). SOM plays an important role in soil health, as it prevents nutrient leaching, makes nutrients accessible to plants, and acts as a buffer to resist strong changes in pH (Leu 2007). Carbon content is also known to be an essential element of an overall healthy soil (Yerima and Van Ranst 2005).

The amount of SOM was highest in the natural forest and lowest in the field road. This could be attributed to the higher clay content found in the natural forest. Soils with relatively high clay contents such as the natural forest tend to stabilize and maintain more SOM than those with low clay contents (Paz-Gonzalez et al. 2000). The lesser amount of litter input in the field road compared to the agricultural land and natural forest could have resulted in the low SOM in the field road (Morris 2004). Furthermore, when natural forest is converted into managed agricultural lands, SOM decomposes rapidly due to changes in temperature, aeration, and water content (Ashagrie et al. 2007). The decrease in SOM associated with land use conversion indicates the necessity of sustainable cropping systems, such as the addition of SOM, crop residues, crop rotation, and agroforestry using fast-growing leguminous trees, to mitigate the negative effects of cultivation. Fallowing a land have been found to not only improve soil fertility, but also reduce soil variability, which is beneficial for both practical and experimental agriculture.

The CV of SOM under the three land uses were generally low (CV < 15% ; Table 4.1 and 4.2) and varied in the order natural forest < field road < agricultural land. The lower CV in the natural forest indicates a more stable spatial pattern (Atwell and Wuddivira 2019).

4.3.1.4 Soil moisture content

Research has shown that land use exerts a significant influence on SMC levels (Xiao et al. 2011; Fu et al. 2003). This primarily occurs due to the differences in water consumption characteristics of vegetation and their impact on the root distribution of the soil. Changes in land use can cause SMC levels to increase, decrease, or fluctuate. Studies have revealed that the effect of trees and shrubs on soil moisture levels is significant and can be observed in the entire soil profile (0–100 cm) after land conversions have taken place (Fu et al. 2003). These changes are attributed to the differences in water uptake, as the variability in root distribution affects soil moisture levels in accordance with land use practices.

The mean SMC values were higher on the first survey day than on the second survey day, which could be attributed to the higher total rainfall (84.2 mm) on the first survey day compared to the second survey day (19.3 mm) (Figure 4.2). Furthermore, the mean SMC values were higher in the natural forest than in the agricultural land and field road. This could be ascribed to the deep litter layer (high SOM) found in the natural forest, which reduces surface evaporation and improves water retention capabilities. This finding agrees with that of Morris (2004), who noted the expansion of fine soil pores that retain water against gravitational drainage in coarser textured soils such as podzolic soils. Conversely, the low SMC in agricultural land and field road is likely due to the higher rate of evaporation that exists in the surface horizon of the agricultural land and field road, caused by factors such as ploughing as well as the higher surface runoff due to surface crusting and compaction. The SMC was significantly higher on field roads relative to the agricultural land. This could be explained by the mechanical disruption of pore arrangements by

practices such as tillage that lowers SMC in cultivated soils such as agricultural land (Celik 2005). SMC differed significantly under each land use (Table 4.1 and 4.2) indicating that SMC is sensitive to land use changes.

The spatial variability of SMC across land uses was generally low (CV< 15%) (Warrick 1998). Agricultural land and field road displayed a higher CV of SMC compared to the natural forest (Table 4.1 and Table 4.2), suggesting the influence of management practices such as tillage, compaction influence the heterogeneity of SMC (Atwell and Wuddivira 2019).

4.3.1.5 Apparent electrical conductivity

In the study area, EC_a values recorded at shallower depths (VCP C1, i.e., DOI of 0 – 0.25 m) were generally higher than at deeper depths (VCP C2, DOI = 0 – 0.5 m and HCP C1, DOI = 0 – 0.5 m) across the land use (Table 4.1 and Table 4.2) indicating that conductivity decreases with depth in the study area. The MC-EMI sensor's VCP C3, HCP 2, and HCP 3 provided more than 50 % negative values and hence could not be analyzed. Aside from the 38 kHz frequency (HCP) from the MF-EMI sensor, all other frequencies registered negative values (more than 50% of the data); hence, their measurements could not be analyzed. This is indicative that the use of MF-EMI is of limited usefulness in shallow soil investigations (Calamita et al. 2015). However, its ability to characterize wood areas and acquire more data is an added value in the exchange of information between hydrology and geophysics (Calamita et al. 2015).

EC_a had medium sensitivity (15% < CV < 35%) to land use in agricultural land and field road while low sensitivity was observed in natural forests due to low anthropogenic activities (Atwell and Wuddivira 2019). Interestingly, CV for EC_a generally increased with coil depth of exploration which deviated from expectations since deeper depths are not typically exposed to climate or anthropogenic disturbances. One-way ANOVA revealed low EC_a readings across different land uses with significant differences between natural forests and other land uses on both survey days; this difference could be attributed to high SOM, SMC, and clay content in natural forests (Jonard et al. 2013).

Table 4.1 Analysis of variance showing the effects of agricultural land, field road, and natural forest on soil properties for the first survey day

Survey Day 1	Agricultural land				Field road				Natural forest				
Variable	LSME	CV	Min	Max	LSME	CV	Min	Max	LSME	CV	Min	Max	SE
Soil Properties													
Sand	68.20[a]	2.99	64.8	68.8	70.40[a]	4.84	64.20	76.12	65.20[a]	3.04	62.91	68.00	2.66
Silt	18.70[a]	7.00	16.20	20.4	19.20[a]	10.31	15.10	23.22	17.30[a]	5.84	13.44	21.25	2.47
Clay	13.10[b]	7.23	12.05	16.08	11.4[b]	10.26	6.60	17.51	18.50[a]	6.27	14.47	22.14	1.24
SMC	33.71[c**‡]	8.35	30.00	37.84	38.01[b**]	8.31	33.42	42.57	42.98[a***]	6.08	40.00	47.25	1.45
SOM	3.87[b⁋**]	7.75	3.06	5.02	2.08[c**]	4.80	1.43	3.28	8.37[a**]	4.78	7.96	10.02	1.08
BD (depth 1)	1.17[a*]	8.70	0.98	1.30	1.20[a*]	8.3	1.10	1.32	0.90[b*]	11.1	0.85	1.0	0.24
BD (depth 2)	1.22[a*]	7.81	1.20	1.34	1.24[a*]	8.1	1.12	1.29	0.94[b*]	10.6	0.87	1.1	0.22
Average BD	1.20[a*]	8.33	0.98	1.34	1.22[a*]	8.20	1.10	1.32	0.92[b*]	10.87	0.85	1.1	0.24
MC EMI													
EC_a VCP C1[†]	0.08[b**]	13.5	0.05	0.10	0.07[b**]	14.29	0.04	0.06	0.18[a***]	5.56	0.14	0.22	0.04
EC_a VCP C2	0.06[b**]	16.7	0.05	0.10	0.04[b**]	25.00	0.03	0.05	0.13[a**]	7.69	0.10	0.20	0.03
EC_a HCP C1	0.05[b**]	20.0	0.04	0.11	0.05[b**]	20.00	0.03	0.07	0.15[a**]	6.69	0.13	0.19	0.03
MF EMI													
HCP-38kHz	0.06[b**]	31.15	0.05	0.07	0.08[b**]	25.10	0.08	0.10	0.25[a**]	8.01	0.20	0.28	0.006

[†]EC_a = apparent electrical conductivity; VCP = vertical coplanar mode; HCP = horizontal coplanar mode C1 = Coil 1; C2 = Coil 2; SMC = soil moisture content; SOM = soil organic matter; BD-1 = bulk density at 0-10cm depth; BD-2 = bulk density at 10-20cm depth; Average BD = average of BD-1 and BD-2; SE – Standard Error; LSME – Least square mean estimate; CV = Coefficient of variability; Min = Minimum; Max = Maximum

[‡]Significance is reported at 0.1 (*) and 0.05 (**)

⁋ Means that do not share a common letter are significantly different according to Fisher's Least Significant Difference Test

Table 4.2 Analysis of variance showing the effects of agricultural land, field road, and natural forest on soil properties for the second survey day

Survey Day 2	Agricultural land				Field road				Natural forest				
Variable	LSME	CV	Min	Max	LSME	CV	Min	Max	LSME	CV	Min	Max	SE
Soil Properties													
Sand	68.2[a]	2.99	64.8	68.8	70.40[a]	4.84	64.20	76.12	65.20[a]	3.04	62.91	68.00	2.66
Silt	18.7[a]	7.00	16.20	20.4	19.20[a]	10.31	15.10	23.22	17.30[a]	5.84	13.44	21.25	2.47
Clay	13.10[b]	7.23	12.05	16.08	10.4[b]	10.26	6.60	17.51	17.50[a]	6.27	14.47	22.14	2.74
SMC	26.0[c**]	11.40	20.00	30.03	32.67[b**]	8.48	27.65	38.07	38.23[a***]	7.70	30.94	52.13	3.56
SOM	3.67[b**]	10.89	3.00	5.02	2.01[c**]	7.46	1.43	3.28	9.37[a**]	7.43	7.96	10.02	1.36
BD (depth 1)	1.19[a*]	8.40	1.10	1.30	1.24[a*]	8.06	1.17	1.30	0.90[b*]	11.1	0.85	1.0	0.20
BD (depth 2)	1.22[a*]	8.20	1.20	1.34	1.25[a*]	8.0	1.19	1.29	0.94[b*]	10.6	0.87	1.1	0.20
Average BD	1.21[a*]	8.26	1.10	1.34	1.25[a*]	8.0	1.17	1.30	0.92[b*]	10.87	0.85	1.1	0.20
MC EMI													
EC_a VCP C1[†]	0.06[b**‡]	16.7	0.04	0.08	0.05[b**]	20.0	0.04	0.06	0.15[a***]	13.3	0.11	0.19	0.08
EC_a VCP C2	0.04[b**]	25.0	0.04	0.09	0.04[b**]	25.0	0.03	0.07	0.10[a**]	20.0	0.08	0.18	0.05
EC_a HCP C1	0.05[b**]	20.0	0.04	0.07	0.04[b**]	25.0	0.03	0.06	0.12[a**]	16.7	0.09	0.19	0.05
EC_a MF-EMI													
EC_a HCP-38kHz	0.05[b**]	26.87	0.04	0.07	0.07[b**]	28.56	0.06	0.08	0.23[a**]	17.39	0.19	0.26	0.05

[†]EC_a = apparent electrical conductivity; VCP = vertical coplanar mode; HCP = horizontal coplanar mode C1 = Coil 1; C2 = Coil 2; SMC = soil moisture content; SOM = soil organic matter; BD-1 = bulk density at 0-10cm depth; BD-2 = bulk density at 10-20cm depth; Average BD = average of BD-1 and BD-2; SE – Standard Error; LSME – Least square mean estimate; CV = Coefficient of variability; Min = Minimum; Max = Maximum

[‡]Significance is reported at 0.1 (*) and 0.05 (**)

[¶] Means that do not share a common letter are significantly different according to Fisher's Least Significant Difference Test

Table 4.3 Analysis of variance showing the effects of agricultural land, field road, and natural forest on soil properties between survey days

Land use Condition	Agricultural Land			Field Road			Natural Forest		
Soil properties	Survey Day 1 (LSME)	Survey Day 2 (LSME)	SE	Survey Day 1 (LSME)	Survey Day 2 (LSME)	SE	Survey Day 1 (LSME)	Survey Day 2 (LSME)	SE
SOM	3.87[a**‡]	3.67[a**]	1.22	2.08[a**]	2.01[a**]	1.25	8.37[a**]	9.37[a**]	1.25
SMC	33.7[a⁋**]	26.0[b**]	1.74	38.0[a**]	32.7[b**]	1.89	43.0[a***]	38.2[b***]	1.33
BD (Depth 1)	1.17[a*]	1.19[a*]	0.1	1.20[a*]	1.30[a*]	0.1	0.90[a*]	0.90[a*]	0.1
BD (Depth 2)	1.22[a*]	1.22[a*]	0.1	1.24	1.25[a*]	0.1	0.94[a*]	0.94[a*]	0.1
Average BD	1.20[a*]	1.21[a*]	0.1	1.22	1.25[a*]	0.1	0.92[a*]	0.92[a*]	0.1
EC_a VCP C1[†]	0.05[a**]	0.05[b**]	0.001	0.05[a**]	0.05[b**]	0.001	0.15[a***]	0.14[b***]	0.004
ECa VCP C2	0.08[a**]	0.06[b**]	0.002	0.08[a**]	0.05[b**]	0.002	0.17[a**]	0.17[b**]	0.004
ECa HCP C1	0.07[a**]	0.06[b**]	0.002	0.07[a**]	0.03[b**]	0.002	0.19[a**]	0.18[b**]	0.004
ECa HCP-38kHz	0.06[a**]	0.05[b**]	0.01	0.08[a**]	0.07[b**]	0.01	0.25[a**]	0.23[b**]	0.02

[†]EC_a = apparent electrical conductivity; VCP = vertical coplanar mode; HCP = horizontal coplanar mode C1 = Coil 1; C2 = Coil 2; SMC = soil moisture content; SOM = soil organic matter; BD-1 = bulk density at 0-10cm depth; BD-2 = bulk density at 10-20cm depth; Average BD = average of BD-1 and BD-2; SE – Standard Error; LSME – Least square mean estimate

[‡]Significance is reported at 0.1 (*) and 0.05 (**)

⁋ Means that do not share a common letter are significantly different according to Fisher's Least Significant Difference Test

4.3.2 Correlation analysis

EC_a was positively correlated with silt and clay content across different land uses (Tables 4.4, 4.5, and 4.6). Although several studies have demonstrated that EC_a is significantly affected by clay contents due to the physical contact between soil particles which typically increases soil EC_a by increasing the electrical conductivity of the soil solid particles (Brogi et al. 2019; Grubbs et al. 2019), the low clay content in the study area could have accounted for the non-significant connection between EC_a and clay content across different land uses. Negative significant correlations were observed between sand contents and mainly EC_a from the MC-EMI sensor across various land use conditions (Tables 4.4, 4.5, and 4.6), this result suggests that as the sand content increases, the EC_a measured by the MC-EMI sensor decreases. This result implies that the MC-EMI is better suited to represent the variations in sand and silt contents of the soil in the study area, when compared to the MF-EMI sensor.This result was expected as an increase in sand content which typically decreases EC_a due to its non-conductive nature (Carroll and Oliver 2005).

The strong significant correlation was noticed between EC_a and SMC for all three land uses (Tables 4.4, 4.5, and 4.6), indicating that SMC is the major driver of EC_a in this study site. An increase in SMC has been reported to increase EC_a due to the contribution from the solutes present in the soil solution, the clustering of conductive particles as well as a decrease in air thicknesses (Knight and Endres 1990). Wet soils contain more moisture and hence higher EC_a than dry soil (Nocco et al. 2019) which explains why the relationship between EC_a and SMC under natural forest was stronger than that of agricultural land or field road shown in Tables 4.4 and 4.5. Although EC_a may

be a proxy of SMC (Badewa et al. 2018), its relationship with ECa is affected by other factors such as compaction which could be amplified in managed ecosystems like agricultural land or field road resulting in lower correlations between EC_a and SMC than those found in natural forest shown in Table 4.6. The correlation results suggest that EC_a values are higher when SMC increases along with retained ions present in soil solution.

The relationship between EC_a and SOM was much stronger under natural forest than agricultural or field road conditions; however, it was not significant in field road possibly due to lower levels of SOM present there. The most significant influence of SOM was observed on CMD VCP C1 probably because of its lower DOI of 0 – 25 cm and within sampling depth according to Sadatcharam (2019). This could be attributed to practices such as application of fertilizers or compaction resulting into change of concentration of dissolved ions and variability of EC_a thus reducing strength of correlations between EC_a and SOM for field road and agricultural land when compared with natural forest (Table 4.6), as natural forests provide better niche for these investigations than converted forest lands into managed lands like agricultural lands.

Surprisingly, both sensors showed a general negative correlation with BD across different land use conditions, similar to the result found by Sadatcharam (2019) using same instruments on a nearby field. However, it was expected that as BD increased, EC_a increase due to reduced pore spaces, which resulted in more solid contacts and ions for conducting electricity through the water phase connected within the soil solution. This was in accordance with the findings of Corwin and Scudiero (2016).

These results indicated that the electromagnetic induction (EMI) may not be a reliable method for representing BD variations at the study site. Results, as displayed in Tables 4.4, 4.5 and 4.6, indicated that, aside from two depth intervals of BD, the relation among the independent variables was not significant across different land uses, suggesting the absence of multicollinearity among these variables at the study site.

Table 4.4 Correlation matrix of soil properties under agricultural land for first survey day

Soil Properties	ECa VCP C1[†]	ECa VCP C2	ECa HCP C1	ECa HCP 38 kHz	SMC	SOM	Sand	Silt	Clay	BD - 1	BD - 2	Average BD
ECa VCP C1		***[‡]	***	**	***	**	*	**	*NS*	*	*	*
ECa VCP C2	0.80[⁋]		***	**	*	*NS*	*NS*	*	*NS*	*NS*	*NS*	*NS*
ECa HCP C1	0.81	0.95		*	*	*	*	*	*NS*	**	*	*
ECa HCP 38kHz	0.53	0.26	0.45		**	*	*NS*	*	*NS*	*	*	*NS*
SMC	0.83	0.72	0.75	0.77		*NS*	*NS*	*NS*	*NS*	*NS*	*NS*	*NS*
SOM	0.75	0.47	0.53	0.30	0.36		*NS*	*NS*	*NS*	*NS*	*NS*	*NS*
Sand	-0.23	-0.29	-0.31	-0.68	-0.18	-0.12		*NS*	*NS*	*NS*	*NS*	*NS*
Silt	0.49	0.40	0.37	0.43	0.36	0.31	-0.26		*NS*	*NS*	*NS*	*NS*
Clay	0.13	0.20	0.22	0.12	0.17	0.25	-0.18	0.30		*NS*	*NS*	*NS*
BD - 1	-0.41	-0.28	-0.38	-0.63	-0.38	-0.40	0.10	-0.25	-0.26		**	*
BD - 2	-0.25	-0.34	-0.40	-0.44	-0.20	-0.35	0.13	-0.19	-0.40	0.95		*
Average BD	-0.32	-0.40	-0.44	-0.17	-0.09	-0.17	0.06	-0.15	-0.57	0.87	0.89	

Correlation Coefficient (r)

[†]EC_a = apparent electrical conductivity; VCP = vertical coplanar mode; HCP = horizontal coplanar mode C1 = Coil 1; C2 = Coil 2; SMC = soil moisture content; SOM = soil organic matter; BD-1 = bulk density at 0-10cm depth; BD-2 = bulk density at 10-20cm depth; Average BD = average of BD-1 and BD-2

[‡]Significance is reported at 0.1 (*), 0.05 (**) and 0.001 (***), NS (non-significant correlations)

[⁋]Correlation coefficient (r) is reported in coloured boxes

Table 4.5 Correlation matrix of soil properties under field road for first survey day

Soil Properties	ECa VCP C1[†]	ECa VCP C2	ECa HCP C1	ECa HCP 38 kHz	SMC	SOM	Sand	Silt	Clay	BD-1	BD - 2	Average BD
ECa VCP C1		*NS*[‡]	*NS*	***	**	*NS*	*	*	*NS*	*NS*	*NS*	*NS*
ECa VCP C2	0.43[⁋]		***	*NS*	**	*NS*	*NS*	*	*NS*	*NS*	*NS*	*NS*
ECa HCP C1	0.36	0.91		*NS*	*	*NS*	*	*	*NS*	*NS*	*NS*	*NS*
ECa HCP 38 kHz	0.82	0.48	0.40		***	*NS*	*NS*	*	*NS*	*NS*	*NS*	*NS*
SMC	0.78	0.43	0.49	0.78		*NS*	*NS*	*NS*	*NS*	*NS*	*NS*	*NS*
SOM	0.30	0.19	0.18	0.31	0.43		*NS*	*NS*	*NS*	*NS*	*NS*	*NS*
Sand	-0.50	-0.23	-0.22	-0.51	-0.33	-0.14		*NS*	*NS*	*NS*	*NS*	*NS*
Silt	0.58	0.34	0.30	0.45	0.27	0.22	-0.96		*NS*	*NS*	*NS*	*NS*
Clay	0.29	0.21	0.10	0.38	0.31	0.24	-0.45	0.18		*NS*	*NS*	*NS*
BD - 1	-0.21	-0.37	-0.32	-0.35	-0.20	-0.27	0.25	-0.22	-0.37		**	**
BD - 2	-0.20	-0.31	-0.36	-0.20	-0.25	-0.30	0.14	-0.15	-0.40	0.93		**
Average BD	-0.22	-0.40	-0.44	-0.17	-0.09	-0.17	0.06	-0.15	-0.57	0.87	0.89	

Correlation Coefficient (r)

[†]EC_a = apparent electrical conductivity; VCP = vertical coplanar mode; HCP = horizontal coplanar mode C1 = Coil 1; C2 = Coil 2; SMC = soil moisture content; SOM = soil organic matter; BD-1 = bulk density at 0-10cm depth; BD-2 = bulk density at 10-20cm depth; Average BD = average of BD-1 and BD-2

[‡]Significance is reported at 0.1 (*), 0.05 (**) and 0.001 (***), NS (non-significant correlations)

[⁋]Correlation coefficient (r) is reported in coloured boxes

Table 4.6 Correlation matrix of soil properties under natural forest for first survey day

Soil Properties	ECa VCP C1[†]	ECa VCP C2	ECa HCP C1	ECa HCP 38 kHz	SMC	SOM	Sand	Silt	Clay	BD - 1	BD - 2	Average BD
ECa VCP C1		*NS*[‡]	*NS*	***	***	***	*	*	*NS*	*	*NS*	*
ECa VCP C2	0.10[⁋]		**	*NS*	**	*NS*	*NS*	*	*NS*	*NS*	*NS*	*NS*
ECa HCP C1	0.55	0.95		*NS*	**	*	*NS*	*	*NS*	*NS*	*NS*	*NS*
ECa HCP 38 kHz	0.94	0.23	0.41		***	***	*NS*	**	*NS*	*	*	*
SMC	0.88	0.35	0.40	0.82		*NS*	*NS*	*NS*	*NS*	*NS*	*NS*	*NS*
SOM	0.80	0.27	0.29	0.78	0.57		*NS*	*NS*	*NS*	*NS*	*NS*	*NS*
Sand	-0.11	-0.13	-0.11	-0.16	-0.37	-0.77		*NS*	*NS*	*NS*	*NS*	*NS*
Silt	0.47	0.34	0.21	0.29	0.24	0.43	-0.77		*NS*	*NS*	*NS*	*NS*
Clay	0.22	0.12	0.09	0.21	0.29	0.53	-0.61	-0.04		*NS*	*NS*	*NS*
BD - 1	-0.36	-0.18	-0.12	-0.35	-0.27	-0.57	0.66	-0.83	0.12		**	**
BD - 2	-0.29	-0.18	-0.14	-0.40	-0.22	-0.55	0.60	-0.80	0.14	0.96		**
Average BD	-0.40	-0.19	-0.20	-0.38	-0.27	-0.60	0.64	-0.78	0.15	0.90	0.90	

[†]EC_a = apparent electrical conductivity; VCP = vertical coplanar mode; HCP = horizontal coplanar mode C1 = Coil 1; C2 = Coil 2; SMC = soil moisture content; SOM = soil organic matter; BD-1 = bulk density at 0-10cm depth; BD-2 = bulk density at 10-20cm depth; Average BD = average of BD-1 and BD-2

[‡]Significance is reported at 0.1 (*), 0.05 (**) and 0.001 (***), NS (non-significant correlations)

[⁋]Correlation coefficient (r) is reported in coloured boxes

4.3.3 Regression analysis

The use of multiple regression is a valuable tool for evaluating the relationships between SMC and EC_a when considering the texture, SOM, and BD contents of a soil. This is due to the presence of multiple predictors, which allows for a comprehensive exploration of the relationship between soil parameters. Multiple regression analysis can identify how each predictor influences the soil moisture, as well as whether the combination of predictors is sufficient to accurately estimate the soil moisture. Such an analysis provides valuable insights into the soil's hydrological properties, and can help optimize agricultural practices, such as irrigation and fertilization, to promote the growth of crops. Regardless, MLR predictions were compared to simple linear regression predictions during data processing, and it was found that MLR predictions were more accurate relative to simple linear regression predictions based on a higher R^2 and lower RMSE values. The VIF obtained from the MLR ranged from 1.00 – 1.51 (Table 4.7) across different land use conditions, indicating the absence of multi-collinearity in the developed regression models (Shrestha 2020). The accuracy of prediction improved significantly with increasing SMC, which is in line with findings of other researchers, demonstrating high sensitivity of both sensors to measure SMC with increasing SMC level (Fernández-Gálvez 2008). The generated MLR models generally over-predicted SMC across different land use conditions.

The best model for agricultural land was obtained using coil 1 of the MC-EMI sensor in the VCP mode (Table 4.7). This was possibly due to the similar depth of exploration (DOE) between EC_a (DOE = 25cm), and the soil samples taken at 20 cm depth. EC_a from this coil orientation significantly explained approximately 92.11% of the variations in SMC, SOM, and silt collectively

at approximately 0-25 cm depth range. EC_a did not explain variations in sand and clay in this land use regardless of the EMI sensor used and were subsequently removed from all generated models for this land use (Table 4.7). EC_a readings from the MC-EMI sensor in coil orientations VCP C2 and HCP C1 could only explain significant variations in SMC (68.06% and 82.95%, respectively). SMC and BD were the dominant significant factors being explained by the variation in EC_a recorded from the MF-EMI sensor (Table 4.7). The high depth of investigation coupled with the highly sensitive nature of the MF sensor (Won et al. 1996) could have resulted in low R^2 values relative to VCP C1 and HCP 1 due to significant influence of external features and other shallow soil properties (Farooque et al. 2012).

Generally, EC_a was able to explain more variations in soil properties in the natural forest compared to the field road, where it was only seen to be able to explain variations related to SMC. This is likely due to external factors such as soil-to-sensor distance variation, plant roots, and residues which affect EMI measurement accuracy (Mouazen et al. 2006). Additionally, moist soils are more favorable for EC_a surveys than dry soils (Brevik et al. 2006) which can also account for higher predictive accuracy found in natural forest relative to other land uses such as agricultural land and field roads (Sadatcharam 2019). Measurement errors associated with measuring BD via core sampling, transportation and drying may account for some limitations when predicting soil properties such as BD as well as errors associated with core drying method when measuring SMC (Mouazen and Al-Asadi 2018).

In conclusion, both sensors used can be successfully employed for predicting near-surface soil properties based on EC_a readings; however, results suggest that MC-EMI sensor was better suited

for predicting these properties relative to MF-EMI sensor particularly in managed agricultural lands such as field roads where measurement errors associated with core drying method can be minimized by keeping samples sealed until drying test is conducted (Mouazen and Al-Asadi 2018).

Table 4.7 Multiple regression using backward elimination of predictors between soil moisture content (SMC) and investigated soil properties at 90% confidence

Land use condition	Multiple Linear Regression equation (Backward elimination method)	R^2	Validated R^2	RMSE	Variance Inflation Factor (VIF)
		%	%	%	
Agricultural land	EC_a VCP C1† = -0.09 + 0.003 SMC + 0.02 SOM + 0.28 Silt	92.1	88.6	3.05	SMC= 1.25 Silt = 1.20 SOM = 1.20
	EC_a VCP C2 = -0.11 + 0.005 SMC	68.1	57.8	5.31	SMC = 1.00
	EC_a HCP C1 = -0.09 + 0.004 SMC	82.9	63.2	3.64	SMC = 1.00
	EC_a HCP 38 kHz = 0.06 + 0.002 SMC – 0.04 BD	77.8	62.4	3.91	SMC = 1.02 BD = 1.02
Field road	EC_a VCP C1 = 0.04 + 0.002 SMC	78.9	71.5	4.41	SMC = 1.0
	EC_a VCP C2 = 0.01 + 0.002 SMC	57.7	47.6	6.67	SMC = 1.0
	EC_a HCP C1 = 0.02 + 0.001 SMC	78.9	71.1	4.92	SMC = 1.0
	EC_a HCP 38 kHz = 0.04 + 0.001 SMC	78.3	70.4	5.18	SMC = 1.0
Natural forest	EC_a VCP C1 = -1.95 + 0.006 SMC+ 0.012 SOM + 3.77 Silt – 0.32 BD	95.1	84.9	1.30	SMC = 1.51 SOM = 1.29 Silt = 1.18 BD = 1.03
	EC_a VCP C2 = -0.73 + 0.008 SMC + 6.48 Silt	65.6	54.6	3.25	SMC = 1.32 Silt = 1.30
	EC_a HCP C1 = 0.04 + 0.003 SMC + 0.004 SOM + 0.001 Silt	91.1	81.5	2.44	SMC = 1.51 SOM= 1.27 Silt = 1.20
	EC_a HCP 38 kHz = 0.03 + 0.004 SMC - 0.059 BD	88.2	80.9	2.65	SOM= 1.01 BD = 1.01

†EC_a = apparent electrical conductivity; VCP = vertical coplanar mode; HCP = horizontal coplanar mode C1 = Coil 1; C2 = Coil 2; SMC = soil moisture content; SOM = soil organic matter; BD = bulk density at 0-20cm depth; RMSE = root mean square error; R^2 = coefficient of determination

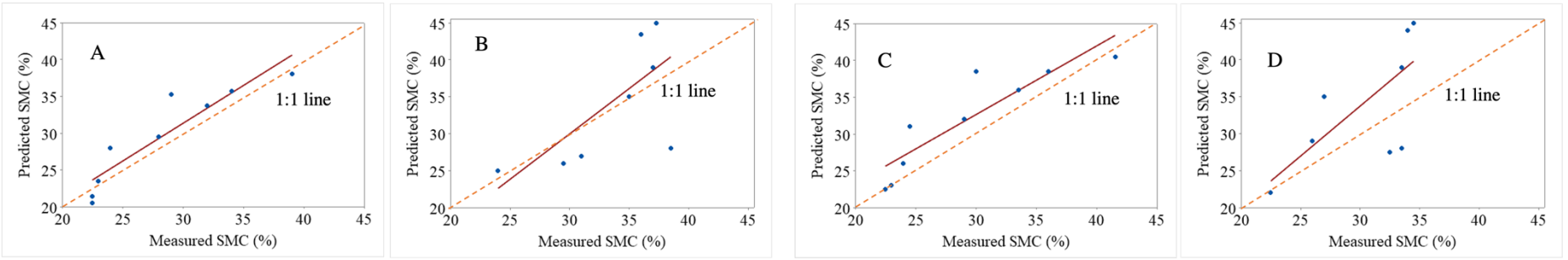

Figure 4.5: Relationship between measured and predicted soil moisture content (SMC) measurements obtained from MLR in (A) MC-EMI VCP C1, (B) MC-EMI VCP C2 (C) MC-EMI HCP C1 and (D)MF-EMI HCP 38kHz under the agricultural land.

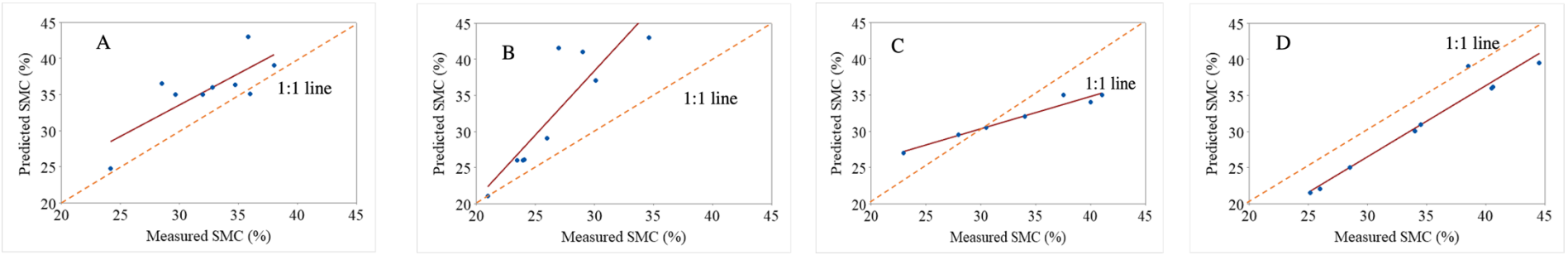

Figure 4.6: Relationship between measured and predicted soil moisture content (SMC) measurements obtained from MLR in (A) MC-EMI VCP C1, (B) MC-EMI VCP C2 (C) MC-EMI HCP C1 and (D)MF-EMI HCP 38kHz under the field road.

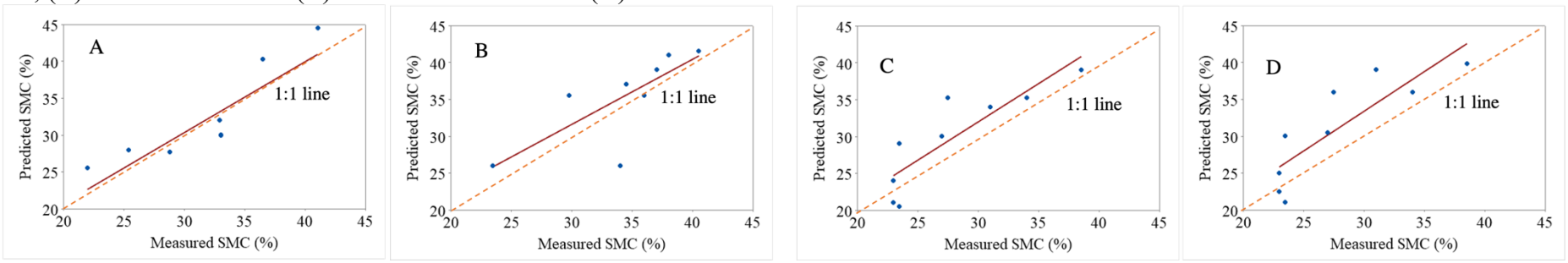

Figure 4.7: Relationship between TDR-measured and model predicted soil moisture content (SMC) measurements obtained from MLR in (A) MC-EMI VCP C1, (B) MC-EMI VCP C2 (C) MC-EMI HCP C1 and (D)MF-EMI HCP 38kHz under the natural forest.

4.3.4 Statistical comparison of measured soil moisture content with Time Domain Reflectometer against predicted soil moisture content using selected models under the different land use.

Comparison of the measured SMC from TDR against the predicted SMC from VCP C1 MLR from 1:1 line at $\alpha = 0.1$ revealed that no significant difference (slope = 1 and intercept = 0) for agricultural land (Table 4.8). This result indicates that the MLR model was able to accurately predict SMC using EC_a VCP C1 (Figure 4.5a) and was possibly attributable to the similarity in exploration depths between EC_a VCP C1 and the TDR. However, significant differences were observed between the prediction lines obtained using EC_a VCP C2, EC_a HCP C1 and EC_a HCP 38 kHz and their respective 1:1 lines at $\alpha = 0.1$ in the agricultural land (slope $\neq$ 1 and intercept = 0) (Table 4.8). The error of prediction of SMC was generally higher when EC_a VCP C2, EC_a HCP C1 and EC_a HCP 38 kHz coil orientations were used, with the predictions being underestimated from the 1:1 line (Figure 4.5b, 4.5c and 4.5d, respectively). The higher error of prediction of SMC in EC_a VCP C2, EC_a HCP C1 and EC_a HCP 38 kHz coil orientations could be due to the disparity in sampling depths between the TDR and these coil orientations since the sampling depths of these EMI coil orientations are deeper (> 20cm) than those of the TDR sampling depths (measured SMC) taken 0-20cm depth (Altdorff et al. 2017; Calamita et al. 2015).

The analysis also revealed that there were no significant differences between the prediction line obtained from EC_a HCP 38 kHz and the 1:1 line at $\alpha = 0.1$ in the field road (slope = 1 and intercept = 0) (Table 4.8). However, t-test revealed that significant differences existed between the 1:1 line and prediction lines obtained using EC_a VCP C1 (slope $\neq$ 1 and intercept = 0), EC_a VCP C2 (slope

≠ 1 and intercept ≠ 0), and EC_a HCP C1 (slope ≠ 1 and intercept ≠ 0) at $\alpha = 0.1$ in the field road (Table 4.8; Figure 4.6a, 4.6b and 4.6c, respectively). The insignificant difference between the prediction line and the 1:1 line when using the MF-EMI sensor could be attributed to GEM-2's capacity to produce thermally stable measurements in dry soils such as those found in the field road (Won et al. 1996).

Lastly, the results of the comparison between the TDR-measured SMC and the predicted SMCs obtained from ECa VCP C1, ECa HCP C1, and ECa HCP 38 kHz from their respective 1:1 lines revealed that there was no significant difference in the natural forest (Table 4.7; Figure 4.7a, 4.7c and 4.7d, respectively). The slope of the regression line between the measured and predicted SMCs was equal to 1 and the intercept was 0, indicating that the predicted SMCs closely correlated with the measured values. These findings suggest that more EMI coil orientations could be used to reliably estimate soil moisture content in the natural forest relative to the other land use conditions.

There were significant differences between the prediction line obtained from EC_a VCP C2 and its 1:1 line in the natural forest (slope ≠ 1 and intercept = 0) (Figure 4.7b). While the MLR techniques may be able to accurately predict SMC in a natural forest, more research is needed to better understand using EC_a VCP C2.

Table 4.8 Summary of statistical comparison of measured soil moisture against predicted soil moisture obtained from MLR under the different land use ($\alpha = 0.1$)

Land use condition	Coil Orientation	t-calculated		Analysis from 1:1		Deviation from 1:1 Line
		Intercept	Slope	Intercept	Slope	
Agricultural land	EC_a VCP C1	0.1	0.2	NS	NS	NO
	EC_a VCP C2	0.2	-1.5	NS	S	YES
	EC_a HCP C1	0.9	-1.4	NS	S	YES
	EC_a HCP 38 kHz	-0.5	1.7	NS	S	YES
Field road	EC_a VCP C1	1.0	-1.4	NS	S	YES
	EC_a VCP C2	-1.5	2.2	S	S	YES
	EC_a HCP C1	13.8	-15.2	S	S	YES
	EC_a HCP 38 kHz	-1.0	-0.14	NS	NS	NO
Natural forest	EC_a VCP C1	1.2	-1.2	NS	NS	NO
	EC_a VCP C2	0.5	-1.4	NS	S	YES
	EC_a HCP C1	0.1	0.2	NS	NS	NO
	EC_a HCP 38 kHz	0.1	0.4	NS	NS	NO

$t_{.90} = 1.4$, df = 8, NS (Non-significant), S (Significant)

4.3.5 Variography and kriging interpolated surface of soil moisture content

Interpolation methods are increasingly being used as a tool to improve the prediction of SMC spatial distribution due to limited access to accurate observation data (Xie et al. 2020). 4002, 1142, and 1037 EC_a data were collected from agricultural land, field roads, and natural forest, respectively using the MC-EMI VCP C1. In comparison, SMC was sampled fewer times, only 9 data points. Generally, visual differences were present between maps of measured SMC obtained from cokriging with EC_a as covariate, and maps of predicted SMC from cokriging with EC_a as covariate across different land use conditions. However, the trends in the variability of both the measured and predicted SMC were similar. Various variograms are shown in Appendix B for further reference.

4.3.5.1 Agricultural land

The interpolated spatial maps for measured SMC for the agricultural land are displayed in Figure 4.8a, for which a spherical variogram model was the best fit for the spatiotemporal representation in the cokriging interpolation. The nugget effect of 5 indicated that additional sampling of SMC at smaller distances might be needed to detect spatial dependence and create an accurate map. The range value of 8 m indicated that SMC values influenced neighboring SMC values over higher distances compared to other land use conditions, and the spatial dependence was judged to be medium (nugget/sill = 0.3), based on the classification of Cambardella et al. (1994). The most accurate SMC prediction in this land use was obtained from the MLR model with the MC-EMI VCP C1, and cokriging with measured EC_a as a covariate was used to generate the spatial maps (Figure 4.9a). The predicted SMC maps depicted low SMC content similar to the measured SMC

maps, and an experimental variogram with a range of 8m, nugget effect of 0, and a partial sill of 20 showed strong spatial dependence (nugget/sill = 0). The accuracy of the measured SMC map was approximately 50% higher (RMSE = 0.09 %) relative to the predicted SMC map (RMSE = 0.18 %) possibly due to the influence of other soil properties such as SOM and silt, as seen in the MLR model, and numerical instability from the predicted models.

4.3.5.2 Field road

The interpolated spatial maps for measured SMC for the field road are displayed in Figure 4.8b, using a spherical variogram model as the best fit for the spatiotemporal representation of the measured SMC in the cokriging interpolation. The measured SMC maps in field road generally depicted higher SMC content (35-40 %) relative to the agricultural land (25-35 %), as indicated by the results from the ANOVA (Table 4.3). The small range (4m) of SMC values in this land use was indicative that SMC values influenced neighbouring SMC values over shorter distances relative to agricultural land. This was reflected in the partial sill of 10 and the high nugget value (10), which suggest that additional sampling of SMC at smaller distances might be needed to detect spatial dependence and create a more accurate map. Further, the spatial dependence was judged to be medium (nugget:sill = 0.5). It was found that the most accurate SMC prediction in this land use was obtained from the MLR generated with the MC-EMI VCP C1. Consequently, interpolated spatial maps of the predicted SMC from this regression model were generated with cokriging using measured EC_a as a covariate (Figure 4.9b). The accuracy of the measured SMC map obtained from cross-validation was increased by approximately 60% (RMSE = 0.12 %) relative to the predicted SMC map (RMSE = 0.20 %).

4.3.5.3 Natural forest

The interpolated spatial maps of the measured SMC in the natural forest, displayed in Figure 4.8c, were generated using cokriging with a spherical variogram model as the best-fit representation of its spatiotemporal variation. The measured SMC maps generally showed a high SMC content of 40-50 %, with range values at 2m, nugget values of 1, and partial sill values of 5.5. The small nugget value indicated that further sampling of SMC at shorter distances may not be necessary to demonstrate spatial dependence. Compared to other land use conditions, the range values were lower for wet soils (natural forest) and increased with decreasing SMC (field road and agricultural land). This result is consistent with Lakhankar et al. (2010). The land use also exhibited a high spatial dependence (nugget/sill = 0.15), and the moistest land use (natural forest) recorded the strongest spatial dependence. This is due to SMC patterns being at their strongest prior to the dry-down phase, which tends to weaken the spatial patterns as each value converges to lower levels. The most accurate SMC maps in this land use were obtained from the MLR model generated with the MC-EMI VCP C1, and the corresponding interpolated spatial maps of the predicted SMC were generated with cokriging using measured EC_a as a covariate (Figure 4.9c). The variogram of the predicted SMC maps had a range of 3.4 m, nugget of 0, and partial sill of 20, and showed a strong spatial dependence (nugget/sill = 0). The accuracy of the measured SMC map obtained from cross-validation was higher (RMSE = 0.05 %) compared to the predicted SMC map (RMSE = 0.15 %), this is likely due to the significant influence of other soil properties such as SOM, BD, and silt as seen in the MLR model.

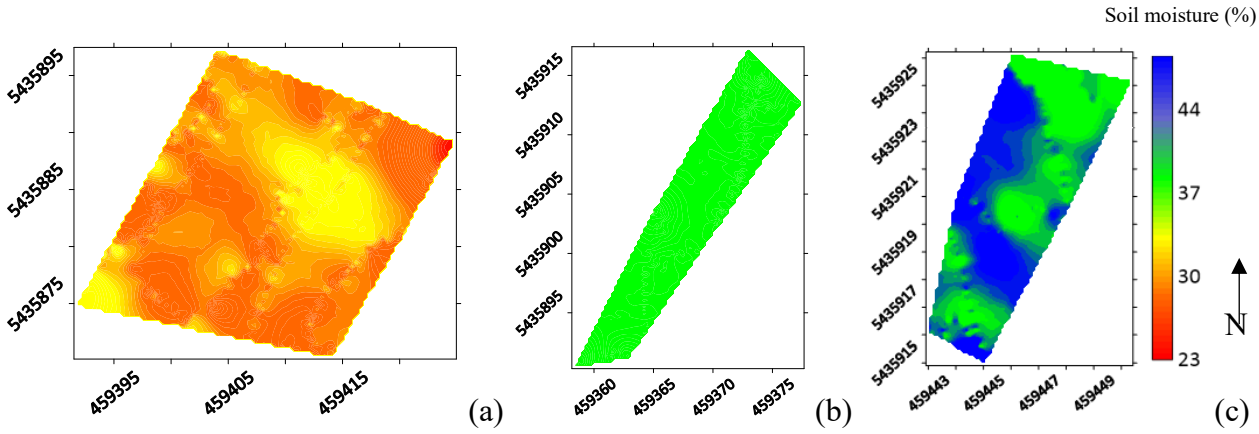

Figure 4.8: Spatial variability maps of measured soil moisture content (a) Agricultural land; (b) Field road; (c) Natural forest obtained from cokriging with apparent electrical conductivity (ECa) as a covariate.

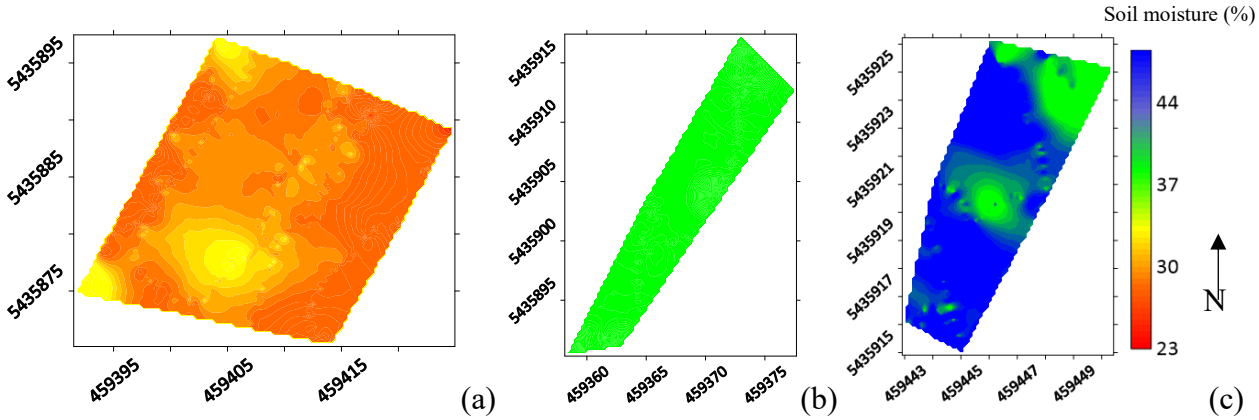

Figure 4.9: Spatial variability maps of predicted soil moisture content (a) Agricultural land; (b) Field road; (c) Natural forest obtained from cokriging with apparent electrical conductivity (ECa) as a covariate.

4.4 Conclusion

Measuring EC_a using MC-EMI and MF-EMI sensors provided important information for maximizing the accuracy of SMC prediction in different land by giving a workable relationship between EC_a and the other investigated soil properties sampled at 20 cm across the different land use conditions. Generally, EC_a was found to be significantly correlated to SMC and SOM, with SMC exhibiting the strongest relation with EC_a across the different land use conditions in this study site. The correlation results between EC_a and SMC were the strongest in moist soils.

Measuring EC_a using the MC-EMI (C1- VCP) provided the best predictions across the different land use conditions relative to the other EMI coils employed in this study. Cokriging of measured SMC with EC_a as covariate revealed more accurate maps relative to cokriging predicted SMC with EC_a as a covariate. The comparison of both sensors revealed that although MF-EMI used 8 integral depths from 4 different frequencies in 2 coil orientations, only the EC_a 38 kHz in HCP coil orientation revealed significant interactions with the other soil properties. On the other hand, the MC-EMI showed 6 integral depths to displayed significant interactions with the other soil properties. The results of this study demonstrate that the MC-EMI sensor is the more appropriate choice for the characterizing SMC in the study area, as it offers a higher degree of accuracy and precision. This is especially beneficial in land use applications, where precise and reliable data is crucial. Additionally, the findings suggest that georeferenced mobile soil EC_a measurements, carried out with either an MF-EMI or MC-EMI, can be used to rapidly assess the spatial variability. Moreover, EC_a serves as a valuable indicator of soil quality in relation to productivity, and its incorporation can facilitate the implementation of site-specific agronomic management. This is an important consideration in land use conversion.

Further studies are needed to investigate inverse modeling to obtain 3D maps of SMC, as well as considering other environmental factors such as temperature and vegetation cover, in order to create more comprehensive understanding of soil spatial variability and formulate more accurate prediction models. Additionally, more extensive field measurements should be conducted to enhance the robustness and reliability of the prediction models by including additional covariates such as temperature, which could help improve accuracy in predicting SMC across different land use conditions.

4.5 Competing interests

The authors declare there are no competing interests.

4.6 Data availability

Data generated or analyzed during this study are available from the corresponding author upon reasonable request.

4.7 Acknowledgement

The authors would like to acknowledge the financial support from the Natural Science and Engineering Research Council Discovery Grant (NSERC-DG: RGPIN-2019-04614), Industry, Energy and Technology of the Government of NL (IET Grant: 5404-1962-102) and the Memorial University of Newfoundland and Labrador (MUNF). Special thanks to Dr. Dmitry Sveshnikov for the guidance and constructive comments given for the methodology and data analysis. We thank Sashini Pathirana and Salman Afzal for their assistance in collecting the EMI and soil moisture data, respectively. We also thank Sabrina Ellsworth, Dr. Vanessa Kavanagh and Adrian David Reid from the Department of Fisheries, Forestry and Agriculture of the Government of NL, Canada for providing necessary facilities and management of the Clean Tech Crop Rotation Experimental site at the Western Agriculture Center and Research Station in Pasadena, Newfoundland.

Appendix B

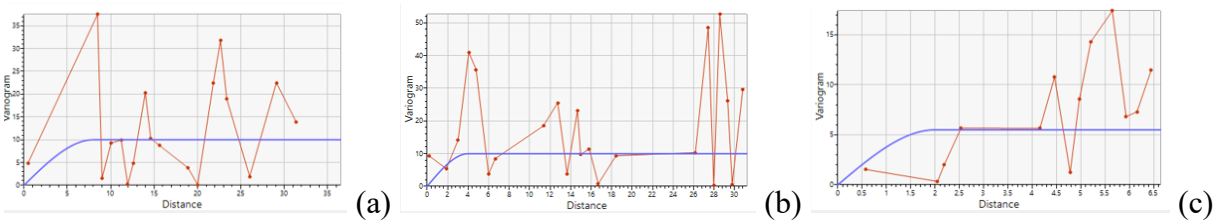

Figure B1. Variogram models of TDR-measured soil moisture content obtained from cokriging for agricultural land (a), field road (b), and natural forest (c).

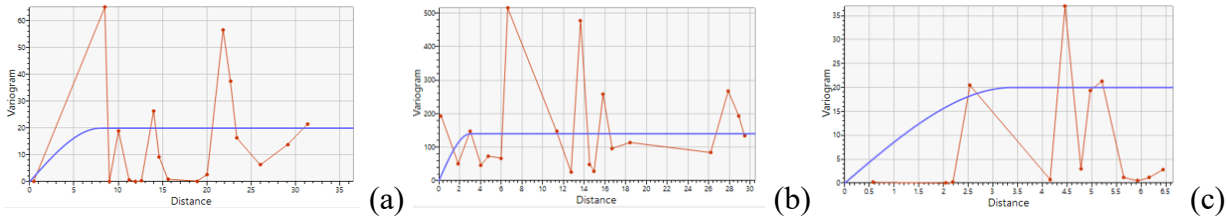

Figure B2. Variogram models of predicted soil moisture content from MLR models obtained from cokriging for agricultural land (a), field road (b) and natural forest (c).

4.8 References

Abd El-Wahab, R., Al-Rashed, A. and Al-Dousari, A., 2018. Influences of physiographic factors, vegetation patterns and human impacts on aeolian landforms in arid environment. Arid Ecosystems, 8, pp.97-110.

Allred, B.J., Ehsani, M.R. and Daniels, J.J., 2008. General considerations for geophysical methods applied to agriculture. Handbook of Agricultural Geophysics, pp.3-16.

Altdorff, D., Galagedara, L., Nadeem, M., Cheema, M. and Unc, A., 2018. Effect of agronomic treatments on the accuracy of soil moisture mapping by electromagnetic induction. Catena, 164, pp.96-106.

Altdorff, D., Sadatcharam, K., Unc, A., Krishnapillai, M. and Galagedara, L., 2020. Comparison of multi-frequency and multi-coil electromagnetic induction (EMI) for mapping properties in shallow podsolic soils. Sensors, 20, pp.2330.

Altdorff, D., Von Hebel, C., Borchard, N., Van Der Kruk, J., Bogena, H.R., Vereecken, H. and Huisman, J.A., 2017. Potential of catchment-wide soil water content prediction using electromagnetic induction in a forest ecosystem. Environmental Earth Sciences, 76, pp.1-11.

Atwell, M.A. and Wuddivira, M.N., 2019. Electromagnetic-induction and spatial analysis for assessing variability in soil properties as a function of land use in tropical savanna ecosystems. SN Applied Sciences, 1, pp.856.

Ayoubi, S., Emami, N., Ghaffari, N., Honarjoo, N. and Sahrawat, K.L., 2014. Pasture degradation effects on soil quality indicators at different hillslope positions in a semiarid region of western Iran. Environmental Earth Sciences, 71, pp.375-381.

Badewa, E., Unc, A., Cheema, M., Kavanagh, V. and Galagedara, L., 2018. Soil moisture mapping using multi-frequency and multi-coil electromagnetic induction sensors on managed podzols. Agronomy, 8, pp.224.

Brevik, E.C., Fenton, T.E. and Lazari, A., 2006. Soil electrical conductivity as a function of soil water content and implications for soil mapping. Precision Agriculture, 7, pp.393-404.

Brogi, C., Huisman, J., Pätzold, S., Von Hebel, C., Weihermüller, L., Kaufmann, M., Van Der Kruk, J. and Vereecken, H., 2019. Large-scale soil mapping using multi-configuration EMI and supervised image classification. Geoderma, 335, pp.133-148.

Buta, M., Paulette, L., Man, T., Bartha, I., Negruşier, C. and Bordea, C., 2019. Spatial assessment of soil salinity by electromagnetic induction survey. Environmental Engineering and Management Journal (EEMJ), 18(9), pp.2073-2081

Calamita, G., Perrone, A., Brocca, L., Onorati, B. and Manfreda, S., 2015. Field test of a multi-frequency electromagnetic induction sensor for soil moisture monitoring in southern Italy test sites. Journal of Hydrology, 529, pp.316-329.

Cambardella, C. and Karlen, D., 1999. Spatial analysis of soil fertility parameters. Precision Agriculture, 1, pp.5-14.

Carroll, Z. and Oliver, M.A., 2005. Exploring the spatial relations between soil physical properties and apparent electrical conductivity. Geoderma, 128, pp.354-374.

Carter, M.R. and Gregorich, E.G., 2007. Soil sampling and methods of analysis, CRC press.

Celik, I., 2005. Land-use effects on organic matter and physical properties of soil in a southern Mediterranean highland of Turkey. Soil and Tillage research, 83, pp.270-277.

Corwin, D.L. and Scudiero, E., 2019. Mapping soil spatial variability with apparent soil electrical conductivity (ECa) directed soil sampling. Soil Science Society of America Journal, 83, pp.3-4.

Croquet, E.G., 2016. Late Wisconsinan paleosols and macrofossils in Chehalis Valley: paleoenvironmental reconstruction and regional significance.

Farzamian, M., Paz, M.C., Paz, A.M., Castanheira, N.L., Gonçalves, M.C., Monteiro Santos, F.A. and Triantafilis, J., 2019. Mapping soil salinity using electromagnetic conductivity imaging—A comparison of regional and location-specific calibrations. Land Degradation and Development, 30, pp.1393-1406.

Feigin, A., Ravina, I. and Shalhevet, J., 2012. Irrigation with treated sewage effluent: management for environmental protection, Springer Science and Business Media, 17.

Fernández-Gálvez, J., 2008. Errors in soil moisture content estimates induced by uncertainties in the effective soil dielectric constant. International Journal of Remote Sensing, 29, pp.3317-3323.

Franzluebbers, A., Stuedemann, J. and Schomberg, H., 2000. Spatial distribution of soil carbon and nitrogen pools under grazed tall fescue. Soil Science Society of America Journal, 64, pp.635-639.

Grubbs, R.A., Straw, C.M., Bowling, W.J., Radcliffe, D.E., Taylor, Z. and Henry, G.M., 2019. Predicting spatial structure of soil physical and chemical properties of golf course fairways using an apparent electrical conductivity sensor. Precision Agriculture, 20, pp.496-519.

Jonard, F., Mahmoudzadeh, M., Roisin, C., Weihermüller, L., André, F., Minet, J., Vereecken, H. and Lambot, S., 2013. Characterization of tillage effects on the spatial variation of soil properties using ground-penetrating radar and electromagnetic induction. Geoderma, 207, pp.310-322.

Kakaire, J., Makokha, G.L., Mwanjalolo, M., Mensah, A.K. and Emmanuel, M., 2015. Effects of mulching on soil hydro-physical properties in Kibaale Sub-catchment, South Central Uganda.

Kar, S.K., Patra, S., Singh, R., Sankar, M., Kumar, S., Singh, D., Madhu, M. and Singla, S., 2022. Impact of land use reformation on soil hydraulic properties and recovery potential of conservation tillage in India's North-West Himalayan region. Ecohydrology and Hydrobiology.

Khan, F.S., Zaman, Q.U., Chang, Y.K., Farooque, A.A., Schumann, A.W. and Madani, A., 2016. Estimation of the rootzone depth above a gravel layer (in wild blueberry fields) using electromagnetic induction method. Precision Agriculture, 17, pp.155-167.

Kilic, K., Kilic, S. and Kocyigit, R., 2012. Assessment of spatial variability of soil properties in areas under different land use. Bulgarian Journal of Agricultural Science, 18, pp.722–732

Kizilkaya, R. and Dengiz, O., 2010. Variation of land use and land cover effects on some soil physico-chemical characteristics and soil enzyme activity. Zemdirbyste-Agriculture, 97, pp.15-24.

Knight, R. and Endres, A.L., 1990. A new concept in modeling the dielectric response of sandstones; defining a wetted rock and bulk water system. Geophysics, 55, pp.586-594.

Lakhankar, T., Jones, A.S., Combs, C. L., Sengupta, M., Vonder Haar, T.H. and Khanbilvardi, R., 2010. Analysis of large-scale spatial variability of soil moisture using a geostatistical method. Sensors, 10, pp.913-932.

Leeper, G.W. and Uren, N.C., 1993. Soil science: an introduction, Melbourne University Press.

Lobe, I., Amelung, W. and Du Preez, C.C., 2001. Losses of carbon and nitrogen with prolonged arable cropping from sandy soils of the South African Highveld. European Journal of Soil Science, 52, pp.93-101.

McNeill, J.D., 1980. Electromagnetic terrain conductivity measurement at low induction numbers. In Technical Note TN-6. Geonics Limited, Mississauga, Ontario, Canada pp.1-15.

Morris, L.A., 2004. Soil biology and tree growth-soil organic matter forms and functions. Elsevier, pp.1201-1207

Mouazen, A.M. and Al-Asadi, R.A., 2018. Influence of soil moisture content on assessment of bulk density with combined frequency domain reflectometry and visible and near infrared spectroscopy under semi field conditions. Soil and Tillage Research, 176, pp.95-103.

Mouazen, A.M., Karoui, R., De Baerdemaeker, J. and Ramon, H., 2006. Characterization of soil water content using measured visible and near infrared spectra. Soil Science Society of America Journal, 70, pp.1295-1302.

Murty, D., Kirschbaum, M.U., Mcmurtrie, R.E. and Mcgilvray, H., 2002. Does conversion of forest to agricultural land change soil carbon and nitrogen? A review of the literature. Global Change Biology, 8, pp.105-123.

Narjary, B., Meena, M.D., Kumar, S., Kamra, S.K., Sharma, D.K. and Triantafilis, J., 2019. Digital mapping of soil salinity at various depths using an EM38. Soil Use and Management, 35, pp.232-244.

Nieto, O., Castro, J., Fernández, E. and Smith, P., 2010. Simulation of soil organic carbon stocks in a Mediterranean olive grove under different soil-management systems using the RothC model. Soil Use and Management, 26, pp.118-125.

Nocco, M.A., Ruark, M.D. and Kucharik, C.J., 2019. Apparent electrical conductivity predicts physical properties of coarse soils. Geoderma, 335, pp.1-11.

Nwite, J., Orji, J. and Okolo, C., 2018. Effect of different land use systems on soil carbon storage and structural indices in Abakaliki, Nigeria. Indian Journal of Ecology, 45, pp.522-527.

Paz-Gonzalez, A., Vieira, S. and Castro, M.T.T., 2000. The effect of cultivation on the spatial variability of selected properties of an umbric horizon. Geoderma, 97, pp.273-292.

Perera, K., 2021. The adaptability of empirical equations to calculate potential evapotranspiration and trend analysis of hydroclimatological parameters for agricultural areas in Newfoundland. Master's Thesis. Memorial University of Newfoundland.

Rhoton, F., Bruce, R., Buehring, N., Elkins, G., Langdale, C. and Tyler, D., 1993. Chemical and physical characteristics of four soil types under conventional and no-tillage systems. Soil and Tillage Research, 28, pp.51-61.

Robinson, D., Lebron, I., Lesch, S. and Shouse, P., 2004. Minimizing drift in electrical conductivity measurements in high temperature environments using the EM-38. Soil Science Society of America Journal, 68, pp.339-345.

Roose, E. and Barthes, B., 2001. Organic matter management for soil conservation and productivity restoration in Africa: a contribution from Francophone research. Managing Organic Matter in Tropical Soils: Scope and Limitations: Proceedings of a Workshop organized by the Center for Development Research at the University of Bonn (ZEF Bonn)—Germany, 7–10 June 1999, Springer, pp.159-170.

Sadatcharam, K., 2019. Assessing potential applications of multi-coil and multi-frequency electromagnetic induction sensors for agricultural soils in western Newfoundland. Master's Thesis. Memorial University of Newfoundland.

Sağlam, M. and Dengiz, O., 2012. Influence of selected land use types and soil texture interactions on some soil physical characteristics in an alluvial land. International Journal of Agronomy and Plant Production, 3, pp.508-513.

Shrestha, N., 2020. Detecting multicollinearity in regression analysis. American Journal of Applied Mathematics and Statistics, 8, pp.39-42.

Shrestha, S.L., 2022. Quantifying effects of meteorological parameters on air pollution in Kathmandu valley through regression models. Environmental Monitoring and Assessment, 194, pp.684.

Sishodia, R.P., Ray, R.L. and Singh, S.K., 2020. Applications of remote sensing in precision agriculture: A review. Remote Sensing, 12, pp.3136.

Sówka, I., Badura, M., Pawnuk, M., Szymański, P. and Batog, P., 2020. The use of the GIS tools in the analysis of air quality on the selected University campus in Poland. Archives of Environmental Protection, 46, pp.100-106.

Von Hebel, C., Van Der Kruk, J., Huisman, J.A., Mester, A., Altdorff, D., Endres, A.L., Zimmermann, E., Garré, S. and Vereecken, H., 2019. Calibration, conversion, and quantitative multi-layer inversion of multi-coil rigid-boom electromagnetic induction data. Sensors, 19, pp.4753.

Warrick, A.W., 1988. Additional solutions for steady-state evaporation from a shallow water table. Soil Science, 146, pp.63-66.

Won, I., Keiswetter, D.A., Fields, G.R. and Sutton, L.C., 1996. GEM-2: A new multifrequency electromagnetic sensor. Journal of Environmental and Engineering Geophysics, 1, pp.129-137.

Xia, Q., Rufty, T. and Shi, W., 2020. Soil microbial diversity and composition: Links to soil texture and associated properties. Soil Biology and Biochemistry, 149, pp.107953.

Xiao, L.-P., Sun, Z.-J., Shi, Z.-J., Xu, F. and Sun, R.-C., 2011. Impact of hot compressed water pretreatment on the structural changes of woody biomass for bioethanol production. BioResources, 6, pp.1576-1598.

Xie, B., Jia, X., Qin, Z., Zhao, C. and Shao, M.A., 2020. Comparison of interpolation methods for soil moisture prediction on China's Loess Plateau. Vadose Zone Journal, 19, pp.20025.

Yerima, B.P. and Van Ranst, E., 2005. Introduction to soil science: Soils of the tropics, Trafford Publishing.

CHAPTER FIVE: General conclusion and recommendations

5.1 General discussion and conclusion

This thesis assessed the application of multi-coil (MC) and multi-frequency (MF) electromagnetic induction (EMI) sensors in characterizing the variability of a range of soil properties in three different land uses. The surveys were conducted during the wet period, as MF–EMI is more effective in detecting ECa variability in wet soils than in dry soils. The thesis is comprised of two studies conducted on Boreal podzolic soil, specifically in the Western Agriculture Center and Research Station, managed by the Department of Fisheries, Forestry and Agriculture, Government of Newfoundland, Canada.

The first study (Chapter 3) presents evidence that proximal surveys of apparent electrical conductivity (EC_a) using GEM-2 (MF–EMI) could serve as a valuable surrogate for evaluating intra-field spatial variability of soil moisture content (SMC). The impact of soil moisture on EC_a was analyzed under three distinct land use conditions (agricultural land, recently cleared natural forest, and field road) on a boreal podzolic soil. Results from the linear regression analysis indicated that soil moisture was a major factor contributing to EC_a in the study area. The application of cokriging with EC_a as a covariate raised the sensitivity level of spatial variability prediction of SMC than maps produced using ordinary kriging, with additional improvements in the prediction accuracies of soil moisture maps. It was found that EC_a obtained using EMI has the potential to be a reliable auxiliary variable for accurately predicting soil moisture in boreal podzolic soils, with the best prediction and strongest correlation observed in the natural forest. Analysis of EC_a - SMC correlations revealed weaker correlations for agricultural land and field

road. This can be attributed to the presence of fertilizer on the agricultural land, which increases the concentration of dissolved ions in the pore water and thus its pore water electrical conductivity (EC_w), as well as heavy compaction and shallow water depths in parts of the field road that cause poor drainage. These two factors are responsible for the higher EC_a variability in the agricultural land and field road, which in turn has a direct effect on the EC_a-SMC relation in these land uses. These findings indicate that cokriging of SMC with a densely sampled EC_a as covariates may provide an improved characterization of soil moisture variability within the study area. Specifically, the number of EC_a data points taken across all land uses in this study were greater than one thousand (1000) data points. This suggests that the cokriging of SMC with densely sampled EC_a may be a reliable tool for accurately assessing soil moisture variability in the study area. Consequently, this study confirms the efficacy of the georeferenced MF–EMI technique to rapidly assess intra-field variability under different land uses.

The second study (Chapter 4) revealed that measuring EC_a using MC–EMI and MF–EMI sensors provided significant information for maximizing the accuracy of SMC prediction under different land use conditions. EC_a had a significant positive correlation to both SMC and soil organic matter (SOM), with SMC exhibiting the strongest correlation. The correlation results between EC_a and SMC were found to be the strongest in moist soils. This is because EC_a has been reported to increase with water content and potentially ions retained in soil solution. Coil 1 in vertical coplanar mode MC-EMI sensor was the most accurate method for predicting land use conditions, compared to other EMI coils orientations, according to multiple linear regression analysis. SMC was the primary driving EC_a parameter in the study area, however, the other variables such as SOM, silt content, and bulk density were also had a significant impact on EC_a. These findings demonstrate

the importance of considering several soil parameters such as clay content, bulk density, and organic matter when analyzing soil-related variables like EC_a since EC_a is affected by these parameters. Cokriging of TDR-measured SMC with EC_a as a covariate revealed more accurate maps than cokriging predicted SMC with EC_a as a covariate. Additionally, findings from the comparison of both sensors indicate that MC–EMI sensors are more suitable for SMC characterization in the study area than MF–EMI sensors, as they provide a higher level of accuracy and precision. These results illustrate that georeferenced mobile soil EC_a measurements with statistical and geostatsical techniques can aid in characterizing soil spatial variability of SMC rapidly and serve as a soil quality indicator for soil productivity.

5.2 Recommendations for future work

It is recommended that:

1. Further studies should be conducted to compare the prediction accuracy of several interpolation techniques such as inverse distance weighting for the soil properties under different land uses in the study area.
2. More studies should be carried out on other subregions for further validation and assess the gradual variability (gradient) of soil properties between natural and managed lands.
3. More extensive field measurements should be conducted to enhance the reliability of the prediction models through intensive calibration and validation with ground truth data at both vertical and horizontal scales.
4. Ground-truthing of soil parameters should be conducted at deeper depths to ascertain the variability of EC_a associated with soil parameters in those levels. The use of MC and MF-EMI sensors permits a greater depth of investigation than was used in this study, which

only extended to a depth of 0-20 cm. A deeper look into the soil profile will provide a greater understanding of the variability of EC_a throughout the soil profile.

5. A spatial smoothing filter should be applied to reduce the noises due to the EMI sensor positioning (height and tilting) and the difference in the investigated soil volume of the EMI sensors and TDR.
6. Further studies should be conducted to apply inverse modeling to obtain 3D maps of SMC, while considering other environmental factors such as temperature, land slope, water level and vegetation cover, to create more comprehensive understanding of soil spatial variability.
7. Investigation is undertaken on whether magnetic susceptibility could be used as an auxiliary variable to improve the accuracy of maps of the targeted soil properties in this study.
8. EC_a readings obtained from other frequencies of the MF-EMI sensor should be investigated to determine if significant relationships can be identified between these readings and soil parameters. Such an analysis could provide valuable information that may be utilized to better understand the characteristics and behavior of the soil within an area of interest.

References and Bibliography

Abd El-Wahab, R., Al-Rashed, A. and Al-Dousari, A., 2018. Influences of physiographic factors, vegetation patterns and human impacts on aeolian landforms in arid environment. Arid Ecosystems, 8, pp.97-110.

Adejuwon, J.O. and Ekanade, O., 1988. A comparison of soil properties under different landuse types in a part of the Nigerian cocoa belt. Catena, 15(3-4), pp.319-331.

Afrizal, R. and Masunaga, T., 2013. Assessment erosion 3D hazard with USLE and surfer tool: a case study of Sumani Watershed in West Sumatra Indonesia. Journal of Tropical Soils, 18(1), pp.81-92.

Al-Asadi, R.A. and Mouazen, A.M., 2014. Combining frequency domain reflectometry and visible and near infrared spectroscopy for assessment of soil bulk density. Soil and Tillage Research, 135, pp.60-70.

Allred, B.J., Ehsani, M.R. and Daniels, J.J., 2008. General considerations for geophysical methods applied to agriculture. Handbook of Agricultural Geophysics, pp.3-16.

Altdorff, D. and Dietrich, P., 2014. Delineation of areas with different temporal behavior of soil properties at a landslide affected Alpine hillside using time-lapse electromagnetic data. Environmental Earth Sciences, 72, pp.1357-1366.

Altdorff, D., Bechtold, M., Van der Kruk, J., Vereecken, H. and Huisman, J.A., 2016. Mapping peat layer properties with multi-coil offset electromagnetic induction and laser scanning elevation data. Geoderma, 261, pp.178-189.

Altdorff, D., Galagedara, L., Nadeem, M., Cheema, M. and Unc, A., 2018. Effect of agronomic treatments on the accuracy of soil moisture mapping by electromagnetic induction. Catena, 164, pp.96-106.

Altdorff, D., Sadatcharam, K., Unc, A., Krishnapillai, M. and Galagedara, L., 2020. Comparison of multi-frequency and multi-coil electromagnetic induction (EMI) for mapping properties in shallow podzolic soils. Sensors, 20, pp.2330.

Altdorff, D., Von Hebel, C., Borchard, N., Van Der Kruk, J., Bogena, H.R., Vereecken, H. and Huisman, J.A., 2017. Potential of catchment-wide soil water content prediction using electromagnetic induction in a forest ecosystem. Environmental Earth Sciences, 76, pp.1-11.

André, F., Van Leeuwen, C., Saussez, S., Van Durmen, R., Bogaert, P., Moghadas, D., De Resseguier, L., Delvaux, B., Vereecken, H. and Lambot, S., 2012. High-resolution imaging of a vineyard in south of France using ground-penetrating radar, electromagnetic induction and electrical resistivity tomography. Journal of Applied Geophysics, 78, pp.113-122.

Archie, G.E., 1942. The electrical resistivity log as an aid in determining some reservoir characteristics. Transactions of the AIME, 146(01), pp.54-62.

Atwell, M.A. and Wuddivira, M.N., 2019. Electromagnetic-induction and spatial analysis for assessing variability in soil properties as a function of land use in tropical savanna ecosystems. SN Applied Sciences, 1(8), pp.856.

Ayoubi, S., Emami, N., Ghaffari, N., Honarjoo, N. and Sahrawat, K.L., 2014. Pasture degradation effects on soil quality indicators at different hillslope positions in a semiarid region of western Iran. Environmental Earth Sciences, 71, pp.375-381.

Badewa, E., Unc, A., Cheema, M., Kavanagh, V. and Galagedara, L., 2018. Soil moisture mapping using multi-frequency and multi-coil electromagnetic induction sensors on managed podzols. Agronomy, 8, pp.224.

Bai, Y., Ochuodho, T.O. and Yang, J., 2019. Impact of land use and climate change on water-related ecosystem services in Kentucky, USA. Ecological Indicators, 102, pp.51-64.

Batte, M.T., 2000. Factors influencing the profitability of precision farming systems. Journal of Soil and Water Conservation, 55(1), pp.12-18.

Battikhi, A.M. and Suleiman, A.A., 1999. Effect of tillage system on soil strength and bulk density of vertisols. Journal of Agronomy and Crop Science, 183(2), pp.81-89.

Belkhiri, L., Tiri, A. and Mouni, L., 2020. Spatial distribution of the groundwater quality using kriging and co-kriging interpolations. Groundwater for Sustainable Development, 11, pp.100473.

Binley, A., Hubbard, S.S., Huisman, J.A., Revil, A., Robinson, D.A., Singha, K. and Slater, L.D., 2015. The emergence of hydrogeophysics for improved understanding of surface soil processes over multiple scales. Water Resources Research, 51(6), pp.3837-3866.

Brevik, E.C., Fenton, T.E. and Lazari, A., 2006. Soil electrical conductivity as a function of soil water content and implications for soil mapping. Precision Agriculture, 7, pp.393-404.

Brevik, E.C. and Fenton, T.E., 2002. Influence of soil water content, clay, temperature, and carbonate minerals on electrical conductivity readings taken with an EM-38. Soil Survey Horizons, 43(1), pp.9-13.

Brevik, E.C., 2000. A comparison of soil properties in compacted versus non-compacted Bryant soil series twenty-five years after compaction ceased. Soil Survey Horizons, 41(2), pp.52-58.

Brevik, E.C., Fenton, T.E. and Lazari, A., 2003. Differences in EM-38 readings taken above crop residues versus readings taken with instrument-ground contact. Precision Agriculture, 4, pp.351-358.

Briggs, M.A., Wang, C., Day-Lewis, F.D., Williams, K.H., Dong, W. and Lane, J.W., 2019. Return flows from beaver ponds enhance floodplain-to-river metals exchange in alluvial mountain catchments. Science of the Total Environment, 685, pp.357-369.

Brogi, C., Huisman, J., Pätzold, S., Von Hebel, C., Weihermüller, L., Kaufmann, M., Van Der Kruk, J. and Vereecken, H., 2019. Large-scale soil mapping using multi-configuration EMI and supervised image classification. Geoderma, 335, pp.133-148.

Buol, S.W. and Stokes, M.L., 1997. Soil profile alteration under long-term, high-input agriculture. Replenishing Soil Fertility in Africa, 51, pp.97-109.

Buta, M., Paulette, L., Man, T., Bartha, I., Negruşier, C. and Bordea, C., 2019. Spatial assessment of soil salinity by electromagnetic induction survey. Environmental Engineering and Management Journal (EEMJ), 18(9), pp.2073-2081

Calamita, G., Perrone, A., Brocca, L., Onorati, B. and Manfreda, S., 2015. Field test of a multi-frequency electromagnetic induction sensor for soil moisture monitoring in southern Italy test sites. Journal of Hydrology, 529, pp.316-329. Doi:https://doi.org/10.1016/j.jhydrol.2015.07.023.

Cambardella, C. and Karlen, D., 1999. Spatial analysis of soil fertility parameters. Precision Agriculture, 1, pp.5-14.

Carrière, S.D., Martin-StPaul, N.K., Doussan, C., Courbet, F., Davi, H. and Simioni, G., 2021. Electromagnetic induction is a fast and non-destructive approach to estimate the influence of surface heterogeneity on forest canopy structure. Water, 13(22), pp.3218.

Carroll, Z. and Oliver, M.A., 2005. Exploring the spatial relations between soil physical properties and apparent electrical conductivity. Geoderma, 128, pp.354-374.

Carter, M.R. and Gregorich, E.G., 2007. Soil sampling and methods of analysis, CRC press.

Celik, I., 2005. Land-use effects on organic matter and physical properties of soil in a southern Mediterranean highland of Turkey. Soil and Tillage research, 83, pp.270-277.

Chalise, K.S., Singh, S., Wegner, B.R., Kumar, S., Pérez-Gutiérrez, J.D., Osborne, S.L., Nleya, T., Guzman, J. and Rohila, J.S., 2019. Cover crops and returning residue impact on soil organic carbon, bulk density, penetration resistance, water retention, infiltration, and soybean yield. Agronomy Journal, 111(1), pp.99-108.

Cho, Y., Sudduth, K.A. and Chung, S.O., 2016. Soil physical property estimation from soil strength and apparent electrical conductivity sensor data. Biosystems Engineering, 152, pp.68-78.

Choi, M., and Jacobs, J.M., 2007. Soil moisture variability of root zone profiles within SMEX02 remote sensing footprints. Advances in Water Resources, 30(4), pp.883-896. https://doi.org/10.1016/j.advwatres.2006.07.007.

Chrétien, M., Lataste, J.F., Fabre, R. and Denis, A., 2014. Electrical resistivity tomography to understand clay behavior during seasonal water content variations. Engineering Geology, 169, pp.112-123.

Ciampalini, A., André, F., Garfagnoli, F., Grandjean, G., Lambot, S., Chiarantini, L. and Moretti, S., 2015. Improved estimation of soil clay content by the fusion of remote hyperspectral and proximal geophysical sensing. Journal of Applied Geophysics, 116, pp.135-145.

Corwin, D.L. and Scudiero, E., 2019. Mapping soil spatial variability with apparent soil electrical conductivity (ECa) directed soil sampling. Soil Science Society of America Journal, 83, pp.3-4.

Corwin, D.L. and Lesch, S.M., 2003. Application of soil electrical conductivity to precision agriculture: theory, principles, and guidelines. Agronomy Journal, 95(3), pp.455-471.

Corwin, D.L. and Lesch, S.M., 2005. Apparent soil electrical conductivity measurements in agriculture. Computers and Electronics in Agriculture, 46(1-3), pp.11-43.

Corwin, D.L., 2008. Past, present, and future trends in soil electrical conductivity measurements using geophysical methods. Handbook of Agricultural Geophysics, pp.17-44.

Croquet, E.G., 2016. Late Wisconsinan paleosols and macrofossils in Chehalis Valley: paleoenvironmental reconstruction and regional significance (Doctoral dissertation, Science: Department of Earth Sciences).

Dakak, H., Dekkaki, H.C., Zouahri, A., Moussadek, R., Iaaich, H., Yachou, H., Ghanimi, A. and Douaik, A., 2023. Soil salinity prediction and mapping using electromagnetic induction and spatial interpolation. Environmental Sciences Proceedings, 16(1), pp.76.

Dale, V.H., 1997. The relationship between land-use change and climate change. Ecological Applications, 7(3), pp.753-769.

De Benedetto, D., Castrignanò, A., Rinaldi, M., Ruggieri, S., Santoro, F., Figorito, B., Gualano, S., Diacono, M. and Tamborrino, R., 2013. An approach for delineating homogeneous zones by using multi-sensor data. Geoderma, 199, pp.117-127.

De Souza Lima, E., Lovera, L.H., Montanari, R., De Souza, Z.M. and Torres, J.L.R., 2017. Spatial variability of apparent electrical conductivity and physicochemical attributes of the soil. Revista Cultura Agronômica, 26(3), pp.469-482.

Deidda, G.P., De Carlo, L., Caputo, M.C. and Cassiani, G., 2022. Frequency domain electromagnetic induction imaging: An effective method to see inside a capped landfill. Waste Management, 144, pp.29-40.

Doolittle, J., Noble, C. and Leinard, B., 2000. An electromagnetic induction survey of a riparian area in southwest Montana. Soil Survey Horizons, 41(2), pp.27-36.

Doolittle, J.A. and Brevik, E.C., 2014. The use of electromagnetic induction techniques in soils studies. Geoderma, 223, pp.33-45.

Doolittle, J.A. and Collins, M.E., 1998. A comparison of EM induction and GPR methods in areas of karst. Geoderma, 85(1), pp.83-102.

Doolittle, J.A., Sudduth, K.A., Kitchen, N.R. and Indorante, S.J., 1994. Estimating depths to claypans using electromagnetic induction methods. Journal of Soil and Water Conservation, 49(6), pp.572-575.

Drummond, S.T., Sudduth, K.A., Joshi, A., Birrell, S.J. and Kitchen, N.R., 2003. Statistical and neural methods for site–specific yield prediction. Transactions of the ASAE, 46(1), pp.5. Doi:10.13031/2013.12541.

DualEM, Inc., 2005. DUALEM-1S and Dualem- S User's Manual. Milton, Ontario, Canada.

Enakiev, Y.I., Bahitova, A.R. and Lapushkin, V.M., 2018. Microelements (Cu, Mo, Zn, Mn, Fe) in corn grain according to their availability in the fallow SOD-Podzolic soil profile. Bulgarian Journal of Agricultural Science, 24(2), pp.285-289.

Farzamian, M., Paz, M.C., Paz, A.M., Castanheira, N.L., Gonçalves, M.C., Monteiro Santos, F.A. and Triantafilis, J., 2019. Mapping soil salinity using electromagnetic conductivity imaging—A

comparison of regional and location-specific calibrations. Land Degradation and Development, 30, pp.1393-1406.

Feigin, A., Ravina, I. and Shalhevet, J., 2012. Irrigation with treated sewage effluent: management for environmental protection, Springer Science and Business Media, 17.

Fernández-Gálvez, J., 2008. Errors in soil moisture content estimates induced by uncertainties in the effective soil dielectric constant. International journal of remote sensing, 29, pp.3317-3323.

Fortes, R., Millán, S., Prieto, M.H. and Campillo, C., 2015. A methodology based on apparent electrical conductivity and guided soil samples to improve irrigation zoning. Precision Agriculture, 16(4), pp.441-454.

Franzen, D.W., 2018. Soil variability and fertility management. Precision Agriculture Basics, pp.79-92.

Franzluebbers, A., Stuedemann, J. and Schomberg, H., 2000. Spatial distribution of soil carbon and nitrogen pools under grazed tall fescue. Soil Science Society of America Journal, 64, pp.635-639.

Friedman, S.P., 2005. Soil properties influencing apparent electrical conductivity: a review. Computers and Electronics in Agriculture, 46(1-3), pp.45-70.

Funes, I., Savé, R., Rovira, P., Molowny-Horas, R., Alcañiz, J.M., Ascaso, E., Herms, I., Herrero, C., Boixadera, J. and Vayreda, J., 2019. Agricultural soil organic carbon stocks in the north-eastern Iberian Peninsula: Drivers and spatial variability. Science of the Total Environment, 668, pp.283-294

Ganjegunte, G.K., Clark, J.A., Sallenave, R., Sevostianova, E., Serena, M., Alvarez, G. and Leinauer, B., 2017. Soil salinity of an urban park after long-term irrigation with saline ground water. Agronomy Journal, 109(6), pp.3011-3018.

Ganjegunte, G.K., Sheng, Z. and Clark, J.A., 2014. Soil salinity and sodicity appraisal by electromagnetic induction in soils irrigated to grow cotton. Land Degradation and Development, 25(3), pp.228-235.

Gao, X., Wu, P., Zhao, X., Shi, Y., Wang, J. and Zhang, B., 2011. Soil moisture variability along transects over a well-developed gully in the Loess Plateau, China. Catena, 87(3), pp.357-367.

García-Tomillo, A., Mirás-Avalos, J.M., Dafonte-Dafonte, J. and Paz-González, A., 2017. Mapping soil texture using geostatistical interpolation combined with electromagnetic induction measurements. Soil Science, 182(8), pp.278-284.

Gebbers, R., Lück, E. and Heil, K., 2007. Depth sounding with the EM38-detection of soil layering by inversion of apparent electrical conductivity measurements. Precision Agriculture, 7, pp.95-102.

Gebrehiwot, S.G., Bewket, W., Mengistu, T., Nuredin, H., Ferrari, C.A. and Bishop, K., 2021. Monitoring and assessment of environmental resources in the changing landscape of Ethiopia: a focus on forests and water. Environmental Monitoring and Assessment, 193(10), pp.1-13

Geonics, 2005. EM38. Available from: http://www.geonics.com/html/em38.html (Accessed 17 February 2005).

GF Instruments, 2011. CMD Electromagnetic conductivity meter user manual V. 1.5. Geophysical Equipment and Services, Czech Republic. Available at: http://www.gfinstruments.cz/index.php?menu=gi&smenu=iem&cont=cmd_&ear=ov.

Gooley, L., Huang, J., Page, D. and Triantafilis, J., 2014. Digital soil mapping of available water content using proximal and remotely sensed data. Soil Use and Management, 30(1), pp.139-151.

Goovaerts, P., 1997. Geostatistics for natural resources evaluation. Oxford University Press on Demand.

Goovaerts, P., 1999. Using elevation to aid the geostatistical mapping of rainfall erosivity. Catena, 34(3-4), pp.227-242.

Government of Newfoundland and Labrador., 2017. The Way Forward on Agriculture. Sector Work Plan. Retrieved 20 Nov. 2021. From https://www.gov.NF.ca/ffa/files/agriculture-Sector-Workplan_Final.pdf

Greco, R. and Guida, A., 2009. TDR water content inverse profiling in layered soils during infiltration and evaporation. In EGU General Assembly Conference Abstracts pp.7038.

Greenhouse, J.P. and Slaine, D.D., 1983. The use of reconnaissance electromagnetic methods to map contaminant migration: These nine case studies can help determine which geophysical techniques are applicable to a given problem. Groundwater Monitoring and Remediation, 3(2), pp.47-59.

Grisso, R.D., Alley, M.M., Holshouser, D.L. and Thomason, W.E., 2005. Precision farming tools. Soil Electrical Conductivity. Virginia State University Cooperative Extension, pp.442–508.

Grubbs, R.A., Straw, C.M., Bowling, W.J., Radcliffe, D.E., Taylor, Z. and Henry, G.M., 2019. Predicting spatial structure of soil physical and chemical properties of golf course fairways using an apparent electrical conductivity sensor. Precision Agriculture, 20(3), pp.496-519.

Guber, A.K., Gish, T.J., Pachepsky, Y.A., van Genuchten, M.T., Daughtry, C.S.T., Nicholson, T.J. and Cady, R.E., 2008. Temporal stability in soil water content patterns across agricultural fields. Catena, 73(1), pp.125-133.

Guo, X., Fu, Q., Hang, Y., Lu, H., Gao, F. and Si, J., 2020. Spatial variability of soil moisture in relation to land use types and topographic features on hillslopes in the black soil (mollisols) area of northeast China. Sustainability, 12(9), pp.3552.

Guo, Y., Boughton, E.H., Liao, H.L., Sonnier, G. and Qiu, J., 2023. Direct and indirect pathways of land management effects on wetland plant litter decomposition. Science of the Total Environment, 854, pp.158-189.

Guo, Y., Shi, Z., Huang, J., Zhou, L., Zhou, Y. and Wang, L., 2016. Characterization of field scale soil variability using remotely and proximally sensed data and response surface method. Stochastic Environmental Research and Risk Assessment, 30, pp.859-869.

Haining, R.P., 2009. Spatial autocorrelation and the quantitative revolution. Geographical Analysis, 41(4), pp.364-374.

Heil, K. and Schmidhalter, U., 2012. Characterisation of soil texture variability using the apparent soil electrical conductivity at a highly variable site. Computers and Geosciences, 39, pp.98-110.

Hendrickx, J.M.H., Baerends, B., Raza, Z.I., Sadig, M. and Chaudhry, M.A., 1992. Soil salinity assessment by electromagnetic induction of irrigated land. Soil Science Society of America Journal, 56(6), pp.1933-1941

Hendrickx, J.M.H., Kachanoski, R.G., Dane, J.H. and Topp, G.C., 2002. Nonintrusive electromagnetic induction. Methods of Soil Analysis. Part, 4, pp.1297-1306.

Huang, J., Pedrera-Parrilla, A., Vanderlinden, K., Taguas, E.V., Gómez, J.A. and Triantafilis, J., 2017. Potential to map depth-specific soil organic matter content across an olive grove using quasi-2d and quasi-3d inversion of DUALEM-21 data. Catena, 152, pp.207-217.

Huth, N.I. and Poulton, P.L., 2007. An electromagnetic induction method for monitoring variation in soil moisture in agroforestry systems. Soil Research, 45(1), pp.63-72.

Islam, M.M., Meerschman, E., Saey, T., De Smedt, P., Van De Vijver, E. and Van Meirvenne, M., 2012. Comparing apparent electrical conductivity measurements on a paddy field under flooded and drained conditions. Precision Agriculture, 13, pp.384-392.

Islam, M.M., Meerschman, E., Saey, T., De Smedt, P., Van De Vijver, E., Delefortrie, S. and Van Meirvenne, M., 2014. Characterizing compaction variability with an electromagnetic induction sensor in a puddled paddy rice field. Soil Science Society of America Journal, 78(2), pp.579-588.

Johnson, C.K., Doran, J.W., Duke, H.R., Wienhold, B.J., Eskridge, K.M. and Shanahan, J.F., 2001. Field-scale electrical conductivity mapping for delineating soil condition. Soil Science Society of America Journal, 65(6), pp.1829-1837.

Jonard, F., Mahmoudzadeh, M., Roisin, C., Weihermüller, L., André, F., Minet, J., Vereecken, H. and Lambot, S., 2013. Characterization of tillage effects on the spatial variation of soil properties using ground-penetrating radar and electromagnetic induction. Geoderma, 207, pp.310-322.

Kaffka, S.R., Lesch, S.M., Bali, K.M. and Corwin, D.L., 2005. Site-specific management in salt-affected sugar beet fields using electromagnetic induction. Computers and Electronics in Agriculture, 46(1-3), pp.329-350.

Kakaire, J., Makokha, G. L., Mwanjalolo, M., Mensah, A. K. and Emmanuel, M., 2015. Effects of mulching on soil hydro-physical properties in Kibaale Sub-catchment, South Central Uganda.

Kar, S.K., Patra, S., Singh, R., Sankar, M., Kumar, S., Singh, D., Madhu, M. and Singla, S., 2022. Impact of land use reformation on soil hydraulic properties and recovery potential of conservation tillage in India's North-West Himalayan region. Ecohydrology and Hydrobiology.

Kathuria, D., Mohanty, B.P. and Katzfuss, M., 2019. A nonstationary geostatistical framework for soil moisture prediction in the presence of surface heterogeneity. Water Resources Research, 55(1), pp.729-753.

Kaufmann, M.S., von Hebel, C., Weihermüller, L., Baumecker, M., Döring, T., Schweitzer, K., Hobley, E., Bauke, S.L., Amelung, W., Vereecken, H. and van der Kruk, J., 2020. Effect of fertilizers and irrigation on multi-configuration electromagnetic induction measurements. Soil Use and Management, 36(1), pp.104-116.

Kelley, J., Higgins, C.W., Pahlow, M. and Noller, J., 2017. Mapping soil texture by electromagnetic induction: a case for regional data coordination. Soil Science Society of America Journal, 81(4), pp.923-931.

Khan, F.S., Zaman, Q.U., Chang, Y.K., Farooque, A.A., Schumann, A.W. and Madani, A., 2016. Estimation of the rootzone depth above a gravel layer (in wild blueberry fields) using electromagnetic induction method. Precision agriculture, 17, pp.155-167.

Kilic, K., Kilic, S. and Kocyigit, R., 2012. Assessment of spatial variability of soil properties in areas under different land use. Bulgarian Journal of Agricultural Science, 18, pp.722– 732

Kizilkaya, R. and Dengiz, O., 2010. Variation of land use and land cover effects on some soil physico-chemical characteristics and soil enzyme activity. Zemdirbyste-Agriculture, 97, pp.15-24.

Knight, R. and Endres, A.L., 1990. A new concept in modeling the dielectric response of sandstones; defining a wetted rock and bulk water system. Geophysics, 55, pp.586-594.

Kostić, M., Rajković, M., Ljubičić, N., Ivošević, B., Radulović, M., Blagojević, D. and Dedović, N., 2021. Georeferenced tractor wheel slip data for prediction of spatial variability in soil physical properties. Precision Agriculture, 22(5), pp.1659-1684.

Koszinski, S., Miller, B.A., Hierold, W., Haelbich, H. and Sommer, M., 2015. Spatial modeling of organic carbon in degraded peatland soils of northeast Germany. Soil Science Society of America Journal, 79(5), pp.1496-1508.

Kweon, G., Lund, E. and Maxton, C., 2013. Soil organic matter and cation-exchange capacity sensing with on-the-go electrical conductivity and optical sensors. Geoderma, 199, pp.80-89.

Lakhankar, T., Jones, A.S., Combs, C.L., Sengupta, M., Vonder Haar, T.H. and Khanbilvardi, R., 2010. Analysis of large-scale spatial variability of soil moisture using a geostatistical method. Sensors, 10, pp.913-932.

Lal, R., 2020. Soil organic matter and water retention. Agronomy Journal, 112(5), pp.3265-3277.

Lawrence, I. and Lin, K., 1989. A concordance correlation coefficient to evaluate reproducibility. Biometrics, pp.255-268.

Leeper, G.W. and Uren, N.C., 1993. Soil science: an introduction, Melbourne University Press.

Liao, K.H., Zhu, Q. and Doolittle, J., 2014. Temporal stability of apparent soil electrical conductivity measured by electromagnetic induction techniques. Journal of Mountain Science, 11(1), pp.98-109.

Liu, L.L., Cheng, Y.M., Jiang, S.H., Zhang, S.H., Wang, X.M. and Wu, Z.H., 2017. Effects of spatial autocorrelation structure of permeability on seepage through an embankment on a soil foundation. Computers and Geotechnics, 87, pp.62-75.

Lobe, I., Amelung, W. and Du Preez, C.C., 2001. Losses of carbon and nitrogen with prolonged arable cropping from sandy soils of the South African Highveld. European Journal of Soil Science, 52, pp.93-101.

Lu, C., Zhou, Z., Zhu, Q., Lai, X. and Liao, K., 2017. Using residual analysis in electromagnetic induction data interpretation to improve the prediction of soil properties. Catena, 149, pp.176-184.

Lück, E., Guillemoteau, J., Tronicke, J., Klose, J. and Trost, B., 2022. Geophysical sensors for mapping soil layers–a comparative case study using different electrical and electromagnetic sensors. in information and communication technologies for agriculture—Theme I: Sensors pp. 267-287. Springer International Publishing.

Lund, E.D., Christy, C.D. and Drummond, P.E., 1999. Practical applications of soil electrical conductivity mapping. Precision Agriculture, 99, pp.771-779.

Ma, R., McBratney, A., Whelan, B., Minasny, B. and Short, M., 2011. Comparing temperature correction models for soil electrical conductivity measurement. Precision Agriculture, 12, pp.55-66.

Machado, F.C., Montanari, R., Shiratsuchi, L.S., Lovera, L.H. and Lima, E.D.S., 2015. Spatial dependence of electrical conductivity and chemical properties of the soil by electromagnetic induction. Revista Brasileira de Ciência do Solo, 39, pp.1112-1120.

Mahmood, H.S., Hoogmoed, W.B. and van Henten, E.J., 2012. Sensor data fusion to predict multiple soil properties. Precision Agriculture, 13(6), pp.628-645.

Malicki, M.A., Campbell, E.C. and Hanks, R.J., 1989. Investigations on power factor of the soil electrical impedance as related to moisture, salinity and bulk density. Irrigation Science, 10, pp.55-62.

Mansourian, D., Cornelis, W. and Hermans, T., 2020. Exploring Geophysical Methods for Mapping Soil Strength in Relation to Soil Compaction. Master's thesis. Ghent University.

Martinez, G., Vanderlinden, K., Ordóñez, R. and Muriel, J.L., 2009. Can apparent electrical conductivity improve the spatial characterization of soil organic carbon? Vadose Zone Journal, 8(3), pp.586-593.

Martini, E., Werban, U., Zacharias, S., Pohle, M., Dietrich, P. and Wollschläger, U., 2017. Repeated electromagnetic induction measurements for mapping soil moisture at the field scale: Validation with data from a wireless soil moisture monitoring network. Hydrology and Earth System Sciences, 21(1), pp.495-513.

McNeill, J.D., 1980. Applications of transient electromagnetic techniques. Missasauga, ON, Canada: Geonics Limited. pp.17

Medhioub, E., Bouaziz, M. and Bouaziz, S., 2019. Spatial estimation of soil organic matter content using remote sensing data in southern Tunisia. In Advances in Remote Sensing and Geo Informatics Applications: Proceedings of the 1st Springer Conference of the Arabian Journal of Geosciences (CAJG-1), Tunisia 2018 Springer International Publishing, pp. 215-217.

Miller, W. and Miller, W.M., 1978. Soil Survey of De Witt County, Texas. Department of Agriculture, Soil Conservation Service.

Minsley, B.J., Smith, B.D., Hammack, R., Sams, J.I. and Veloski, G., 2012. Calibration and filtering strategies for frequency domain electromagnetic data. Journal of Applied Geophysics, 80, pp.56-66.

Misra, R.K. and Padhi, J., 2014. Assessing field-scale soil water distribution with electromagnetic induction method. Journal of Hydrology, 516, pp.200-209.

Moghadas, D., Taghizadeh-Mehrjardi, R. and Triantafilis, J., 2016. Probabilistic inversion of EM38 data for 3D soil mapping in central Iran. Geoderma Regional, 7(2), pp.230-238.

Moral, F.J., Terrón, J.M. and Da Silva, J.M., 2010. Delineation of management zones using mobile measurements of soil apparent electrical conductivity and multivariate geostatistical techniques. Soil and Tillage Research, 106(2), pp.335-343. Doi:https://doi.org/10.1016/j.still.2009.12.002.

Morris, L.A., 2004. Soil biology and tree growth-soil organic matter forms and functions. Elsevier, pp.1201-1207

Mouazen, A.M. and Al-Asadi, R.A., 2018. Influence of soil moisture content on assessment of bulk density with combined frequency domain reflectometry and visible and near infrared spectroscopy under semi field conditions. Soil and Tillage Research, 176, pp.95-103.

Mouazen, A.M., Karoui, R., De Baerdemaeker, J. and Ramon, H., 2006. Characterization of soil water content using measured visible and near infrared spectra. Soil Science Society of America Journal, 70, pp.1295-1302.

Murty, D., Kirschbaum, M.U., Mcmurtrie, R.E. and Mcgilvray, H., 2002. Does conversion of forest to agricultural land change soil carbon and nitrogen? A review of the literature. Global Change Biology, 8, pp.105-123.

Naderi-Boldaji, M., Sharifi, A., Alimardani, R., Hemmat, A., Keyhani, A., Loonstra, E.H., Weisskopf, P., Stettler, M. and Keller, T., 2013. Use of a triple-sensor fusion system for on-the-go measurement of soil compaction. Soil and Tillage Research, 128, pp.44-53.

Naimi, S., Ayoubi, S., Zeraatpisheh, M. and Dematte, J.A.M., 2021. Ground observations and environmental covariates integration for mapping of soil salinity: a machine learning-based approach. Remote Sensing, 13(23), pp.4825.

Narjary, B., Meena, M.D., Kumar, S., Kamra, S.K., Sharma, D.K. and Triantafilis, J., 2019. Digital mapping of soil salinity at various depths using an EM38. Soil Use and Management, 35, pp.232-244.

Nearing, G.S., Tuller, M., Jones, S.B., Heinse, R. and Meding, M.S., 2013. Electromagnetic induction for mapping textural contrasts of mine tailing deposits. Journal of Applied Geophysics, 89, pp.11-20.

Neely, H.L., Morgan, C.L., Hallmark, C.T., McInnes, K.J. and Molling, C.C., 2016. Apparent electrical conductivity response to spatially variable vertisol properties. Geoderma, 263, pp.168-175.

Nieto, O., Castro, J., Fernández, E. and Smith, P., 2010. Simulation of soil organic carbon stocks in a Mediterranean olive grove under different soil-management systems using the RothC model. Soil Use and Management, 26, pp.118-125.

Niu, C.Y., Musa, A. and Liu, Y., 2015. Analysis of soil moisture condition under different land uses in the arid region of Horqin sandy land, northern China. Solid Earth, 6(4), pp.1157-1167.

Nocco, M.A., Ruark, M.D. and Kucharik, C.J., 2019. Apparent electrical conductivity predicts physical properties of coarse soils. Geoderma, 335, pp.1-11.

Nwite, J., Orji, J. and Okolo, C., 2018. Effect of different land use systems on soil carbon storage and structural indices in Abakaliki, Nigeria. Indian Journal of Ecology, 45, pp.522-527.

Pan, L., Adamchuk, V.I., Prasher, S., Gebbers, R., Taylor, R.S. and Dabas, M., 2014. Vertical soil profiling using a galvanic contact resistivity scanning approach. Sensors, 14(7), pp.13243-13255.

Paz-Gonzalez, A., Vieira, S. and Castro, M.T.T., 2000. The effect of cultivation on the spatial variability of selected properties of an umbric horizon. Geoderma, 97, pp.273-292.

Pedrera-Parrilla, A., Van De Vijver, E., Van Meirvenne, M., Espejo-Pérez, A.J., Giráldez, J.V. and Vanderlinden, K., 2016. Apparent electrical conductivity measurements in an olive orchard under wet and dry soil conditions: significance for clay and soil water content mapping. Precision Agriculture, 17(5), pp.531-545.

Peralta, N.R., Cicore, P.L., Marino, M.A., da Silva, J.R.M. and Costa, J.L., 2015. Use of geophysical survey as a predictor of the edaphic properties variability in soils used for livestock production. Spanish Journal of Agricultural Research, 13(4), pp.1103.

Perera, K., 2021. The adaptability of empirical equations to calculate potential evapotranspiration and trend analysis of hydroclimatological parameters for agricultural areas in Newfoundland. Master's Thesis. Memorial University of Newfoundland.

Piikki, K., Söderström, M. and Stenberg, B., 2013. Sensor data fusion for topsoil clay mapping. Geoderma, 199, pp.106-116.

Pognant, D., Canone, D., Previati, M. and Ferraris, S., 2013. Using EM equipment to verify the presence of seepage losses in irrigation canals. Procedia Environmental Sciences, 19, pp.836-845.

Polyakov, V. and Lal, R., 2004. Modeling soil organic matter dynamics as affected by soil water erosion. Environment International, 30(4), pp.547-556.

Pouladi, N., Møller, A.B., Tabatabai, S. and Greve, M.H., 2019. Mapping soil organic matter contents at field level with Cubist, Random forest, and kriging. Geoderma, 342, pp.85-92.

Pozdnyakov, A.I., Eliseev, P.I. and Pozdnyakov, L.A., 2015. Electrophysical approach to assessing some cultivation and fertility elements of light soils in the humid zone. Eurasian Soil Science, 48(7), pp.726-734.

Rallo, G., Provenzano, G., Castellini, M. and Sirera, À.P., 2018. Application of EMI and FDR sensors to assess the fraction of transpirable soil water over an olive grove. Water, 10(2), p.168.

Rashid, Q.A., Abuel-Naga, H.M., Leong, E.C., Lu, Y. and Al Abadi, H., 2018. Experimental-artificial intelligence approach for characterizing electrical resistivity of partially saturated clay liners. Applied Clay Science, 156, pp.1-10.

Reedy, R.C. and Scanlon, B.R., 2003. Soil water content monitoring using electromagnetic induction. Journal of Geotechnical and Geoenvironmental Engineering, 129(11), pp.1028-1039.

Revil, A., Coperey, A., Shao, Z., Florsch, N., Fabricius, I.L., Deng, Y., Delsman, J.R., Pauw, P.S., Karaoulis, M., De Louw, P.G.B. and van Baaren, E.S., 2017. Complex conductivity of soils. Water Resources Research, 53(8), pp.7121-7147.

Rhoades, J.D., and Corwin, D.L., 1990. Soil electrical conductivity: effects of soil properties and application to soil salinity appraisal. Communications in Soil Science and Plant Analysis, 21(11-12), pp.837-860.

Rhoades, J.D., Manteghi, N.A., Shouse, P.J. and Alves, W.J., 1989. Soil electrical conductivity and soil salinity: New formulations and calibrations. Soil Science Society of America Journal, 53(2), pp.433-439. https://doi.org/10.2136/sssaj1989.03615995005300020020x

Rhoton, F., Bruce, R., Buehring, N., Elkins, G., Langdale, C. and Tyler, D., 1993. Chemical and physical characteristics of four soil types under conventional and no-tillage systems. Soil and tillage Research, 28, pp.51-61.

Robinet, J., von Hebel, C., Govers, G., van der Kruk, J., Minella, J.P., Schlesner, A., Ameijeiras-Mariño, Y. and Vanderborght, J., 2018. Spatial variability of soil water content and soil electrical conductivity across scales derived from Electromagnetic Induction and Time Domain Reflectometry. Geoderma, 314, pp.160-174.

Rodrigues Jr, F.A., Bramley, R.G.V. and Gobbett, D.L., 2015. Proximal soil sensing for precision agriculture: Simultaneous use of electromagnetic induction and gamma radiometrics in contrasting soils. Geoderma, 243, pp.183-195.

Romero-Ruiz, A., Linde, N., Keller, T. and Or, D., 2018. A review of geophysical methods for soil structure characterization. Reviews of Geophysics, 56(4), pp.672-697.

Roose, E. and Barthes, B., 2001. Organic matter management for soil conservation and productivity restoration in Africa: a contribution from Francophone research. Managing Organic Matter in Tropical Soils: Scope and Limitations: Proceedings of a Workshop organized by the Center for Development Research at the University of Bonn (ZEF Bonn)—Germany, 7–10 June 1999, Springer, pp.159-170.

Roper, W.R., Robarge, W.P., Osmond, D.L. and Heitman, J.L., 2019. Comparing four methods of measuring soil organic matter in North Carolina soils. Soil Science Society of America Journal, 83(2), pp.466-474.

Rossi, R., Amato, M., Pollice, A., Bitella, G., Gomes, J.J., Bochicchio, R. and Baronti, S., 2013. Electrical resistivity tomography to detect the effects of tillage in a soil with a variable rock fragment content. European Journal of Soil Science, 64(2), pp.239-248.

Rostami, A.A., Karimi, V., Khatibi, R. and Pradhan, B., 2020. An investigation into seasonal variations of groundwater nitrate by spatial modelling strategies at two levels by kriging and co-kriging models. Journal of Environmental Management, 270, pp.110843.

Sadatcharam, K., 2019. Assessing potential applications of multi-coil and multi-frequency electromagnetic induction sensors for agricultural soils in western Newfoundland. Master's Thesis. Memorial University of Newfoundland.

Sadatcharam, K., Altdorff, D., Unc, A., Krishnapillai, M. and Galagedara, L., 2020. Depth sensitivity of apparent magnetic susceptibility measurements using multi-coil and multi-frequency electromagnetic induction. Journal of Environmental and Engineering Geophysics, 25(3), pp.301-314. Doi: 10.32389/JEEG20-001.

Sağlam, M. and Dengiz, O., 2012. Influence of selected land use types and soil texture interactions on some soil physical characteristics in an alluvial land. International Journal of Agronomy and Plant Production, 3, pp.508-513.

Sanborn, P., Lamontagne, L. and Hendershot, W., 2011. Podzolic soils of Canada: Genesis, distribution, and classification. Canadian Journal of Soil Science, 91(5), pp.843-880.

Sapkota, T.B., Mazzoncini, M., Bàrberi, P., Antichi, D. and Silvestri, N., 2012. Fifteen years of no till increase soil organic matter, microbial biomass and arthropod diversity in cover crop-based arable cropping systems. Agronomy for Sustainable Development, 32(4), pp.853-863.

Schumann, A.W. and Zaman, Q.U., 2003. Mapping water table depth by electromagnetic induction. Applied Engineering in Agriculture, 19(6), pp.675.

Shanahan, P.W., Binley, A., Whalley, W.R. and Watts, C.W., 2015. The use of electromagnetic induction to monitor changes in soil moisture profiles beneath different wheat genotypes. Soil Science Society of America Journal, 79(2), pp.459-466.

Sheets, K.R. and Hendrickx, J.M., 1995. Noninvasive soil water content measurement using electromagnetic induction. Water Resources Research, 31(10), pp.2401-2409.

Shi, W., Dell, E., Bowman, D. and Iyyemperumal, K., 2006. Soil enzyme activities and organic matter composition in a turfgrass chronosequence. Plant and Soil, 288(1), pp.285-296.

Shrestha, N., 2020. Detecting multicollinearity in regression analysis. American Journal of Applied Mathematics and Statistics, 8, pp.39-42.

Shrestha, S.L., 2022. Quantifying effects of meteorological parameters on air pollution in Kathmandu valley through regression models. Environmental Monitoring and Assessment, 194, pp.684.

Silva Filho, A.M., Silva, C.L.B., Oliveira, M.A.A., Pires, T.G., Alves, A.J., Calixto, W.P. and Narciso, M.G., 2017. Geoelectric method applied in correlation between physical characteristics and electrical properties of the soil. Transactions on Environment and Electrical Engineering, 2(2), pp.37-44.

Simon, F.X., Pareilh-Peyrou, M., Buvat, S., Mayoral, A., Labazuy, P., Kelfoun, K. and Tabbagh, A., 2020. Quantifying multiple electromagnetic properties in EMI surveys: A case study of hydromorphic soils in a volcanic context–The Lac du Puy (France). Geoderma, 361, pp.114084.

Simon, F.X., Tabbagh, A., Donati, J.C. and Sarris, A., 2019. Permittivity mapping in the VLF–LF range using a multi-frequency EMI device: first tests in archaeological prospection. Near Surface Geophysics, 17(1), pp.27-41.

Sishodia, R.P., Ray, R.L. and Singh, S.K., 2020. Applications of remote sensing in precision agriculture: A review. Remote Sensing, 12, pp.3136.

Sówka, I., Badura, M., Pawnuk, M., Szymański, P. and Batog, P., 2020. The use of the GIS tools in the analysis of air quality on the selected University campus in Poland. Archives of Environmental Protection, 46(1), pp.100-106.

Srivastava, P.K., Pandey, P.C., Petropoulos, G.P., Kourgialas, N.N., Pandey, V. and Singh, U., 2019. GIS and remote sensing aided information for soil moisture estimation: A comparative study of interpolation techniques. Resources, 8(2), pp.70.

Stadler, A., Rudolph, S., Kupisch, M., Langensiepen, M., van der Kruk, J. and Ewert, F., 2015. Quantifying the effects of soil variability on crop growth using apparent soil electrical conductivity measurements. European Journal of Agronomy, 64, pp.8-20.

Starr, G.C., 2005. Assessing temporal stability and spatial variability of soil water patterns with implications for precision water management. Agricultural Water Management, 72(3), pp.223-243.

Stavi, I., 2019. Seeking environmental sustainability in dryland forestry. Forests, 10(9), pp.737.

Stępień, M., Samborski, S., Gozdowski, D., Dobers, E.S., Chormański, J. and Szatyłowicz, J., 2015. Assessment of soil texture class on agricultural fields using ECa, Amber NDVI, and topographic properties. Journal of Plant Nutrition and Soil Science, 178(3), pp.523-536.

Sudduth, K.A., Kitchen, N.R., Bollero, G.A., Bullock, D.G. and Wiebold, W.J., 2003. Comparison of electromagnetic induction and direct sensing of soil electrical conductivity. Agronomy Journal, 95(3), pp.472-482.

Susha, S.U., Singh, D.N. and Baghini, M.S., 2014. A critical review of soil moisture measurement. Measurement, 54, pp.92-105. https://doi.org/10.1016/j.measurement.2014.04.007.

Tallon, L.K. and Si, B.C., 2015. Representative soil water benchmarking for environmental monitoring. Journal of Environmental Informatics, 4(1), pp.31-39.

Tang, P., Chen, F., Jiang, A., Zhou, W., Wang, H., Leucci, G., de Giorgi, L., Sileo, M., Luo, R., Lasaponara, R. and Masini, N., 2018. Multi-frequency electromagnetic induction survey for

archaeological prospection: Approach and results in Han Hangu Pass and Xishan Yang in China. Surveys in Geophysics, 39(6), pp.1285-1302.

Tang, S., Farooque, A.A., Bos, M. and Abbas, F., 2020. Modelling DUALEM-2 measured soil conductivity as a function of measuring depth to correlate with soil moisture content and potato tuber yield. Precision Agriculture, 21(3), pp.484-502

Tarr, A.B., Moore, K.J., Bullock, D.G., Dixon, P.M. and Burras, C.L., 2005. Improving map accuracy of soil variables using soil electrical conductivity as a covariate. Precision Agriculture, 6(3), pp.255-270.

Tiwari, S., Singh, C., Boudh, S., Rai, P.K., Gupta, V.K. and Singh, J.S., 2019. Land use change: A key ecological disturbance declines soil microbial biomass in dry tropical uplands. Journal of Environmental Management, 242, pp.1-10.

Topp, G.C., Davis, J.L. and Annan, A.P., 1980. Electromagnetic determination of soil water content: Measurements in coaxial transmission lines. Water Resources Research, 16(3), pp.574-582. Doi:https://doi.org/10.1029/WR016i003p00574.

Toushmalani, R., 2010. Application of geophysical methods in agriculture. Australian Journal Basic Applied Science, 4(12), pp.6433-6439.

Triantafilis, J. and Santos, F.M., 2013. Electromagnetic conductivity imaging (EMCI) of soil using a DUALEM-421 and inversion modelling software (EM4Soil). Geoderma, 211, pp.28-38.

Unc, A., Altdorff, D., Abakumov, E., Adl, S., Baldursson, S., Bechtold, M., Cattani, D.J., Firbank, L.G., Grand, S., Guðjónsdóttir, M. and Kallenbach, C., 2021. Expansion of agriculture in northern cold-climate regions: a cross-sectoral perspective on opportunities and challenges. Frontiers in Sustainable Food Systems, 5, pp.448-663.

Uribeetxebarria, A., Arnó, J., Escolà, A. and Martinez-Casasnovas, J.A., 2018. Apparent electrical conductivity and multivariate analysis of soil properties to assess soil constraints in orchards affected by previous parcelling. Geoderma, 319, pp.185-193.

Von Hebel, C., Van Der Kruk, J., Huisman, J.A., Mester, A., Altdorff, D., Endres, A.L., Zimmermann, E., Garré, S. and Vereecken, H., 2019. Calibration, conversion, and quantitative multi-layer inversion of multi-coil rigid-boom electromagnetic induction data. Sensors, 19(21), pp.4753.

Walter, J., Lück, E., Bauriegel, A., Richter, C. and Zeitz, J., 2015. Multi-scale analysis of electrical conductivity of peatlands for the assessment of peat properties. European Journal of Soil Science, 66(4), pp.639-650.

Wang, F., Yang, S., Wei, Y., Shi, Q. and Ding, J., 2021. Characterizing soil salinity at multiple depth using electromagnetic induction and remote sensing data with random forests: A case study

in Tarim River Basin of southern Xinjiang, China. Science of the Total Environment, 754, pp.142030.

Wang, J., Sun, Q., Shang, J., Zhang, J., Wu, F., Zhou, G. and Dai, Q., 2020. A new approach for estimating soil salinity using a low-cost soil sensor in situ: A case study in saline regions of China's East Coast. Remote Sensing, 12(2), pp.239.

Wang, P., Hu, Z., Yang, J., Wang, F. and Gao, M., 2010. The identification test of soil texture with ground penetrating radar. In 2010 International Conference on Advances in Energy Engineering, pp.81-84.

Warrick, A.W., 1988. Additional solutions for steady-state evaporation from a shallow water table. Soil Science, 146, pp.63-66.

Wilson, B.R., Growns, I. and Lemon, J., 2008. Land-use effects on soil properties on the north-western slopes of New South Wales: implications for soil condition assessment. Soil Research, 46(4), pp.359-367.

Wilson, B.R., Koen, T.B., Barnes, P., Ghosh, S. and King, D., 2011. Soil carbon and related soil properties along a soil type and land-use intensity gradient, New South Wales, Australia. Soil Use and Management, 27(4), pp.437-447.

Won, I.J., Keiswetter, D.A., Fields, G.R. and Sutton, L.C., 1996. GEM-2: A new multifrequency electromagnetic sensor. Journal of Environmental and Engineering Geophysics, 1(2), pp.129-137.Doi:https://doi.org/10.4133/JEEG1.2.129.

Wu, W., Chen, G., Meng, T., Li, C., Feng, H., Si, B. and Siddique, K.H., 2023. Effect of different vegetation restoration on soil properties in the semi-arid Loess Plateau of China. Catena, 220, pp.106630.

Wuddivira, M.N., Robinson, D.A., Lebron, I., Bréchet, L., Atwell, M., De Caires, S., Oatham, M., Jones, S.B., Abdu, H., Verma, A.K. and Tuller, M., 2012. Estimation of soil clay content from hygroscopic water content measurements. Soil Science Society of America Journal, 76(5), pp.1529-1535.

Wulanningtyas, H.S., Gong, Y., Li, P., Sakagami, N., Nishiwaki, J. and Komatsuzaki, M., 2021. A cover crop and no-tillage system for enhancing soil health by increasing soil organic matter in soybean cultivation. Soil and Tillage Research, 205, pp.104749.

Xia, Q., Rufty, T. and Shi, W., 2020. Soil microbial diversity and composition: Links to soil texture and associated properties. Soil Biology and Biochemistry, 149, pp.107953.

Xiao, L.-P., Sun, Z.-J., Shi, Z.-J., Xu, F. and Sun, R.-C., 2011. Impact of hot compressed water pretreatment on the structural changes of woody biomass for bioethanol production. BioResources, 6, pp.1576-1598.

Xie, B., Jia, X., Qin, Z., Zhao, C. and Shao, M. A., 2020. Comparison of interpolation methods for soil moisture prediction on China's Loess Plateau. Vadose Zone Journal, 19, pp.20025.

Xu, G., Huang, M., Li, P., Li, Z. and Wang, Y., 2021. Effects of land use on spatial and temporal distribution of soil moisture within profiles. Environmental Earth Sciences, 80, pp.1-12.

Yang, C.S., Kao, S.P., Lee, F.B. and Hung, P.S., 2004, July. Twelve different interpolation methods: A case study of Surfer 8.0. In Proceedings of the 20th ISPRS congress, 35, pp. 778-785.

Yerima, B.P. and Van Ranst, E., 2005. Introduction to soil science: Soils of the tropics, Trafford publishing.

Yu, B., Liu, G., Liu, Q., Wang, X., Feng, J. and Huang, C., 2018. Soil moisture variations at different topographic domains and land use types in the semi-arid Loess Plateau, China. Catena, 165, pp.125-132. https://doi.org/10.1016/j.catena.2018.01.020.

Zhou, Q., Wu, Y., Guo, Z., Hu, J. and Jin, P., 2020. A generalized hierarchical co-Kriging model for multi-fidelity data fusion. Structural and Multidisciplinary Optimization, 62(4), pp.1885-1904

Appendices

Publications and Presentations:

Abstracts:

Mensah, C., Krishnapillai, M., Galagedara, L. (2022). Multi-frequency electromagnetic induction soil moisture characterization under different land uses in western Newfoundland. Joint Annual Meeting of the Canadian Soil Science Society (CSSS) Alberta Soil Science Workshop (ASSW) on "Soil Science for Sustainable Development", May 23 – 27, 2022. Edmonton, AB, Canada

Research articles:

Mensah, C., Katanda, Y., Krishnapillai, M., Cheema, M. and Galagedara, L., 2023. Multi-frequency electromagnetic induction soil moisture characterization under different land uses in western Newfoundland. Canadian Journal of Soil Science (Status: Accepted, Published)

Mensah, C., Katanda, Y., Krishnapillai, M., Cheema, M. and Galagedara, L., 2023. Using multi-frequency and multi-coil electromagnetic induction sensors to improve soil moisture prediction accuracy in different land use. Environmental Research Communications (Status: In-progress)